Journal of
Medicinal Chemistry

Drug Annotation

Discovery of CRBN E3 Ligase Modulator CC-92480 for the Treatment of Relapsed and Refractory Multiple Myeloma

Joshua D. Hansen, Matthew Correa, Mark Nagy, Matt Alexander, Veronique Plantevin, Virginia Grant, Brandon Whitefield, Dehua Huang, Timothy Kercher, Roy Harris, Rama Krishna Narla, Jim Leisten, Yang Tang, Mehran Moghaddam, Katalin Ebinger, Joseph Piccotti, Courtney G. Havens, Brian E. Cathers, James Carmichael, Thomas O Daniel, Rupert Vessey, Lawrence G. Hamann, Katerina Leftheris, Derek Mendy, Frans Baculi, Laurie LeBrun, Gody Khambatta, and Antonia Lopez-Girona

J. Med. Chem., **Just Accepted Manuscript** • DOI: 10.1021/acs.jmedchem.9b01928 • Publication Date (Web): 04 Mar 2020

Just Accepted

is published by the American Chemical Society. 1155 Sixteenth Street N.W., Washington, DC 20036

Discovery of CRBN E3 Ligase Modulator CC-92480 for the Treatment of Relapsed and Refractory Multiple Myeloma

Joshua D. Hansen, Matthew Correa, Mark A. Nagy, Matt Alexander, Veronique Plantevin, Virginia Grant, Brandon Whitefield, Dehua Huang, Timothy Kercher, Roy Harris, Rama Krishna Narla, Jim Leisten, Yang Tang, Mehran Moghaddam, Katalin Ebinger, Joseph Piccotti, Courtney G. Havens, Brian Cathers, James Carmichael, Thomas Daniel, Rupert Vessey, Lawrence G. Hamann, Katerina Leftheris, Derek Mendy , Frans Baculi, Laurie A. LeBrun, Gody Khambatta, Antonia Lopez-Girona*

Celgene Corporation, 10300 Campus Point Drive, Suite 100, San Diego, California 92121, USA.

KEYWORDS Ikaros, IKZF1, Aiolos, IKZF3, protein degradation, molecular glue, immunomodulatory, CELMoD, lenalidomide-resistant, relapsed refractory multiple myeloma.

ABSTRACT: Many patients with multiple myeloma (MM) initially respond to treatment with modern combination regimens including immunomodulatory agents (lenalidomide and pomalidomide) and proteasome inhibitors. However, some patients lack an initial response to therapy (*i.e.*, are refractory) and, although the mean survival of MM patients has more than doubled in recent years, most patients will eventually relapse. To address this need, we explored the potential of novel Cereblon E3 Ligase Modulators (CELMoDs) for the treatment of patients with relapsed or refractory multiple myeloma (RRMM). We found that optimization beyond potency of degradation, including degradation efficiency and kinetics, could provide efficacy in a lenalidomide-resistant setting. Guided by both phenotypic and protein degradation data, we describe a series of CELMoDs for the treatment of RRMM, culminating in the discovery of CC-92480, a novel protein degrader and the first CELMoD to enter clinical development that was specifically designed for efficient and rapid protein degradation kinetics.

INTRODUCTION

Multiple myeloma (MM) is the second most common hematological malignancy in the US but constitutes less than 1% of all cancer types (~32,000 expected new diagnosed cases in 2020).[1] It is considered an orphan disease by the US Food and Drug Administration. Lenalidomide (**1,** Figure 1) has demonstrated significant improvement of overall survival rates (more than double compared to placebo + dexamethasone) and is approved in combination with dexamethasone for the treatment of MM. The widespread use of immunomodulatory drugs and proteasome inhibitors has come to represent the backbone of current standard-of-care therapy for MM patients. Despite these advances in the overall survival rate, there remains significant unmet medical need in both refractory and relapsed patient populations. [2]

Induction of protein degradation as a therapeutic strategy has been clinically validated by the class of immunomodulatory drugs, which include lenalidomide and pomalidomide (Figure 1). The therapeutic benefits of immunomodulatory drug treatment are connected to their ability to promote recruitment and ubiquitination of substrate proteins by the cullin-damaged DNA-binding-RING box-domain protein (CUL4-DDB1-RBX1-CRBN), or simply

(CRL4^{CRBN}) E3 ubiquitin ligase, with the resulting ubiquitin-tagged proteins directed to and subsequently degraded by the 26S proteasome (Figure 2).[3,4,5] In this manner, lenalidomide directs cereblon (CRBN) to degrade Ikaros (IKZF1) and Aiolos (IKZF3), initiating the downstream effects[6,7,8] which were shown to be associated with the antitumor and immunomodulatory properties of lenalidomide.[9,10]

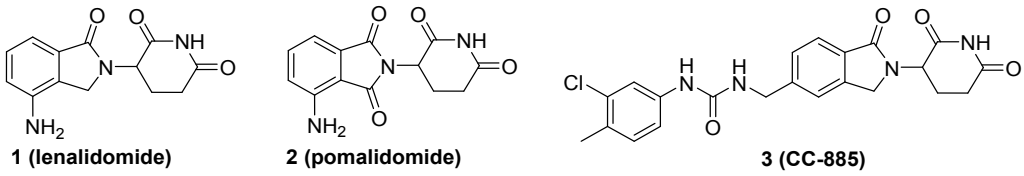

Figure 1. Structures of lenalidomide, pomalidomide, and CC-885.

Figure 2 a)

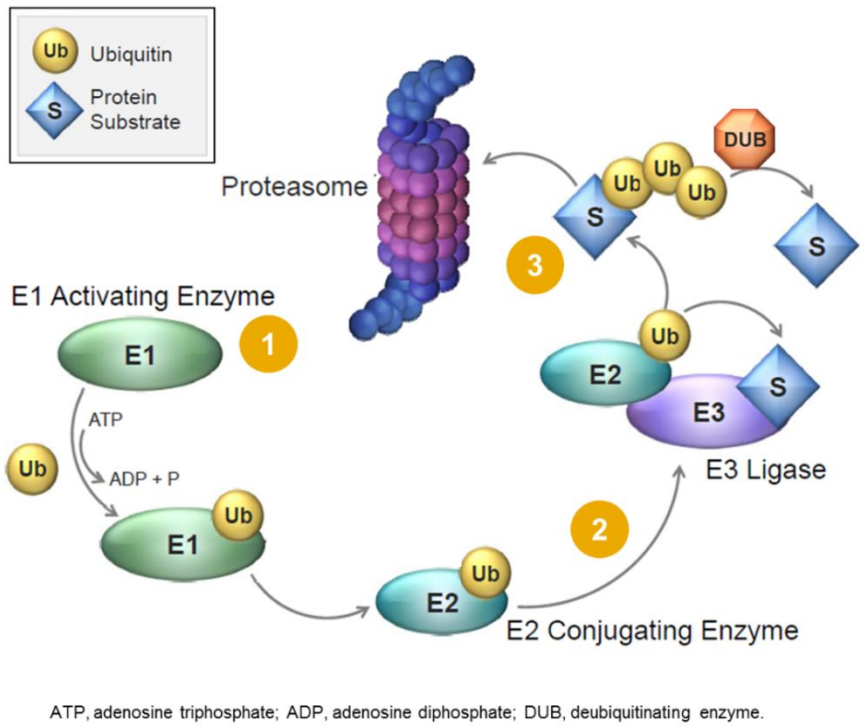

ATP, adenosine triphosphate; ADP, adenosine diphosphate; DUB, deubiquitinating enzyme.

Figure 2 b)

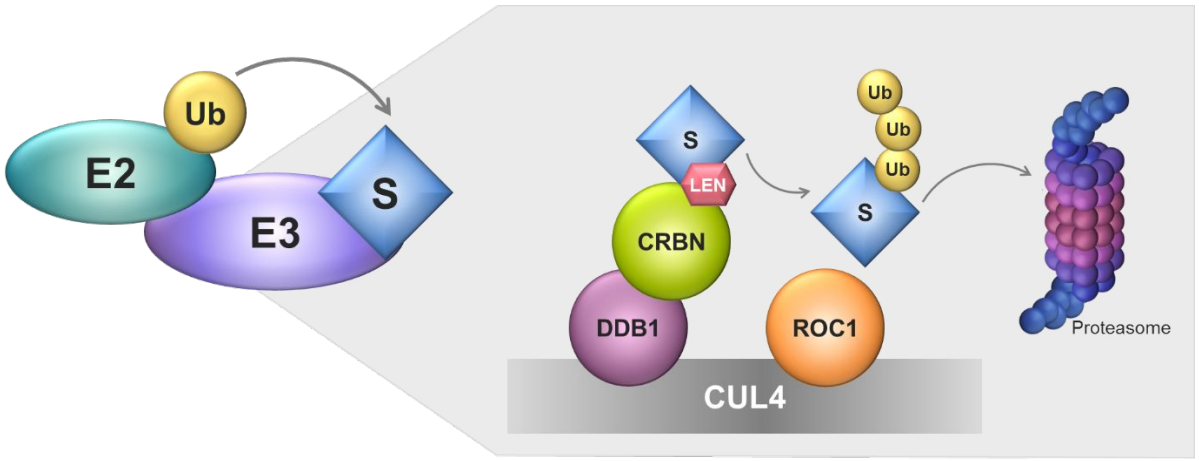

Figure 2. a) Overview of the ubiquitin proteasome system. 1) The E1 enzyme catalyzes the activation of ubiquitin, leading to ubiquitin transfer to E2 conjugating enzyme. 2) Target substrate ubiquitination occurs after E2 transfers ubiquitin via the E3 ligase complex, to which the target is bound. 3) After ubiquitination,

the substrate is recognized by the proteasome for degradation. **b**) Magnified view of the E3 Ligase complex model. Lenalidomide acts as a "molecular glue" to induce the binding of S (substrate; Ikaros/Aiolos) to CRBN and drive the ubiquitination and ultimate degradation by the proteasome. Figure modified from ACS Med. Chem. Lett. **2019**, *10*, 1592-1602.

Focused on a patient-oriented outcome, our goal was to develop a deeper knowledge surrounding the degradation of Ikaros and Aiolos, the aspects of which we believed could provide insight into the development of new protein degraders with enhanced efficacy in MM and particularly in lenalidomide-refractory settings. The establishment and characterization of a lenalidomide-resistant MM cell line, H929 R10-1 has been previously reported, which in brief, results from the continuous treatment of H929 cells with increasing doses of lenalidomide. In order to widen the possibility of finding novel chemical matter as a starting point for investigation, we employed a phenotypic screen of our CRBN modulator library using the lenalidomide-resistant H929 cell line. In conjunction to the phenotypic approach, we screened for protein degradation, and since degradation of Aiolos and Ikaros showed high correlation in previous test sets, and parallel results would be expected, Aiolos was used as the representative target.

Recently, we described the structure-activity relationships of a series of urea-containing compounds represented by **3** (CC-885, Figure 1) which were observed to degrade the key proteins Ikaros and Aiolos, but also effected degradation of GSPT1 (eRF3a) with variable levels of selectivity.[11] Urea **3** was included in the phenotypic screen and displayed potent activity against H929 R10-1. Compound **3** however, was not suitable for further development due to concerns about its toxicity profile. Compound **3** was not tolerated after a single dose in cynomolgus monkeys (data not shown), which we correlated to the lack of an in vitro selectivity ratio between the viability of normal peripheral blood mononuclear cells (PBMCs) from healthy donors versus the target lenalidomide-resistant cells (Figure 3). We removed from consideration compounds like **3** that had little to no *in vitro* selectivity and focused on the leads with high cell viability in PBMCs (IC_{50} > 5 μM). As expected, lenalidomide demonstrated no activity against H929 R10-1, and pomalidomide showed poor activity clustering, with a group of analogs in a half-micromolar potency range. On the other extreme, we identified compound **13** which showed little effect on PBMC viability yet displayed potent single digit-nanomolar antiproliferative activity against the lenalidomide-resistant cell line (Figure 3).

Using **13** as a lead structure, we resolved to explore the SAR of this series (Figure 4) as it related to both lenalidomide-resistance activity as well as preservation of selectivity against PBMCs. Herein, we describe the design and synthesis of a series of potent aryl piperazine-containing compounds that exhibit deep levels of protein degradation with rapid degradation kinetics, leading to preclinical activity for the treatment of RRMM. The optimization of degradation efficiency in this series which translated to strong induction of apoptosis, culminated in the identification of **4** (CC-92480), the first CELMoD entering clinical development that was specifically designed for high efficiency and rapid kinetics of protein degradation.

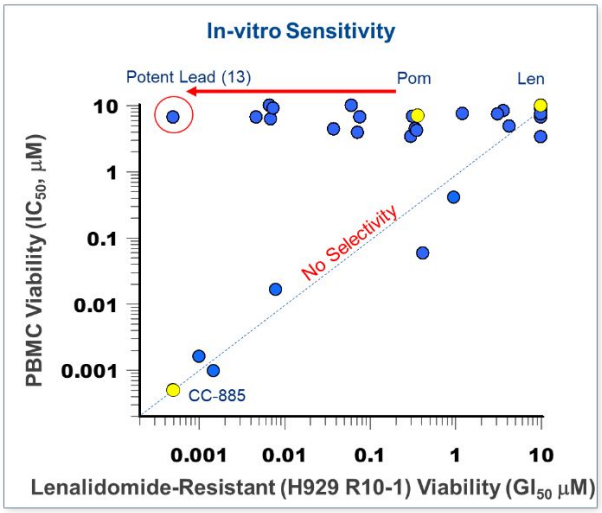

Figure 3. Phenotypic screen of CELMoDs in which in vitro sensitivity toward PBMC viability is plotted against lenalidomide-resistant MM cell viability (H929 R10-1). Compounds above the diagonal line have stronger activity in H929-1051 cells than in PBMC. Lenalidomide (Len), pomalidomide (Pom), and CC-885 are colored in yellow.

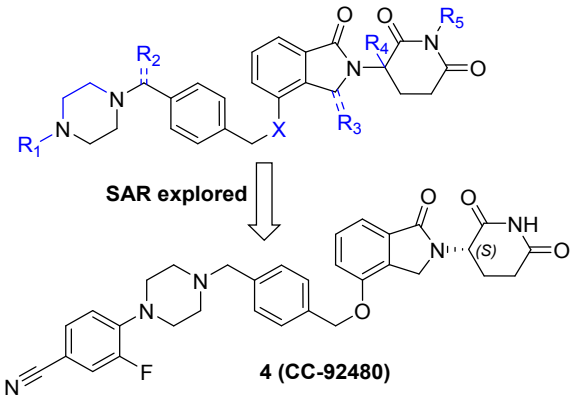

Figure 4. Structures showing the scope of SAR described, leading to **4** (CC-92480).

CHEMISTRY

The chemistry efforts toward CC-92480 (**4**) involved the preparation of several analogs accessed through varying synthetic routes, which are outlined in the following schemes and Supporting Information. Synthesis of key amine **8** (Scheme 1) began with regioselective methyl esterification of the gamma carboxylic acid group of glutamic acid (**5**), followed by boc protection of the amine to give **6**. Conversion of the alpha carboxylic acid to a primary amide followed by acidic boc deprotection gave amine **8**.

The synthesis of the key intermediates **12a-b** (Scheme 2) began with Fischer esterification of 3-hydroxy-2-methylbenzoic acid (**9**), followed by radical bromination of the tolyl-methyl group.[12] Formation of the isoindolinone **11** was accomplished via bromide displacement using methyl 4,5-diamino-5-oxopentanoate (**8**) as the nucleophile, followed by base-mediated cyclization. After silyl deprotection, the requisite benzyl spacer could be installed either via phenol alkylation with 1,4-bis(bromomethyl)benzene or by Mitsunobu reaction with (4-(chloromethyl)phenyl)methanol. In the case of benzyl bromide intermediate **12a**, the glutarimide functionality was obtained through treatment of the primary amide with potassium *tert*-butoxide at low temperature. Alkylation of the benzyl bromide with amines **13-33** afforded the final compounds. For instances involving benzyl chloride intermediate **12b**, alkylation of the chloride with the desired amine nucleophile occurred first and was followed by closure of the glutarimide ring using the low temperature, potassium *tert*-butoxide conditions mentioned above.

To evaluate the dependence of CRBN-binding, the N-methyl analog of **13** (**39**) was accessed through alkylation of the glutarimide functionality as outlined in Scheme 3. Benzyl intermediate **36** was synthesized by silyl protection of benzyl alcohol **35**, followed

by reduction of the ester and subsequent conversion of the resulting benzyl alcohol to benzyl bromide **36**. Closure of the glutarimide ring with potassium *tert*-butoxide was followed by silyl deprotection and alkylation of the glutarimide nitrogen with methyl iodide to provide **38**. Conversion of the benzyl alcohol of **38** to the corresponding mesylate allowed for alkylation with 1-(2,4-difluorophenyl)piperazine to give compound **39**.

SAR exploration of analogs containing the phthalimide core was supported by the synthesis described in Scheme 4 which began with the reaction of phthalic anhydride **41** and 3-aminoglutarimide to give compound **42**. Alkylation of phenol **42** with previously described benzyl bromide **36** was followed by acidic silyl deprotection and conversion of the resulting benzyl alcohol to mesylate **44**. This penultimate intermediate provided a common access point to compounds **45-47**.

For purposes of linker SAR, the nitrogen-linked analog of lead compound **13** was obtained in convergent fashion by reductive amination of lenalidomide (**1**) with functionalized aldehyde **49** which was obtained in one step from commercial 4-(bromomethyl)benzaldehyde (Scheme 5).

The synthesis of chiral alpha-methyl glutarimide analog **58** shown in Scheme 6 began with formation of imine **52** from methyl L-alaninate (**51**) and benzaldehyde. Ensuing addition of prop-2-enamide followed by acidic imine hydrolysis provided racemic 3-amino-3-methylpiperidine-2,6-dione (**53**). Addition of menthol derivative **54** to the amine provided the necessary chiral auxiliary to enrich for the desired S-enantiomer. Compound **56** was obtained in high enantiomeric excess after crystallization of **55** followed by carbamate hydrolysis. Formation of the isoindolinone core was achieved by bromide displacement of **10** and subsequent trimethylaluminum-mediated condensation to give lactam **57**. A one-pot base-mediated silyl deprotection and alkylation of the liberated phenol with benzyl bromide **63** provided the target alpha-methyl glutarimide analog **58**.

Synthesis of amide-linked piperazine analogs shown in Scheme 7 was achieved through a slight modification of the route described in Scheme 2. Alkylation of lactam **11** with benzyl bromide ester **64**, followed by formation of the glutarimide ring with potassium *tert*-butoxide and acidic hydrolysis of the *tert*-butyl ester provided the perfluorophenyl acetate **67** which afforded a common intermediate from which compounds **68-71** were accessed through amide formation with their respective N-aryl piperazines.

Scheme 8 depicts the asymmetric synthesis of **4** that began with intermediate **10** where formation of the lactam proceeded with *tert*-butyl (4S)-4,5-diamino-5-oxo-pentanoate and ensuing silyl deprotection gave hydroxyl **74**. Aryl piperazine intermediate **73** was made through mono-alkylation of 1,4-bis(chloromethyl)benzene with 3-fluoro-4-(piperazin-1-yl)benzonitrile (**72**). The route converged through alkylation of intermediate **74** with benzyl chloride **73**. Formation of the glutarimide ring proceeded via dehydration under acidic conditions at 85 ºC to provide **4** with >98 % enantiomeric excess.

Scheme 1. Synthesis of amine intermediate 8.

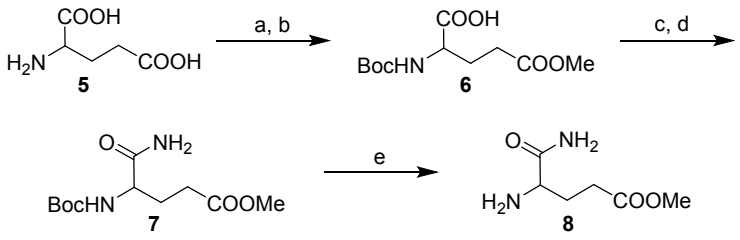

Reagents and conditions: (**a**) TMSCl, MeOH, rt, 30 min; (**b**) Boc_2O, Et_3N, rt, 2 h, 56% over 2 steps; (**c**) Boc_2O, pyridine, rt, 30 min, 1,4-dioxane; (**d**) NH_4HCO_3, rt, 16 h, 90% over 2 steps; (**e**) HCl, rt, 12 h, EtOAc, 95%.

Scheme 2. Synthesis of benzyl piperazine and piperidine analogs.

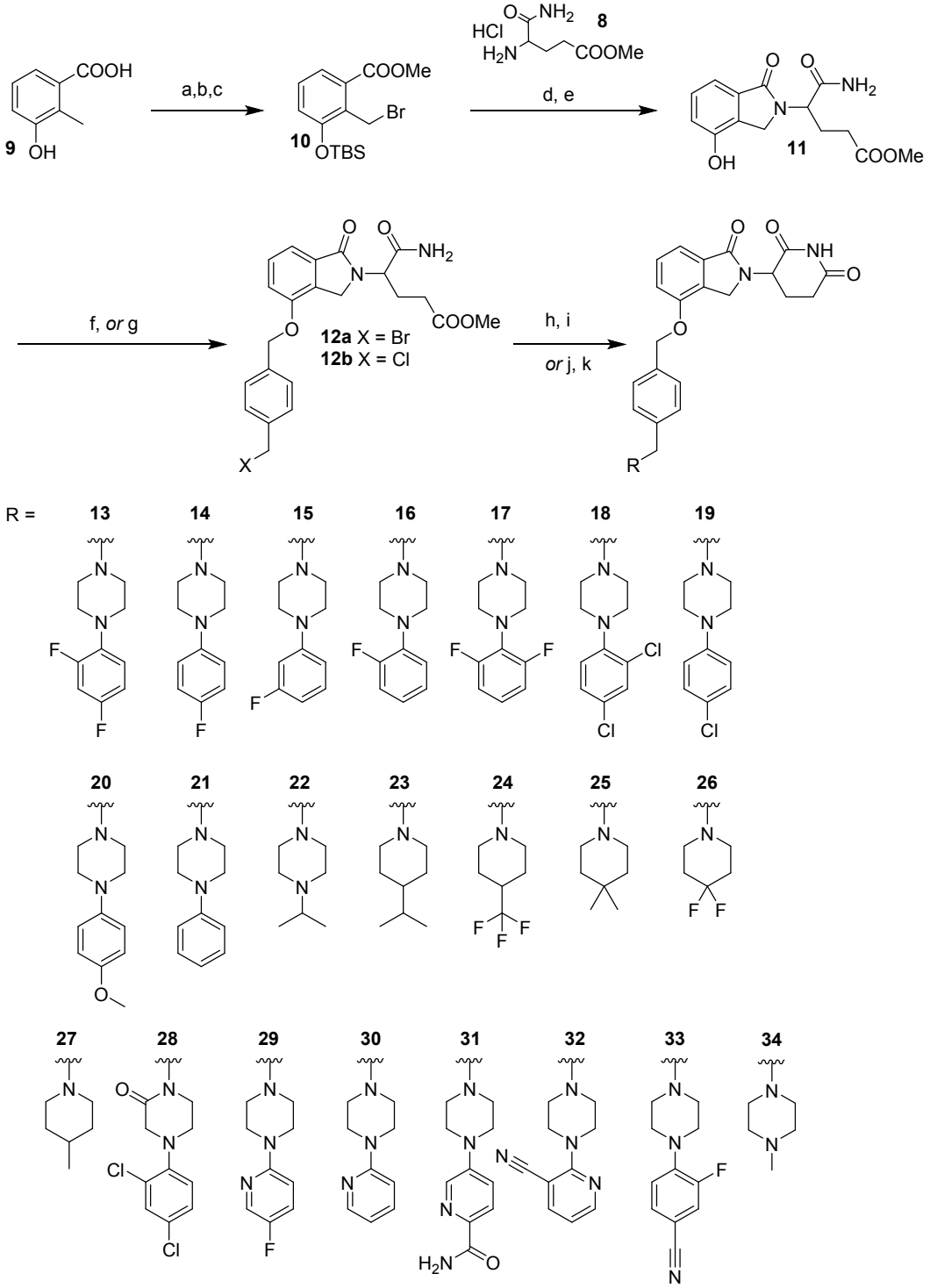

Reagents and conditions: (**a**) H_2SO_4, MeOH, 65 ºC, 17 h, 88%; (**b**) TBSCl, imidazole, 25 ºC, 1 h, DCM, 75%; (**c**) AIBN, NBS, 65 ºC, 2 h, EtOAc, 98%; (**d**) **8**, DIEA, 60 ºC, 16 h, ACN, 76%; (**e**) K_2CO_3, H_2O, RT, 15 h, DMF, then HCl, 77%; (**f**) 1,4-bis(bromomethyl)benzene, K_2CO_3, 60 ºC, 16 h, ACN, 63%; (**g**) (4-(chloromethyl)phenyl)methanol, PPh_3, DIAD, 0 ºC, 1.5 h, THF, 92%; (**h**) *t*-BuOK, -78 ºC, 2 h, THF, 93%; (**i**) Substituted phenyl/alkyl piperazines/piperidines, DIEA, 40 ºC, 18 h, ACN, 18%-90%; (**j**) Substituted

phenyl/alkyl piperazines/piperidines, DIEA, 40 ºC, 18 h, ACN, 45%-60%; (**k**) *t*-BuOK, 0 ºC, 5 min, THF, 36-50%.

Scheme 3. Synthesis of the *N*-methyl glutarimide compound 39.

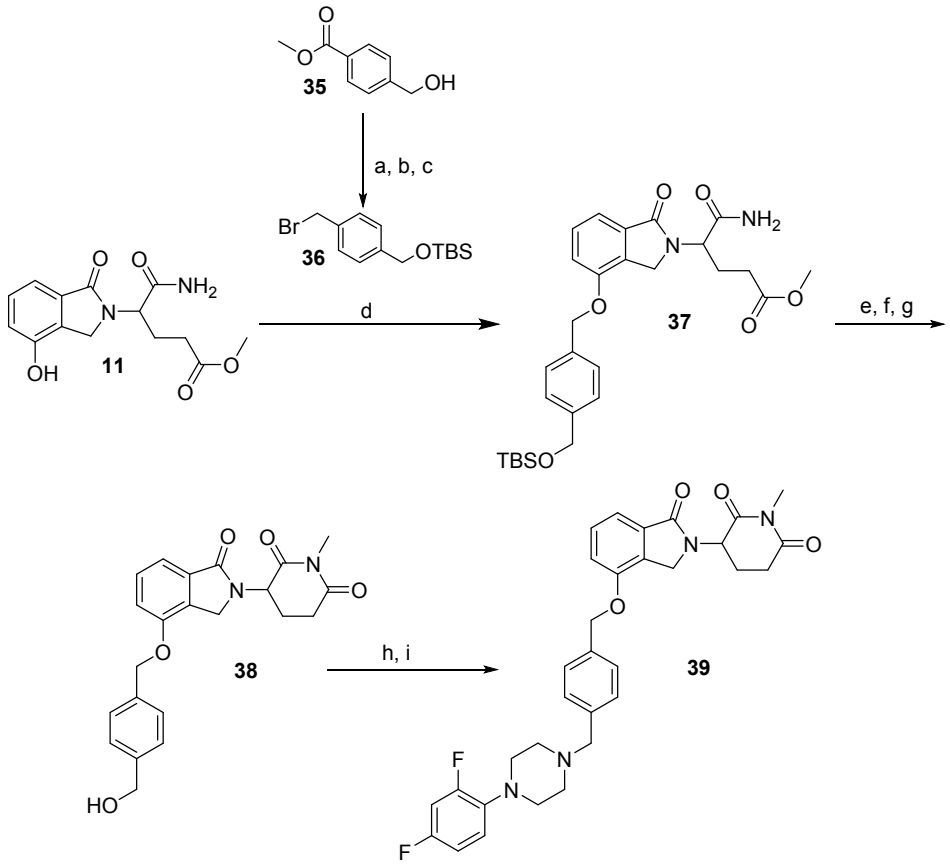

Reagents and conditions: (**a**) TBSCl, imidazole, 0-25 ºC, 16 h, DMF; (**b**) $LiAlH_4$, 0 ºC, 1 h, THF, 80% over 2 steps; (**c**) NBS, Me_2S, -20-25 ºC, 2 h, DCM; (**d**) **37**, K_2CO_3, 30 ºC, 4 h, DMF, 44%; (**e**) *t*-BuOK, 0 ºC, 1 h, THF; (**f**) H_2SO_4, 20 ºC, 2 h, THF, 84% over 2 steps; (**g**) MeI, K_2CO_3, rt, 5 h, DMF, then HCl, 72%; (**h**) MsCl, DIEA, -5 ºC, 1 h, DMF; (**i**) 1-(2,4-difluorophenyl)piperazine, DIEA, 30 ºC, 16 h, DMF, 25% over 2 steps.

Scheme 4. Synthesis of analogs containing the phthalimide core.

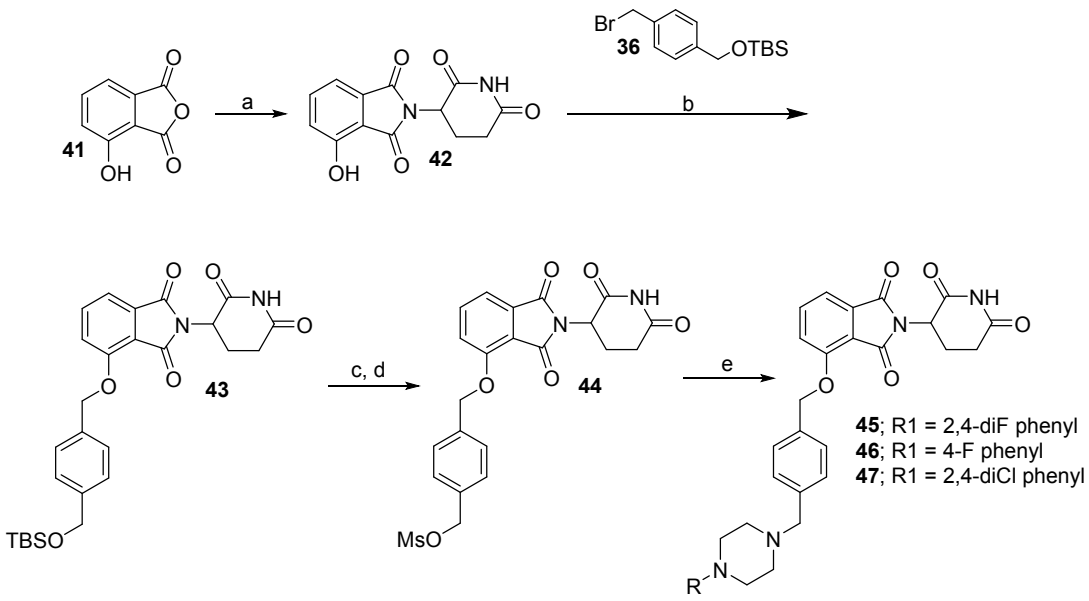

Reagents and conditions: (**a**) 3-aminopiperidine-2,6-dione, AcONa, 100 ºC, 2 h AcOH, 71%; (**b**) **36**, K_2CO_3, 20 ºC, 3 h, DMF, 38% over 2 steps; (**c**) H_2SO_4, 24 ºC, 30 min, THF, 85%; (**d**) MsCl, DIEA, 20 ºC, 2 h, DMF (**e**) Substituted phenyl piperazines, DIEA, 24 ºC, 16 h, DMF, 33-36%.

Scheme 5. Synthesis of the *N*-linked compound 50.

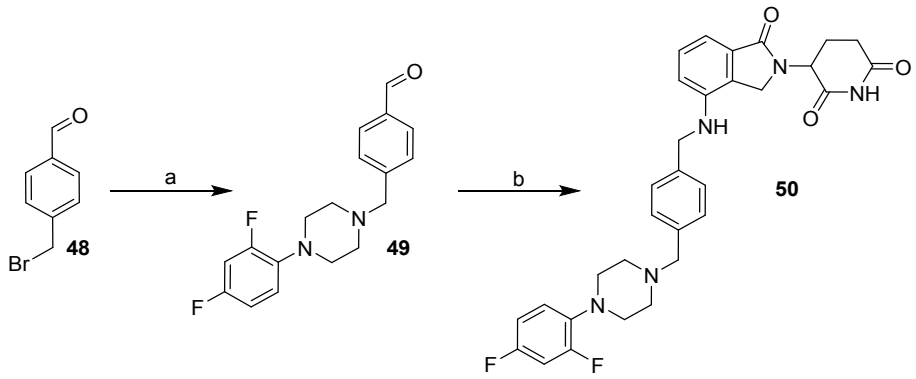

Reagents and conditions: (**a**) 1-(2,4-difluorophenyl)piperazine, TEA, RT, 16 h, ACN, 95%; (**b**) Lenalidomide (**1**), $NaBH_4$, 100 ºC – 25 ºC, 3 h, AcOH, 48% over 2 steps.

Scheme 6. Synthesis of the chiral-methyl glutarimide compound 58.

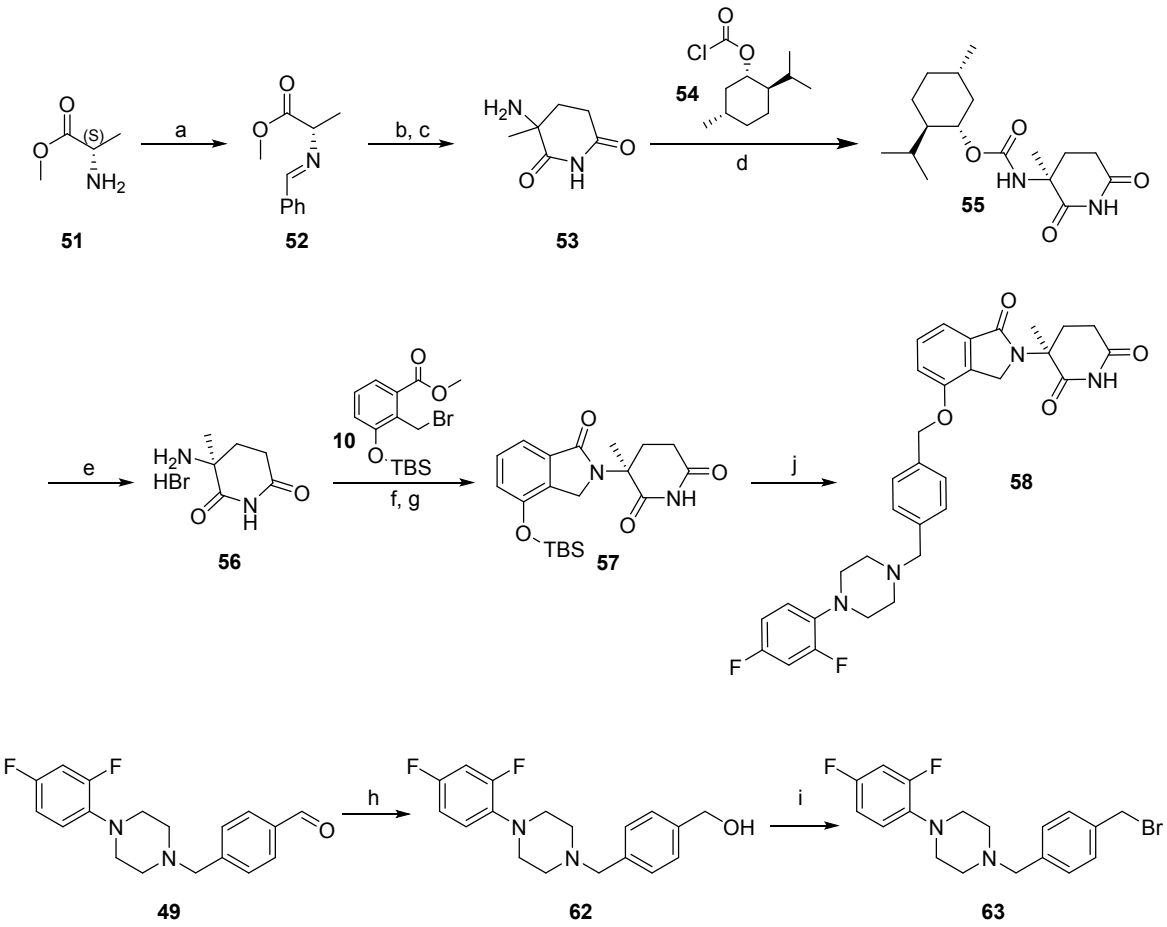

Reagents and conditions: (**a**) $MgSO_4$, TEA, PhCHO, rt, 16 h, DCM; (**b**) prop-2-enamide, *t*-BuOK, NH_4Cl, 0 ºC, 30 min, THF, 75% over 2 steps; (**c**) HCl, 10 ºC, 3 h, THF, 96%; (**d**) **54**, $NaHCO_3$, 0 ºC, 2 h, THF, water, 9%; (**e**) HBr, AcOH, 90 ºC, 6 h, 87%; (**f**) **10**, DIEA, rt, 16 h, ACN; (**g**) $AlMe_3$, 110 ºC, 2 h, toluene, 54% over 2 steps; (**h**) $NaBH_4$, 0 ºC, 2 h, MeOH, 87%; (**i**) $SOBr_2$, rt, 2 h, DCM, 91%; (**j**) **63**, K_2CO_3, rt, 16 h, DMF, 73%.

Scheme 7. Synthesis of amide-linked piperazine analogs.

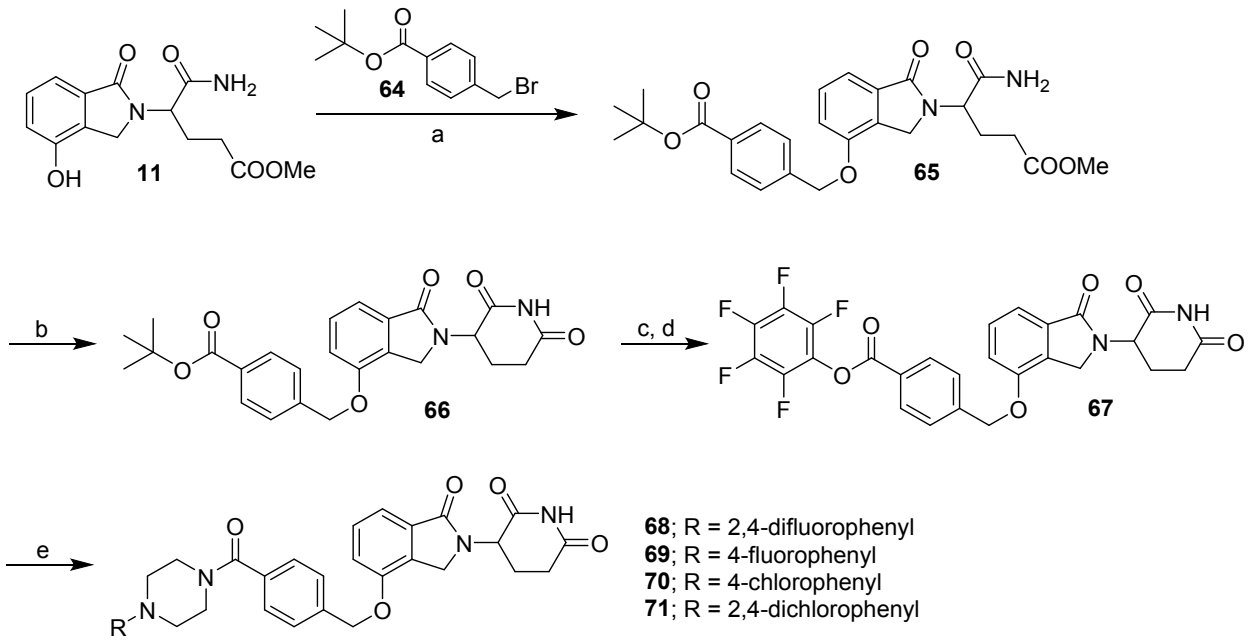

Reagents and conditions: (**a**) **64**, K_2CO_3, 25 ºC, 4 h, NMP, 57%; (**b**) *t*-BuOK, -70 ºC, 90 min, THF, 73%; (**c**) TFA, 25 ºC, 12 h, DCM, 100%; (**d**) Perfluorophenyl 2,2,2-trifluoroacetate, DIEA, THF/DMF, 57%; (**e**) Substituted phenyl piperazines, DIEA, RT, 10 min, DMF, 50-74%.

Scheme 8. Asymmetric synthesis of 4.

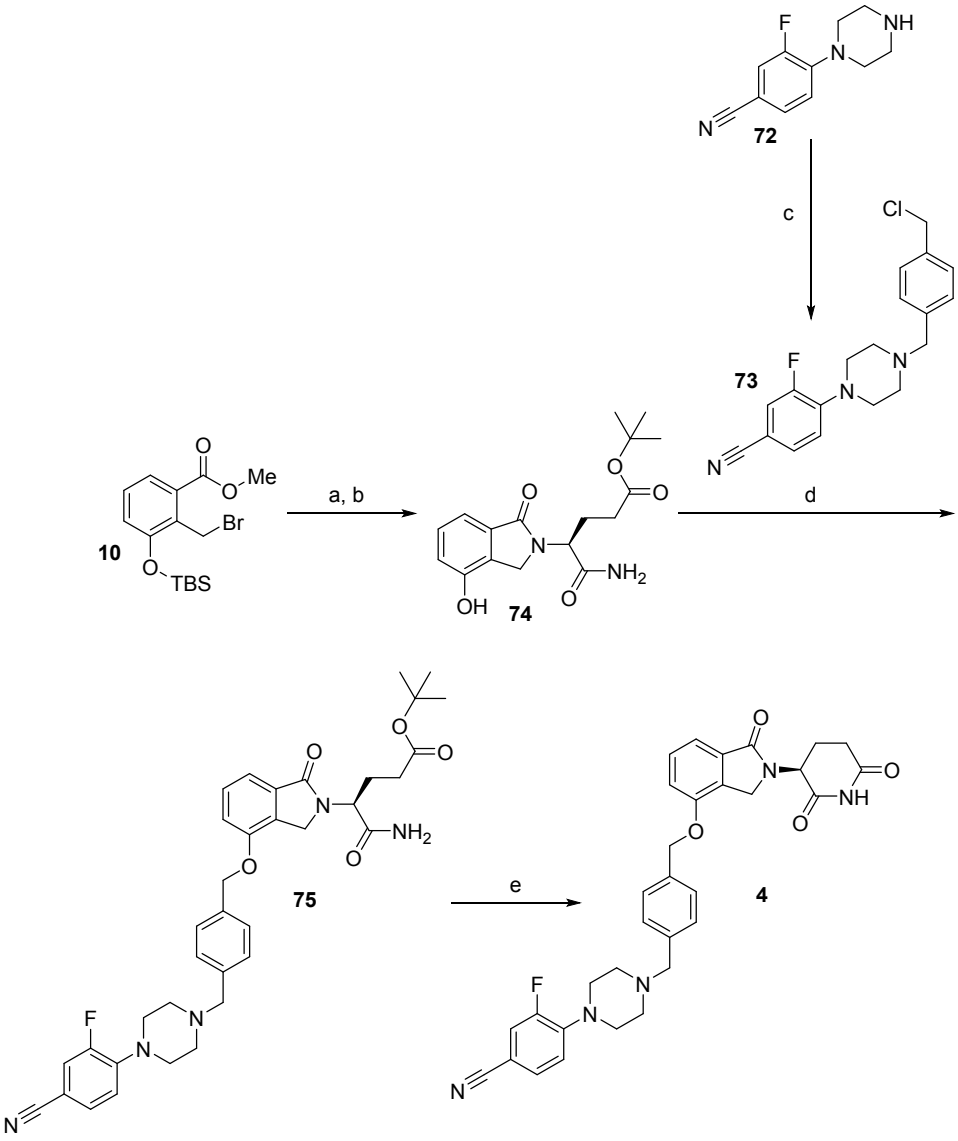

Reagents and conditions: (**a**) tert-butyl (4S)-4,5-diamino-5-oxo-pentanoate, DIEA, 50 ºC, 16 h, ACN; (**b**) TBAF, rt, 16 h, MeOH, 60% over 2 steps; (**c**) 1,4-bis(chloromethyl)benzene, DIEA, 60 ºC, 1 h, ACN/DMF, 67%; (**d**) **73**, K_2CO_3, 45 ºC, 16 h, DMF, 100%; (**e**) benzenesulfonic acid, 85 ºC, 18 h, ACN, 72%, 98% e.e..

RESULTS AND DISCUSSION

Since the mode of action of targeted protein degraders (molecular glue and heterobifunctional molecules/PROTACs) hinges upon removal of a disease-associated protein through an event-driven process (formation of the ternary complex to facilitate ubiquitin transfer) whereby the degrader can facilitate multiple rounds of degradation, the ratio of the number of molecules of target proteins degraded per molecule of degrader compound should be $\geq$ 1:1. After the protein is tagged with ubiquitin and degraded, the degrader molecule becomes available to engage in the formation of a ternary complex with additional protein, thus degraders have the potential for catalytic-like efficiency. The degradation efficiency is inherent to and reflected by the level of protein remaining over a time course of measurement, generally 4 h in the case of work described in this communication. The level of protein remaining is denoted by percent of control on the Y-axis of the degradation curve, and the point at which the curve reaches a minimum (Y_{min}) depicts the minimum percent protein remaining (Figure 5). Percent protein remaining (Y_{min}) is reached when degradation and protein synthesis reach an equilibrium, and thus comparisons of Y_{min} values would reveal which compounds can more effectively induce

protein degradation (lower Y_{min}). It is worth pointing out that for targets with very fast protein resynthesis, a low Y_{min} requires fast degradation kinetics.

Comparison of degradation efficiency can be drawn across groups of compounds assayed under the same conditions and timeframe. As a relevant example, lenalidomide and pomalidomide display a differential in Aiolos degradation efficiency (Figure 5). After 4 hours lenalidomide demonstrates the least efficient degradation at Y_{min} = 35 (35 % protein remaining), and pomalidomide shows improved degradation efficiency with Y_{min} = 18. This differentiated pharmacology is clinically correlated with a greater efficacy of pomalidomide which can achieve responses in lenalidomide-refractory patients.[13] The novel degrader CC-92480 (**4**), in addition to a dramatic increase in potency shows significant improvement in degradation efficiency as measured by the depth of protein degradation (Y_{min} = 5), a parameter we expect to translate into higher clinical efficacy in RRMM patients.

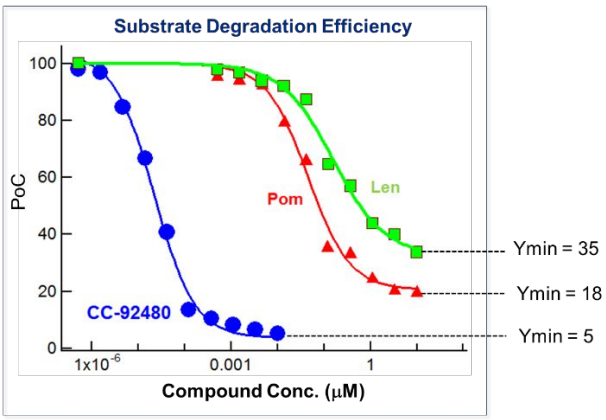

Figure 5. Aiolos degradation curves (4h) of pomalidomide (Pom), lenalidomide (Len), and CC-92840 (**4**). Y_{min} is the lowest point of the dose-response degradation curve and denotes the minimum % protein remaining.

The identified lead **13**, in addition to potent antiproliferative activity in the lenalidomide-resistant line (H929 R10-1), also displays potent and efficient degradation of Aiolos. (Figure 6). To assess the minimum pharmacophore, we explored the effect of a systematic truncation/simplification of the terminal aryl in lead **13**. To begin, the 2,4-difluoro substitution was removed yielding the phenyl analog **21**, which retained both excellent antiproliferative activity as well as Aiolos degradation potency and efficiency. Replacement of phenyl with *i*-propyl, as exemplified in analog **22**, led to a loss in desired antiproliferative activity. It is worth noting that the loss in antiproliferative activity (~20x compared to **13**) was not mirrored by the same loss (3x) of Aiolos degradation potency. However, the degradation efficiency of **22** is lower (13% remaining as compared to 6%

for **13**) and may help rationalize the large loss in antiproliferative potency. A further reduction of size, in which the terminal aryl found in **13** was replaced with methyl (**34**), led to a sharp activity drop (300x) in antiproliferative activity which correlates with concomitant loss in Aiolos degradation potency and efficiency. Finally, removal of the piperazine group in **40**, where the O-benzyl substituent becomes the terminus abolished antiproliferative activity in the H929 R10-1 cell line.

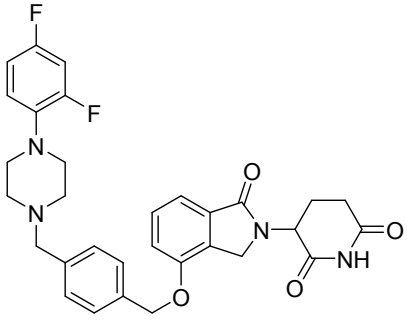

13
H929 R10-1 IC_{50} = 0.0017 μM
Aiolos EC_{50} = 0.00010 μM
Aiolos Y_{min} = 6

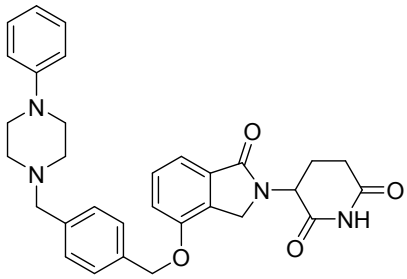

21
H929 R10-1 IC_{50} = 0.0021 μM
Aiolos EC_{50} = 0.00010 μM
Aiolos Y_{min} = 5

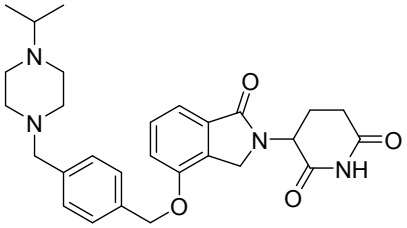

22
H929 R10-1 IC_{50} = 0.035 μM
Aiolos EC_{50} = 0.0003 μM
Aiolos Y_{min} = 13

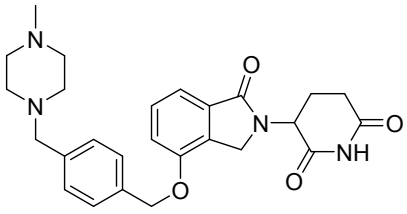

34
H929 R10-1 IC_{50} = 0.51 μM
Aiolos EC_{50} = 0.003 μM
Aiolos Y_{min} = 28

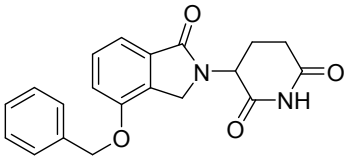

40
H929 R10-1 IC_{50} = > 10 μM
Aiolos EC_{50} = 0.0075 μM
Aiolos Y_{min} = 62

Figure 6. An SAR exploration in which systematic reduction in size from lead **13**, defines the minimum pharmacophore to include an aryl substituted piperazine.

The requirement of the 2,4-difluoro substitution present in **13** was next examined, represented by a selected set of data in Table 1. It is readily apparent that changing the substitution pattern of aryl-fluoro groups (**13**-**17**) made little impact on either antiproliferative activity, or degradation potency/efficiency. Compound **18**, the chloro analog of **13** maintained potency showing only a minimal loss (5x) in antiproliferative activity. Electron donating groups were also assessed as exemplified by **20** and maintained comparable activity to **13**. Taken together, we found the substitution at the terminal aryl to have little impact on antiproliferative activity or Aiolos degradation. Analogs of **13** maintained a similar PBMC viability profile and additionally when measured for degradation selectivity, piperazine **13** and its closely related analogs were devoid of GSPT1 degradation activity.

Table 1. Effect of substitution at the terminal aryl group.[a,b,c]

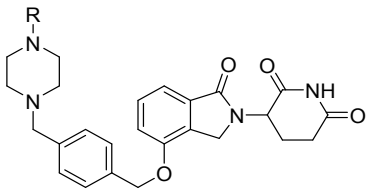

Compd	R	H929 R10-1 IC_{50} (nM)	Aiolos EC_{50} (nM)	Aiolos Y_{min}	GSPT1 EC_{50} (nM)
13	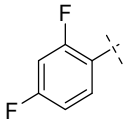	1.7	0.1	6	>10,000
14	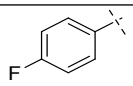	2.8	0.1	5	>10,000
15	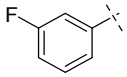	3.7	0.1	6	>10,000
16	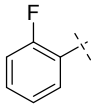	5.0	0.2	6	>10,000
17	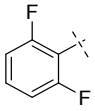	4.0	0.3	7	>10,000
18	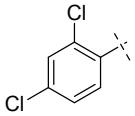	9.2	0.2	8	>10,000
19	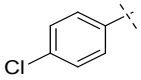	3.6	0.1	6	>10,000
20	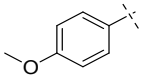	7.1	0.5	9	>10,000
21		2.1	0.1	5	>10,000

[a]All values are the mean of at least three separate assay determinations, [b]SEM for data available in supplemental material, [c]Y_{min} is the % protein remaining followed by treatment with compound concentrations up to 10 μM, and measured after 4 h (see methods).

It was anticipated based on previously established SAR, and confirmed by crystallography,[14] that the glutarimide moiety is an important binding partner to CRBN, and the glutarimide N-H makes a hydrogen-bond interaction with His378 contributing to

CRBN binding affinity. To this end, we synthesized the *N*-methyl glutarimide analog of **13** (**39**). As expected, methylation of the glutarimide disrupts CRBN binding and translated into a >370-fold loss of activity in both degradation and proliferation (Table 2).

Table 2. Effect of *N*-methyl cap at glutarimide. [a,b,c]

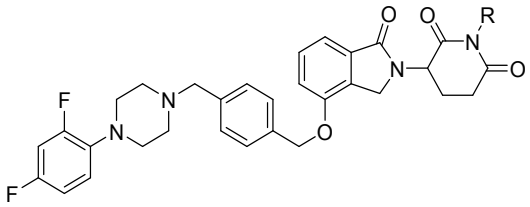

Compd	R	H929 R10-1 IC_{50} (nM)	Aiolos EC_{50} (nM)	Aiolos Y_{min}	GSPT1 EC_{50} (nM)	CRBN Binding IC_{50} (nM)
13	H	1.7	0.1	6	>10,000	55.1
39	Methyl	632	>10,000	93	>10,000	28,000

[a]All values are the mean of at least three separate assay determinations, [b]SEM for data available in supplemental material, [c]Y_{min} is the % protein remaining followed by treatment with compound concentrations up to 10 μM, and measured after 4 h (see methods).

The structural difference between lenalidomide and pomalidomide (Figure 1) is an additional carbonyl group in the scaffold of pomalidomide (oxoisoindoline versus dioxoisoindoline), the presence of which in pomalidomide favorably impacts the efficiency and potency of Aiolos degradation (Figure 5). However, in the context of lead **13**, we found that the dioxoisoindoline core led to the opposite activity profile (Table 3).

Comparison of **13** to **45** reveals that while GSPT1 selectivity was retained, there was a 24-fold loss in Aiolos degradation potency in combination with reduced degradation efficiency by 17%. The loss in degradation efficiency apparently drove the nearly 100-fold loss in H929 R10-1 antiproliferative potency. The trend was similar for related analogs **46** and **47** in which introduction of the second carbonyl into the scaffold had a detrimental effect on activity.

Table 3. Effect of dioxoisoindoline scaffold in terms of antiproliferative activity in the lenalidomide-resistant cell line H929 R10-1, CRBN binding, and the degradation of Aiolos and GSPT1. [a,b,c]

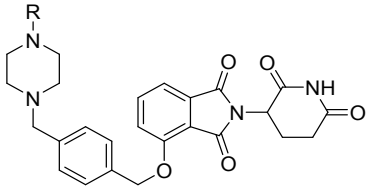

Compd	R	H929 R10-1 IC_{50} (nM)	Aiolos EC_{50} (nM)	Aiolos Y_{min}	GSPT1 EC_{50} (nM)	CRBN Binding IC_{50} (nM)
45	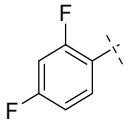	159	2.4	23	>10,000	502
46	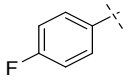	146	2.1	18	>10,000	322

47	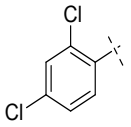	170	3.3	30	>10,000	877

[a]All values are the mean of at least three separate assay determinations, [b]SEM for data available in supplemental material, [c]Y_{min} is the % protein remaining following treatment with compound concentrations up to 10 μM, and measured after 4 h (see methods).

Again, in reference to the structural features of pomalidomide and lenalidomide (Figure 1), both drugs contain an NH_2 functional group at the 4-position of the isoindoline scaffold. To assess the effect exerted by either nitrogen or oxygen as a tether point to the isoindoline core, we synthesized **50** (Table 4) as a direct comparator to **13**. The difference between **13** and **50** asserts the view that the action of binding to CRBN does not directly translate to degradation potency, but rather, is just one of the necessary steps toward formation of the ternary complex requisite for ubiquitination of substrate. In this case, the CRBN binding IC_{50} of the *N*-linked compound **50** was only 2-fold lower than that of **13**, yet the Aiolos degradation potency was reduced by 15-fold and level of protein remaining increased from 6% to 15%, ultimately leading to a 15-fold loss in antiproliferative potency.

Table 4. Effect of oxygen versus nitrogen-linked oxoisoindoline scaffolds. [a,b,c]

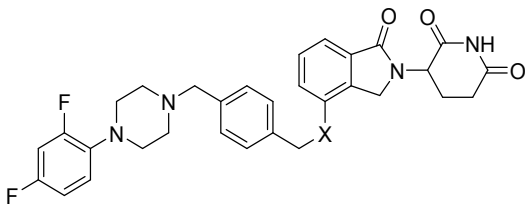

Compd	R	H929 R10-1 IC_{50} (nM)	Aiolos EC_{50} (nM)	Aiolos Y_{min}	GSPT1 EC_{50} (nM)	GSPT1 Y_{min}	CRBN Binding IC_{50} (nM)
13	O	1.7	0.1	6	>10,000	93	502
50	N	26.3	1.5	15	>10,000	90	194

[a]All values are the mean of at least three separate assay determinations, [b]SEM for data available in supplemental material, [c]Y_{min} is the % protein remaining following treatment with compound concentrations up to 10 μM, and measured after 4 h (see methods).

Pomalidomide, lenalidomide, and thalidomide (Figure 1), contain a chiral center at the tertiary glutarimide carbon and this chiral center is known to be unstable and can undergo racemization.[15,16] In the case of thalidomide, crystallographic and binding data supports that the S-enantiomer has stronger binding to CRBN.[17] To identify if a single enantiomer could be largely responsible for the activity, both enantiomers of **13** were independently evaluated (Table 5). In the proliferation assay, we found there was no appreciable difference in activity when comparison was drawn between the two enantiomers (**60** and **61**), or a single enantiomer and the racemate. Additionally, we found that while either enantiomer could degrade equivalent total levels of Aiolos (Y_{min}), the *S*-enantiomer **60** did

have a 5-fold lower Aiolos EC_{50} value than *R*-enantiomer **61**. The largest difference between enantiomers was observed in connection to CRBN binding, where the *S*-enantiomer **60** was clearly more potent (~30-fold) compared to the *R*-enantiomer **61**.

Table 5. Activity table examining the effect of chirality on antiproliferative activity in the lenalidomide-resistant cell line H929 R10-1, CRBN binding affinity, and degradation of Aiolos. [a,b,c]

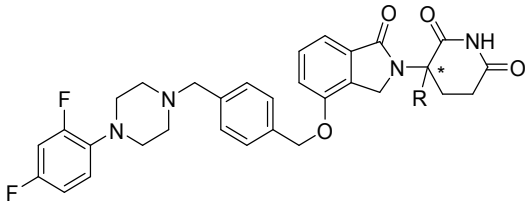

Compd	*	R	H929 R10-1 IC_{50} (nM)	Aiolos EC_{50} (nM)	Aiolos Y_{min}	CRBN Binding IC_{50} (nM)
13	1:1	H	1.7	0.1	6	502
61	(*R*)	H	4.3	0.5	7	1158
60	(*S*)	H	3.8	0.1	5	37
59	(*R*)	Me	> 5,000	> 100	94	9,618
58	(*S*)	Me	496	>10	93	>10,000

[a]All values are the mean of at least three separate assay determinations, [b]SEM for data available in supplemental material, [c]Y_{min} is the % protein remaining following treatment with compound concentrations up to 10 μM, measured after 4 h (see methods).

One possible explanation for the apparent discrepancy between binding affinity and antiproliferative activity of the two enantiomers could be found in the rate of racemization. Figure 6 depicts a measurement of racemization when the *S*-enantiomer **60** was placed in cell media and its concentration measured over time. Increasing concentration of *R*-enantiomer **61** is observed over time corresponding to loss of the *S*-enantiomer, with complete racemization within ~24 h. In the case of the cellular antiproliferation assay, the assay time (120 h) exceeds the time to racemization (~24 h), thus precluding the measurement of single enantiomer activity. On the other hand, the CRBN binding assay (4 h) does not exceed the time to racemization and could potentially discriminate activity between the enantiomers.

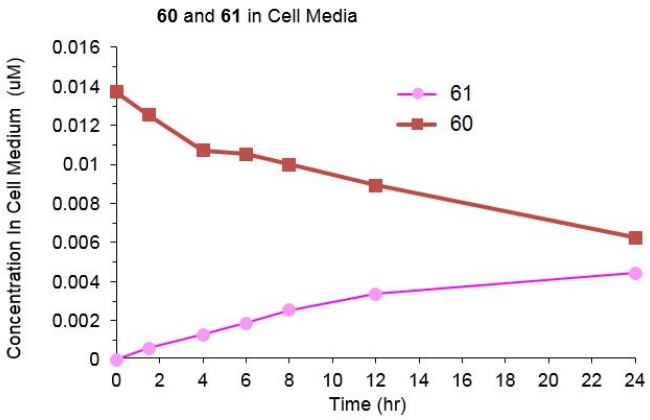

Figure 6. Chiral monitoring over 24 h where the disappearance of the S-enantiomer corresponds with the appearance of the R-enantiomer. This study used the same cell media as the one used for the H929 R10-1 antiproliferative assay.

Additional investigations were made to elucidate the effect of the chiral center on activity. To this end, we placed a methyl group at the glutarimide chiral center (**58** and **59**, Table 5) which would lock defined chirality and remove the potential of racemization over time. Both enantiomers however, suffered a loss in activity both in terms of degradation as well as CRBN binding, showing that substitution at the chiral center was not tolerated.

Having completed an overview of the main SAR about analog **13**, which included exploration of a glutarimide substitution, the core scaffold, linker, and a minimum pharmacophore definition at the piperazine terminus, it was important to identify potential liabilities that might prevent further development of this series. Several preclinical assays were used to evaluate **13**, starting with the *in vitro* safety profile.

Analog **13** was screened against a panel of 80 receptors to assess potential off-target activity. At a concentration of 10 μM, compound **13** demonstrated inhibition equal to or greater than 50% for 26 targets. The % inhibition of the α_1 adrenergic receptor was 101.5% and 99.1% for the dopamine D_{2S} receptor (Table 6). Upon further assessment in

follow-up functional assays, **13** displayed potent activity against multiple targets. For example, the compound had a functional IC_{50} = 14 nM in the α_1 adrenergic receptor assay and a strong agonist activity in the dopamine D_{2S} receptor assay with an EC_{50} = 16 nM (Table 9). The observed in vitro dopamine D_{2S} activity was relevant in vivo.[18] Rodents dosed daily for 7 days with **13**, showed a gut motility suppression in alignment with the observed in vitro activity (data not shown).

To address the off-target activity of **13** a more detailed SAR investigation was carried out at near the piperazine terminus (Table 6). Since isopropyl substituted piperazine **22** was a truncation that maintained activity in the Len-resistant model, we compared **22** to piperidine analog **23**. Compound **23** demonstrated an increased (~25-fold) antiproliferative potency as well as an increased depth of Aiolos degradation (Table 6). Further reduction in terminal group size (**24-27**) decreased antiproliferative potency as well as the depth of Aiolos degradation compared to **23**. Since **23** demonstrated an excellent activity profile, further assessment of off-target binding revealed significant improvement compared to **13**. Using reduction of molecular weight as a general strategy for this series to reduce the number of off-target hits, compounds **24, 25**, and **27**

mentioned above also showed a reduction in the number of off-target activities compared to **13**. However, compounds in this series were not further developed due poor ADME attributes including fast in-vivo clearance and poor bioavailability.

Table 6. Activity table of truncated compounds. [a,b,c,d]

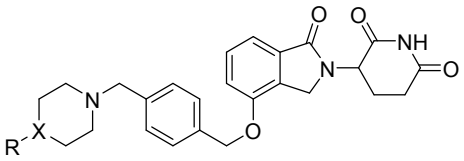

Compd	X	R	H929 R10-1 IC_{50} (nM)	Aiolos EC_{50} (nM)	Aiolos Y_{min}	α_1	D_{2S}
13	CH	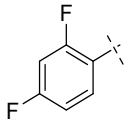	1.7	0.1	6	101.5	99.1
22	N	*i*-Propyl	35.1	0.3	13	ND	ND
23	CH	*i*-Propyl	1.4	0.1	7	63.0	94.0
24	CH	CF_3	8.3	0.6	10	41.5	95.4
25	C	Me, Me	9.9	0.3	11	21.5	66.0
26	C	F, F	20.5	0.5	12	ND	ND
27	CH	Methyl	35.1	1.0	18	40.4	78.4

[a]Antiproliferative and Aiolos degradation values are the mean of at least three separate assay determinations, [b]SEM for data available in supplemental material, [c]Y_{min} is the % protein remaining same comments 10 μM, after treatment for 4 h (see methods). [d]α_1 & D_{2S} reported as % inhibition @ 10 μM, ND, not determined.

To test the hypothesis that the poor off-target receptor profile of **13** was in part due to a combination of higher molecular weight and lipophilicity or the presence of an embedded basic site, a series of non-basic analogs was explored. The direct non-basic comparator to **13**, compound **68**, maintained equivalent antiproliferative activity, and Aiolos degradation depth and potency (Table 7). This activity profile was shared by compounds in the series (**69-71**), while removal of basicity in piperazinone analog **28** did result in a loss of Aiolos degradation efficiency. The lowering of lipophilicity (cLogP = 3.6 (**13**) vs 2.8 (**68**)) in combination with removal of the most basic site which was associated with reduction in the number of off-target receptor hits (26 vs 4, respectively). Where lipophilicity was comparable (**71**), the effect of basic site removal was also significant indicating that the piperazine could be in part responsible for the poor off-target receptor binding profile. Unfortunately, further development of this series was hampered by poor permeability and low solubility (<7 ug/mL).

Table 7. Effect of basic site removal at the piperazine. [a,b,c,d]

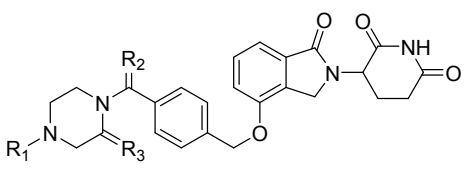

Compd	R_1	R_2	R_3	H929 R10-1 IC_{50} (nM)	Aiolos EC_{50} (nM)	Aiolos Y_{min}	cLogP	α_1	D_{2S}
68	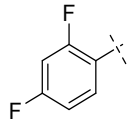	O	H,H	4.9	0.1	7	2.8	70.3	0.4
69	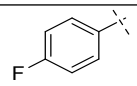	O	H,H	3.7	0.3	8	2.8	ND	ND
70	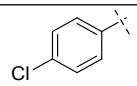	O	H,H	6.2	0.1	7	3.1	33.7	7.9
71	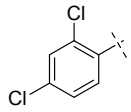	O	H,H	3.3	0.1	7	3.5	74.1	5.6
28	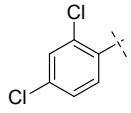	H,H	O	6.7	0.6	11	3.9	ND	ND

[a]Antiproliferative and Aiolos degradation values are the mean of at least three separate assay determinations, [b]SEM for data available in supplemental material, [c]Y_{min} is the % protein remaining same comments 10 μM, after treatment for 4 h (see methods). [d]α_1 & D_{2S} reported as % inhibition @ 10 μM, ND, not determined.

Since it was advantageous from physiochemical property and ADME point of view to maintain the piperazine moiety, we explored the introduction of polarity via heterocycles at the terminal aryl (Table 8). The 4-fluoro pyridyl analog **29** is a direct comparator to **14**. While activity was maintained in both the antiproliferative and degradation assays, the addition of the pyridyl group (**29** or **30)** had little impact toward the improvement of the off-target profile as evident from the strong inhibition of α_1 and D_{2S}. Nevertheless,

encouraged by the activity profile of the pyridyl analog, we examined a series of substituted pyridyl groups with varying polarity. The Aiolos degradation profile was maintained with both the picolinamide as well as aryl nitrile, but there was an interesting subtlety between the effect of these functional groups on the off-target binding profile. While the picolinamide functionality in compound **31** imparted a reduction in α_1 and D_{2S} binding potency, the ortho-aryl nitrile group in **32** effected minimal impact toward off-target binding potency in α_1 and D_{2S} and this analog hit 25/80 receptors in the panel with a potency greater than 50% at 10 μM. Since the nitrile function in **32** did not reduce off-target binding, we were surprised to find that moving the nitrile group to the 4-position both maintained the desired activity profile as well as increased the selectivity against off-target binding. Encouraged by this result, **33** was tested in follow-up assays and determined to have low off-target functional activity compared to **13** (Table 9), and absent of effects on gut motility in rat (data not shown).

Table 8. Effect of polarity and heterocycles on terminal ring.[a,b,c,d]

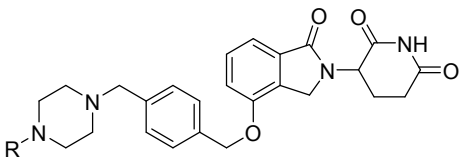

Compd	R	H929 R10-1 IC_{50} (nM)	Aiolos EC_{50} (nM)	Aiolos Y_{min}	cLogP	α_1	D_{2S}
13	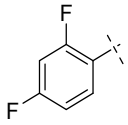	1.7	0.1	6	3.6	101.5	99.1
14	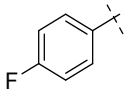	2.8	0.1	5	3.5	100.3	94.7
29	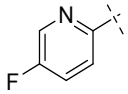	7.4	0.7	11	2.8	97.7	90.8
30		4.6	0.4	8	2.6	99.0	98.0
31	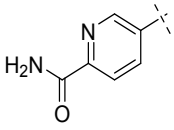	3.5	0.4	9	1.8	25.2	32.9
32	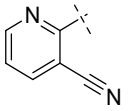	56	1.0	12	2.4	92.1	100
33	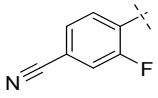	1.7	0.1	6	3.3	67	54.5

[a]Antiproliferative and Aiolos degradation values are the mean of at least three separate assay determinations, [b]SEM for data available in supplemental material, [c]Y_{min} is the % protein remaining same comments 10 μM, after treatment for 4 h (see methods). [d]α_1 & D_{2S} reported as % inhibition @ 10 μM, ND, not determined.

Table 9. Comparison of functional activity between **13** and **33** for the D_{2S} dopamine agonist and α_1 adrenergic receptor.

	13	**33**
Receptor panel, Functional Activity:	α_1 IC_{50}= 14 nM D_{2S} EC_{50} = 16 nM	α_1 IC_{50} = 980 nM D_{2S} EC_{50} > 10,000nM

Having identified a compound with the desired combination of potent MM activity profile and off-target selectivity, we next established which enantiomer of **33** to further characterize. To understand the rate of epimerization that occurred at the chiral center in the pair of enantiomers **4** (*S*-enantiomer) and **76** (*R*-enantiomer), we measured the extent of their respective conversion over time. Racemization was examined in both aqueous buffer (pH 7.4) as well as in cell media. In either context, both compounds underwent full racemization over time. The racemization measurements for both the *R*-enantiomer and *S*-enantiomer in cell media are shown in Figure 7. Since racemization is complete at times sooner than the cellular readout (120 h), the proliferation assay could not be used to discriminate activity.

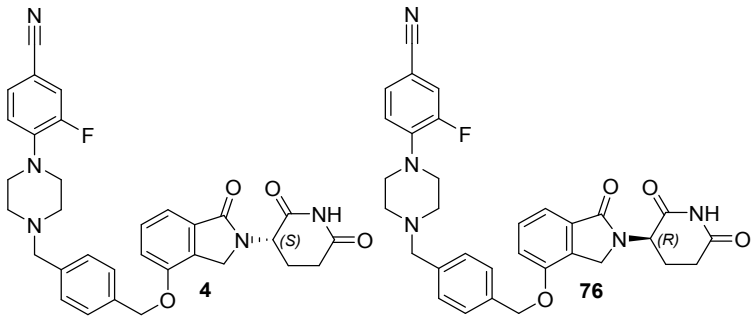

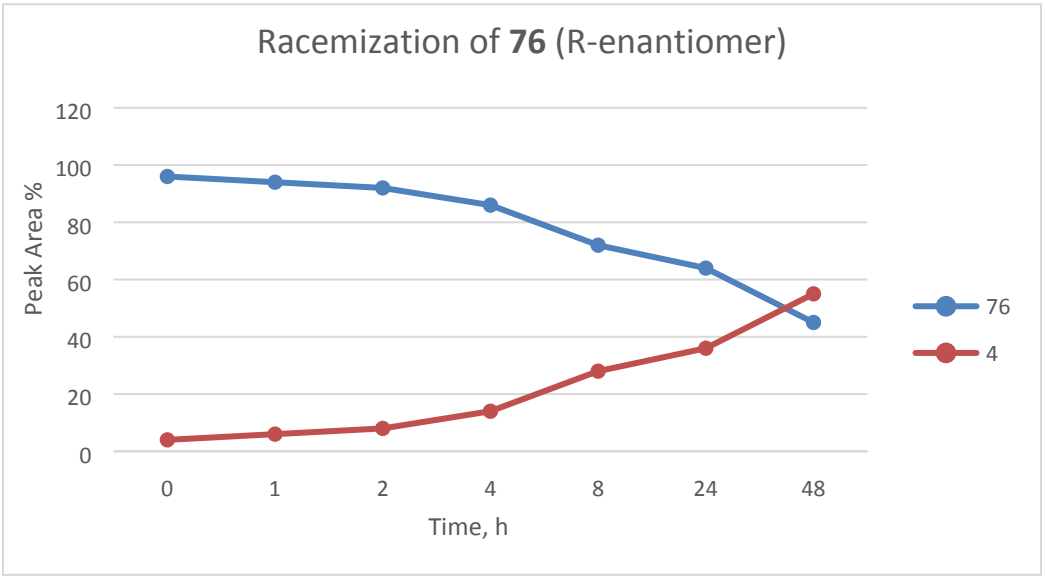

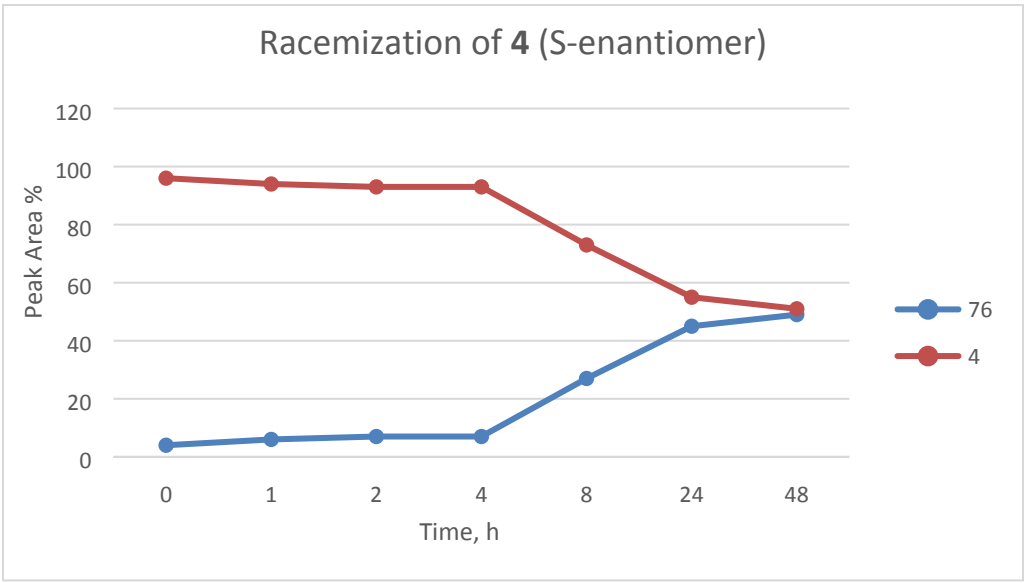

Figure 7. Measurement of racemization at the glutarimide chiral center in cell media. (a) Starting with the *R*-enantiomer, measurement of peak area over time which showed the loss of *R*-enantiomer and appearance of *S*-enantiomer. (b) Peak area measurement over time starting with the *S*-enantiomer.

The CRBN binding assay could be used to discriminate between enantiomers, since the time course (4 h) is shorter than the racemization time for each enantiomer. Measurement of the ability of each enantiomer to bind to CRBN was made at 4 h and showed a large difference in binding affinity in which the *S*-enantiomer was the more potent binder to CRBN (Figure 8).

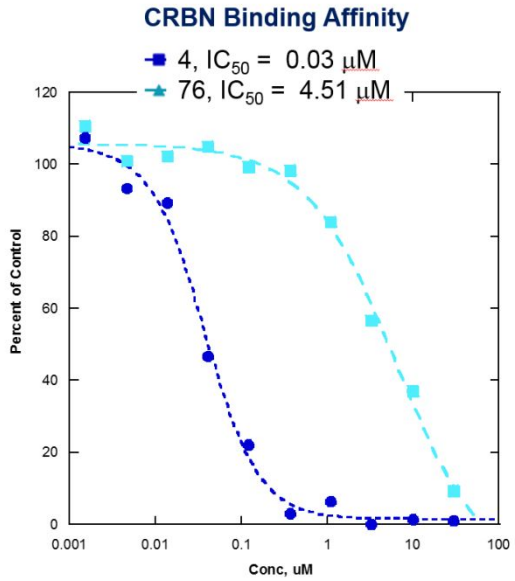

Figure 8. The CRBN binding affinity of the *R*-enantiomer (**76**) and *S*-enantiomer (**4**) measured at 4 h.

Since degradation for Aiolos could also be examined at time points prior to complete racemization, the activity dependence on each enantiomer was estimated in this format. Evaluations were made as early as 45 min and included 1.5 and 3 h (Figure 9). The *S*-

enantiomer (**4**) was determined to be a more potent degrader, while also achieving maximal levels of Aiolos destruction at lower concentrations than the *R*-enantiomer for all time points. Since low level racemization occurred at the timepoints measured, it is difficult to assign absolute activity to either enantiomer. However, taken together, the Aiolos degradation and CRBN binding data supported the *S*-enantiomer as being more active.

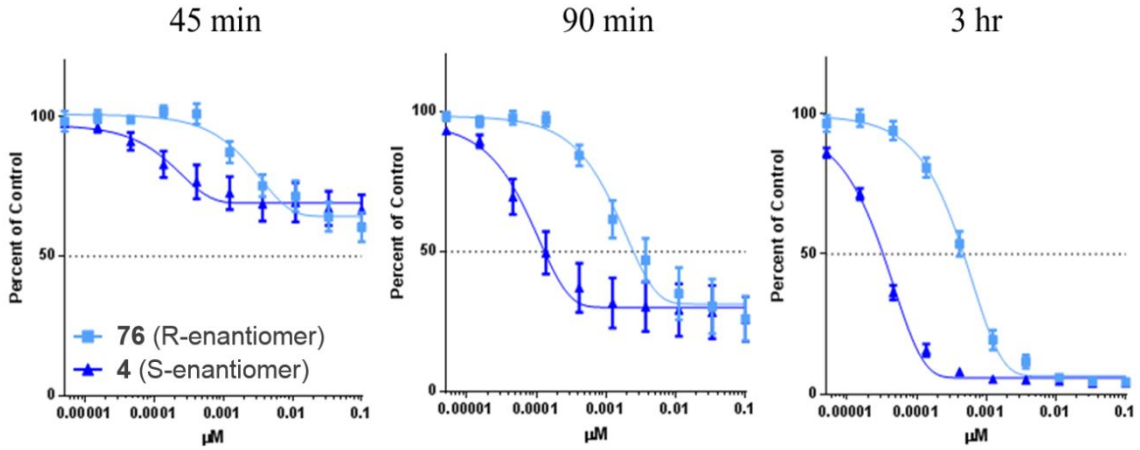

Figure 9. Measurement of Aiolos destruction by either enantiomer at 3 time points.

We hypothesized that the high activity displayed by compound **4** in the lenalidomide-resistant cell line was connected to the rapid kinetics and depth of Aiolos degradation. Thus, the governing activity determinant, particularly in situations of low CRBN cellular concentration, would be two-fold: the potency of degradation, and importantly the

degradation efficiency. When compared to the FDA approved drugs lenalidomide and pomalidomide, **4** is able to degrade Aiolos more extensively, much faster, and at a lower concentration (Figure 10).

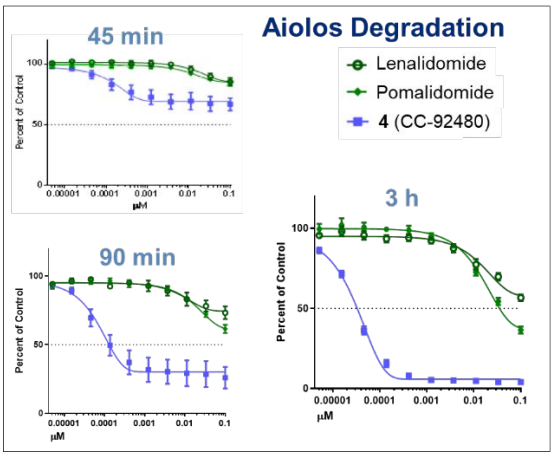

Figure 10. Comparison of the Aiolos degradation curves at early time points for **4** (CC-92480) overlaid with lenalidomide and pomalidomide. ePL degradation assay in DF15 cells.

The more efficient degradation profile of **4** correlated to superior induction of apoptosis in myeloma cells (Figure 11b), and in the lenalidomide-resistant cells treated at concentrations between 1 and 100 nM, nearly complete degradation of Ikaros and Aiolos could be detected in 4 h (Figure 11a). In the same treatment arm, but at 72 h, western blot analysis showed that treatment with **4** stabilized p27 and induced markers of apoptosis (*e.g.* cleaved caspase). Comparatively, pomalidomide showed little to no effect

at similar concentrations and times. The measure of Caspase-3 induction was quantified by live cell imaging and comparison could be drawn between **4**, lenalidomide, and pomalidomide at concentrations from 1 nM to 1 μM over 150 h (Figure 11b). The induction of apoptosis seen for **4** was significant compared to lenalidomide or pomalidomide. For example, at the lowest concentration of **4** tested (1 nM), the level of apoptosis was higher than that observed at the highest concentration tested (1 μM) for either lenalidomide or pomalidomide.

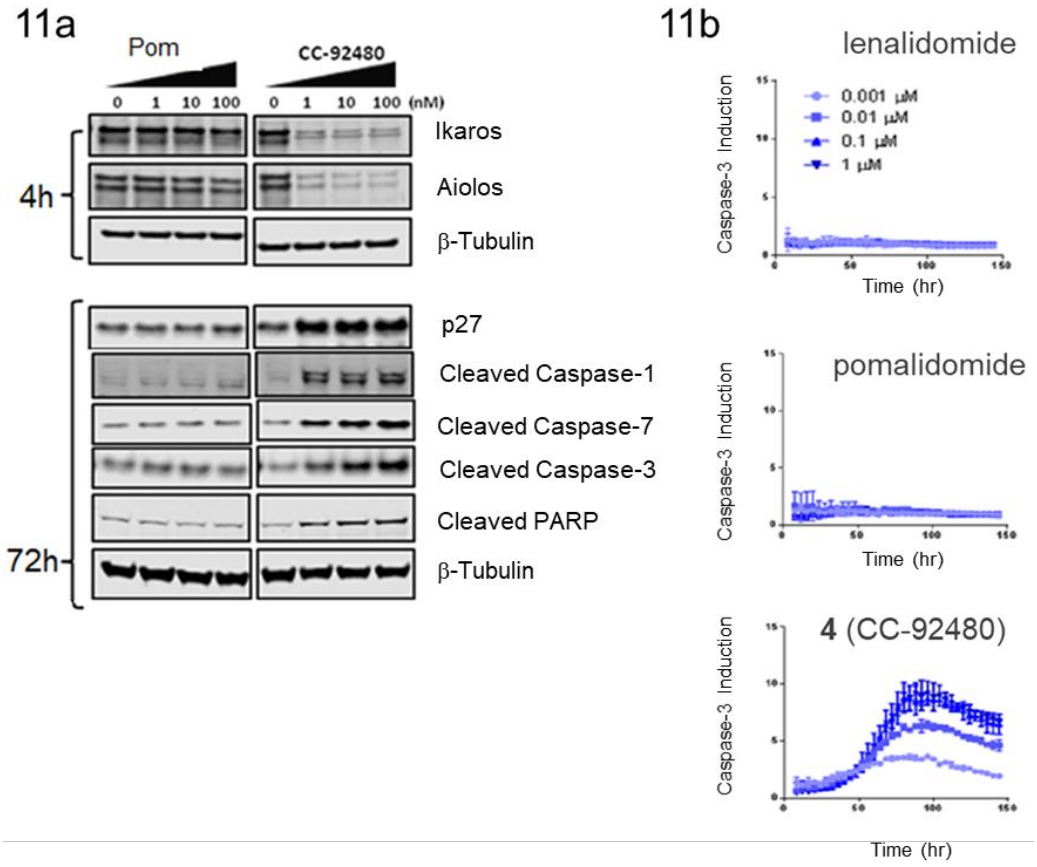

Figure 11. a) Western blot analysis in H929 R10-1 cells showing the fast and deep degradation of Aiolos/Ikaros leads to superior induction of apoptosis. **b)** Comparison of apoptosis measured by caspase-3 induction in lenalidomide-refractory cells (H929 R10-1).

Next, we examined the pharmacokinetic properties of **4** in rat and monkey to support preclinical toxicology studies. The *in vitro* metabolic stability measured by compound incubation in S9 liver fractions for both human and rat was deemed acceptable, and when **4** was dosed in Sprague-Dawley rats as a 2 mg/kg solution intravenously, the observed in vivo clearance was found to be consistent with the predicted clearance from in vitro studies. When dosed orally as a suspension, **4** achieved a C_{max} of 3.2 μM with an oral bioavailability of 38%. In the rat oral PK study, the percentage of racemization was measured and surprisingly determined to be less than 4% when compared to parent AUC or C_{max} levels. A similar finding was observed in monkey; the appearance of the *R*-enantiomer was less than 9% by either C_{max} or AUC comparison to parent (Table 11).

Table 11. Rat and Monkey ADME parameters for **4**.

Assay Parameter	**4**	**76** (*R*-enantiomer)
CaCo-2; A-B / efflux ratio	20 / 1	

Solubility μg/mL at pH 5.0	90	
Rat / Human S9 met. stability[a]	100 / 99	
Rat PK parameter		
iv CL (mL min^{-1} kg^{-1})[b]	6.8 ± 1.0	
po C_{max} (μM)[c]	3.2 ± 0.5	0.06 ± 0.002
po T_{max} (h)	0.8 ± 0.3	
po $AUC_{(0\text{-inf})}$ (μM·hr)	16.4 ± 6.8	0.5 ± 0.3
po F (%)	38% ± 17	
Amount of R-enantiomer formed in vivo (rat)		< 4% by AUC or C_{max}
Monkey PK parameter		
po C_{max} (μM)[d]	0.22 ± 0.08	0.016 ± 0.006
po $AUC_{(0\text{-inf})}$ (μM·hr)	1.1 ± 0.3	0.1 ± 0.04
Amount of R-enantiomer formed in vivo (monkey)		< 9% by AUC or C_{max}

[a] % remaining at 60 min. [b] Dosed 2 mg / kg in 15%DMA/50%PEG/35%D5W. [c] Dosed 10 mg/kg as a suspension in 0.5% CMC / 0.25% Tween-80 / water. [d] Dosed 3.0 mg/kg in 2%NMP / 20% Labrasol / 78% 50mM citrate buffer at pH=3.0.

Compound **4** was evaluated in efficacy models to assess tumor growth inhibition in tumor bearing mice. One model examined used the lenalidomide-resistant cell line H929 R10-1, where tumor-bearing mice were dosed orally for 21 days. Tumor volumes were determined prior to starting treatment and were considered the starting volumes. When tumors reached approximately 150 mm^3, mice were randomized and treated once daily (*q.d.*) orally with vehicle control or various dosage strengths of **4**. After treatment for 21

days, the tumor volumes were measured following the final day of dosing (Figure 12). Both the 3 and 10 mg/kg doses gave near maximal response in this model, while the lowest dose tested (1 mg/kg) showed 75% reduction in tumor volume by the end of the study.

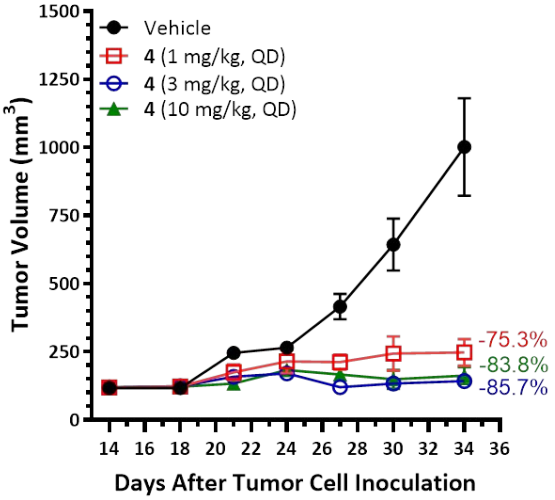

Figure 12. 21-day xenograft study of **4** dosed daily using the lenalidomide-resistant cell line H929 R10-1.

CONCLUSION

The ability to influence protein homeostasis and its association with disease state through targeted protein degradation has exciting implications for drug discovery. In contrast to heterobifunctional protein degraders[19,20,21] that require multiple elements

(target ligand, linker, ligase binder) to employ the CRBN E3 ligase system, CELMoDs are relatively small molecular scaffolds that create an interaction hotspot on the surface of CRBN that promotes direct ligase-target protein interactions.[22] The CELMoDs represent the first clinical examples of intentionally designed, targeted protein degraders.

Guided by the measurement of protein degradation as well as the antiproliferative activity in lenalidomide-resistant cell lines, we discovered a novel series of aryl-piperazine containing compounds with good in vitro selectivity that preferentially kill tumor versus non-tumor cells. Within the aryl piperidine series, we identified candidates with low off-target receptor binding profiles which we hypothesized would also lead to higher safety margins *in vivo*. The phenotypic activity of the series was correlated to Aiolos degradation, and in parallel, by optimizing for rapid and efficient protein degradation, we identified a profile that led to strong induction of apoptosis in a low CRBN context (H929 R10-1 cells). Unlike previously identified compounds, such as lenalidomide and pomalidomide, which require higher concentrations and longer times to degrade protein substrates, CC-92480 (**4**) has a unique and rapid degradation profile: the enhanced efficiency to drive the formation of the protein–protein interaction between Aiolos and cereblon, inducing

targeted docking to the CRL4-CRBN E3 ubiquitin ligase complex. The CC-92480-dependent binding of Aiolos/Ikaros to CRBN leads to polyubiquitination and ultimately proteasome-mediated degradation of protein. Rapid and extensive loss of Aiolos/Ikaros in sensitive cells, such as multiple myeloma cells, results in apoptosis and subsequent cell death.

During the SAR explorations described above, we observed variable levels of activity and *in vitro* selectivity in response to minor structural changes. The subtleties of substitution pattern SAR offer the opportunities to discover compounds across a varied spectrum of degradation, potency, and selectivity, the molecular profiles of which when adjusted properly, have the potential to transform serious diseases and create new landmark therapies.

EXPERIMENTAL SECTION

General. Compounds were named using ChemDraw Ultra. All materials were obtained from commercial sources and used without further purification, unless otherwise noted. Chromatography solvents were HPLC grade and used as purchased. All air-

sensitive reactions were carried out under a positive pressure of an inert nitrogen atmosphere. Chemical shifts (δ) are reported in ppm downfield of TMS and coupling constants (*J*) are given in Hz. Thin Layer Chromatography (TLC) analysis was performed on Whatman thin layer plates. The purity of final tested compounds was ≥ 95% as determined by HPLC using the following method: gradient (5-95% ACN + 0.075% formic acid in water + 0.1% formic acid over 8 min, followed by 95% ACN + 0.075% formic acid for 2 min); flow rate 1 mL/min, column Phenomenex Luna 5μ PFP(2) 100A (150 mm x 4.60 mm). Elemental analysis was performed at Robertson Microlit Laboratories, Ledgewood, New Jersey.

Synthesis.

2-(*tert*-Butoxycarbonylamino) -5-methoxy-5-oxo-pentanoic acid (6). *Step A.* To a suspension of 2-aminopentanedioic acid (**5**) (250 g, 1.70 mol) in dry methanol (2.5 L) under N_2 was added TMSCl (277 g, 2.55 mol) over 30 min. The resulting clear solution was stirred at RT for 30 min. The reaction mixture was carried forward to the next step without further work-up. ^{1}H NMR (400 MHz, CD_3OD) δ 4.17 – 4.15 (m, 1H), 3.71 (s, 3H), 2.70 – 2.60 (m, 2H), 2.33 – 2.25 (m, 2H).

Step B. To the solution from the previous step were added TEA (275 g, 2.72 mol) and Boc_2O (447.35 g, 2.05 mol). The reaction mixture was stirred at 25 °C for 2 h. The solution was concentrated to dryness, then H_2O (2.5 L) was added to dissolve the residue. The resulting aqueous phase was washed with EtOAc (200 mL), then acidified to pH = 3 by HCl (1 N) and extracted with EtOAc (3 x 1 L). The combined organic layers were washed with brine (800 mL), dried over Na_2SO_4, filtered, and concentrated to give **6** (250 g, 957 mmol, 56% yield over 2 steps) as a white solid. ^{1}H NMR (400 MHz, CD_3OD) δ 4.18 – 4.11 (m, 1H), 3.69 (s, 3H), 2.48 – 2.43 (m, 2H), 2.21 – 2.15 (m, 1H), 1.95 – 1.91 (m, 1H), 1.46 (s, 9H).

Methyl 5-amino-4-(tert-butoxycarbonyl amino)-5-oxo-pentanoate (7). To a solution of **6** (200 g, 765 mmol) in dioxane (1.5 L) were added Boc_2O (267 g, 1.22 mol) and pyridine (121 g, 1.53 mol). After the reaction mixture was stirred at 25 °C for 30 min, NH_4HCO_3 (182 g, 2.30 mol) was added to the mixture and stirred for additional 16 h at 25 °C. The organic solvent was removed under reduced pressure. The residue was acidified by HCl (6 M) to pH = 3 and then extracted with EtOAc (3 x 800 mL). The combined organic layer

was washed with brine (800 mL), dried over Na_2SO_4, filtered, and concentrated to give **7** (180 g, 692 mmol, 90% yield) as a white solid. ^{1}H NMR (400 MHz, $CDCl_3$) δ 6.51 (s, 1H), 5.94 (s, 1H), 5.43 (s, 1H), 4.21 (s, 1H), 3.63 (s, 3H), 2.59 – 2.40 (m, 2H), 2.15 – 2.11 (m, 1H), 1.94 – 1.90 (m, 1H), 1.42 (s, 9H).

Methyl 4,5-diamino-5-oxo-pentanoate hydrochloride (8). A mixture of **7** (180 g, 692 mmol) and HCl/EtOAc (300 mL, 4 M) was stirred at 25 °C for 12 h. The precipitated solid was collected by vacuum filtration and washed with EtOAc (500 mL) to give **8** (130 g, 661 mmol, 95% yield) as a white solid. ^{1}H NMR (400 MHz, CD_3OD) δ 4.00 – 3.96 (m, 1H), 3.70 (s, 3H), 2.59 – 2.52 (m, 2H), 2.22 – 2.13 (m, 2H).

Methyl 2-(bromomethyl)-3-[tert-butyl(dimethyl)silyl]oxy-benzoate (10). *Step A.* H_2SO_4 (129.07 g, 1.32 mol) was added dropwise to a mixture of 3-hydroxy-2-methyl-benzoic acid (**9**) (500 g, 3.29 mol) in MeOH (5.00 L) over 30 min. The reaction mixture was stirred at 65 °C for 17 h. The solvent was removed under reduced pressure. To the remaining residue was added water (15 L) slowly at room temperature. A brown solid was formed and the suspension was stirred in an ice bath for 30 min. The solid was collected by

vacuum filtration, washed with water (5 L), and dried to give methyl 3-hydroxy-2-methyl-benzoate (484.5 g, 2.92 mol, 88.7% yield) as a light brown solid. ^{1}H NMR (400 MHz CD_3OD) δ 7.25 (d, J = 8.0 Hz, 1H), 7.05 (t, J = 8.0 Hz, 1H), 6.92 (d, J = 8.0 Hz, 1H), 3.85 (s, 3H), 2.35 (s, 3H).

Step B. To a 10 L three-neck flask equipped with mechanical stir bar and thermometer, were added DCM (5 L), methyl 3-hydroxy-2-methyl-benzoate (475.00 g, 2.86 mol) and imidazole (389.42 g, 5.72 mol, 385.56 mL). Chloro-dimethyl-(1-methyl-1-methyl-ethyl)silane (470.99 g, 3.15 mol) was added to the above solution in portions. After the addition, the mixture was stirred at 25 °C for 1 h. The reaction mixture was quenched with saturated $NaHCO_3$ (400 mL), extracted with DCM (2.5 L), and washed with cold water (2.5 L) and brine (2.5 L). The combined organic layer was dried over Na_2SO_4 and filtered. The filtrate was concentrated and the remaining residue was purified by silica gel column chromatography to give methyl 3-[tert-butyl(dimethyl)silyl]-oxy-2-methyl-benzoate (605.0 g, 2.16 mol, 75.4% yield) as a brown oil. ^{1}H NMR (400 MHz, $CDCl_3$) δ 7.44 (d, J = 7.50

Hz, 1H), 7.10 (t, *J* = 7.94 Hz, 1H), 6.94 (d, *J* = 7.94 Hz, 1H), 3.89 (s, 3H), 2.43 (s, 3H), 1.04 (s, 9H), 0.23 (s, 6H).

Step C. To a solution of methyl 3-[tert-butyl(dimethyl)silyl]oxy-2-methyl-benzoate (342.00 g, 1.22 mol) in EtOAc (3.40 L) was added AIBN (6.01 g, 36.60 mmol) and NBS (249.61 g, 1.40 mol) at 20 ºC to give a suspension. The suspension was stirred and refluxed at 65 °C for 2 h under a tungsten lamp. The reaction was cooled to RT, washed with aqueous Na_2SO_3 (3 L), brine (3 x 1500 mL), dried over Na_2SO_4, filtered, and concentrated to give **10** (431.2 g, 1.20 mol, 98.5% yield) as a brown oil. ^{1}H NMR (400 MHz, $CDCl_3$) δ 7.52 (d, *J* = 7.94 Hz, 1H), 7.21 – 7.27 (m, 1H), 6.99 (d, *J* = 7.94 Hz, 1H), 5.03 (s, 2H), 3.94 (s, 3H), 1.07 (s, 9H), 0.31 (s, 6H).

Methyl 5-amino-4-[4-[hydroxy-1-oxo-isoindolin-2-yl]-5-oxo-pentanoate (11). *Step A.* To a stirred solution of **8** (74.5 g, 379 mmol) in ACN (2.50 L) was added **10** (125 g, 348 mmol). To the suspension was added DIEA (89.9 g, 696 mmol) through an addition funnel over 10 min and then the mixture was stirred at 60 °C for 16 h. The reaction mixture was diluted with EtOAc (1 L), and washed with HCl (1N, 1 L), aqueous NaHCO3 (saturated, 1 L) and

brine (1 L). The organic layer was concentrated to give crude methyl 5-amino-4-[4-[tert-butyl(dimethyl)silyl]oxy-1-oxo- isoindolin-2-yl]-5-oxo-pentanoate (108 g, 266 mmol, 76% yield) as a light yellow solid. MS (ESI) *m/z* 407.3 $[M+1]^+$.

Step B. To a stirred cold solution of methyl 5-amino-4-[4-[tert-butyl(dimethyl)silyl]oxy-1-oxo-isoindolin-2-yl]-5-oxo-pentanoate (108 g, 266 mmol) in DMF (350 mL) was added K_2CO_3 (14.7 g, 106 mmol) in H_2O (40 mL) by portions over 5 min. The resulting reaction mixture was stirred at 15 °C for 15 h. The reaction mixture was cooled to 0 °C and HCl (12 M, 15 mL) was slowly added. Acetonitrile (200 mL) was added to the mixture and a precipitate solid formed. The suspension was stirred at RT for 10 min and filtered. The filter cake was washed with EtOAc (200 mL x 5) to give desired product (55 g). The filtrate was concentrated under reduced pressure to give a crude product (100 g) which was dissolved in DCM (1 L) and left to stand at 15 °C for 16 h. A white solid was formed which was collected by filtration to give an additional 5 g of desired product. A total 60 g of **11** (60 g, 205 mmol, 77% yield) was obtained as a white solid. ^{1}H NMR (400 MHz, DMSO-d_6) δ 7.58 (s, 1H), 7.31 (t, J = 8.0 Hz, 1H), 7.19 – 7.14 (m, 2H), 7.01 (d, J = 7.6 Hz, 1H),

4.75 – 4.71 (m, 1H), 4.50 (d, *J* = 17.6 Hz, 1H), 4.32 (d, *J* = 17.6 Hz, 1H), 3.51 (s, 3H), 2.29 – 2.18 (m, 3H), 2.09 – 1.99 (m, 1H).

Methyl-5-amino-4-[4-[[4-(bromomethyl)phenyl]methoxy]-1-oxo-isoindolin-2-yl]-5-oxo-pentanoate (12a). A mixture of 1,4-bis(bromomethyl)benzene (67.7 g, 257 mmol), K_2CO_3 (11.8 g, 85.5 mmol) and methyl 5-amino-4-(4-hydroxy-1-oxo- isoindolin-2-yl)-5-oxo-pentanoate (25 g, 85.5 mmol) in ACN (1 L) were stirred at 60 °C for 16 h. The reaction mixture was cooled to RT and filtered. The filtrate was concentrated and purified by silica gel column chromatography to afford **12a** (25.5 g, 54 mmol, 63% yield) as a white solid. ^{1}H NMR (400 MHz DMSO-d_6) δ 7.59 (s, 1H), 7.50 – 7.44 (m, 5H), 7.32 – 7.28 (m, 2H), 7.19 (s, 1H), 5.26 (s, 2H), 4.79 – 4.71 (m, 3H), 4.55 (d, *J* = 17.6 Hz, 1H), 4.43 (d, *J* = 17.6 Hz, 1H), 3.52 (s, 3H), 2.30 – 2.19 (m, 3H), 2.10 – 2.08 (m, 1H).

4-Carbamoyl-4-[4-(4-chloromethyl-benzyloxy)-1-oxo-1,3-dihydro-isoindol-2-yl]-butyric acid methyl ester (12b). Polymer-supported triphenylphosphine (1.6 mmol/g, 10 g, 16 mmol) was added to a stirred suspension of **11** (2.49 g, 8.52 mmol) in THF (100 mL) at 0 °C, followed by diisopropyl diazene-1,2-dicarboxylate (3.36 mL, 17.04 mmol). After

stirring for 30 min, (4-(chloromethyl) phenyl)methanol (2.00 g, 12.78 mmol) was added. The mixture was stirred for 1 h then filtered. The resin was washed with methanol (3 x 30 mL) and DCM (3 x 30 mL). The combined filtrate was concentrated under reduced pressure to give an oil, which was purified by silica gel column chromatography to give **12b** as an oil (3.38 g, 92% yield). ^{1}H NMR (DMSO-d_6) δ 7.58 (d, J = 0.4 Hz, 1H), 7.41 – 7.54 (m, 5H), 7.25 – 7.35 (m, 2H), 7.19 (d, 1H), 5.26 (s, 2H), 4.78 (s, 2H), 4.73 (dd, J = 4.8, 10.3 Hz, 1H, NCH), 4.35 – 4.62 (m, 2H), 3.50 (s, 3H), 1.97 – 2.35 (m, 4H).

3-(4-((4-((4-(2,4-Difluorophenyl)piperazin-1-yl)methyl)benzyl)oxy)-1-oxoisoindolin-2-yl)piperidine-2,6-dione (13). *Step A.* A solution of **12a** (28.5 g, 60.0 mmol) in THF (720 mL) was cooled in a dry ice/acetone bath to -78 °C. While stirring, t-BuOK (7.4 g, 66.0 mmol) was added in one portion to the clear solution. Stirring continued for an additional 2 h at -78 °C. A cooled 1N aqueous solution of HCl (260 mL) was added to the reaction mixture while maintaining a temperature of -78 °C. The mixture was concentrated under reduced pressure until a white slurry remained. The white slurry was diluted with water (250 mL) and then collected by filtration. The filter cake was washed with water (250 mL)

and dried, then washed with EtOAc (250 mL) to give 3-(4-((4-(bromomethyl)benzyl)oxy)-1-oxoisoindolin-2-yl)piperidine-2,6-dione (24.7 g, 55.7 mmol, 93% yield) as a light yellow solid. ^{1}H NMR (400 MHz, DMSO-d_6) δ 10.95 (s, 1H), 7.51 – 7.41 (m., 5H), 7.35 – 7.28 (m, 2H), 5.23 (s, 2H), 5.12 – 5.07 (m, 1H), 4.70 (s, 2H), 4.41 (d, J = 17.6 Hz, 1H), 4.25 (d, J = 17.6 Hz, 1H), 2.90 – 2.84 (m, 1H), 2.58 – 2.53 (m, 1H), 2.44 – 2.41 (m, 1H), 1.98 – 1.95 (m, 1H).

Step B. 3-(4-((4-(Bromomethyl)benzyl)oxy)-1-oxoisoindolin-2-yl)piperidine-2,6-dione (17.44 g, 39.4 mmol) was placed in a flask with 1-(2,4-difluorophenyl)piperazine (7.80 g, 39.4 mmol), DIEA (20.62 mL, 118 mmol), and ACN (200 mL). The reaction mixture was stirred at 40 °C for 18 h. Volatile organics were removed under reduced pressure to give an off-white solid. The solid was taken up in DMSO and purified using reverse-phase semi-preparative HPLC. Fractions containing the desired product were combined and volatile organics were removed under reduced pressure to give a white solid. The solid was slurried in ethanol and volatile organics were removed under reduced pressure to give a white solid. The solid was slurried in water and filtered to give **13** (10.1 g, 18.02

mmol, 45.8% yield, HPLC purity >99%) as a white solid. ^{1}H NMR (400 MHz, DMSO-d_6) δ 10.97 (s, 1H), 7.43 – 7.52 (m, 3H), 7.30 – 7.39 (m, 4H), 7.17 (ddd, J = 2.81, 9.20, 12.44 Hz, 1H), 7.01 – 7.10 (m, 1H), 6.94 – 7.01 (m, 1H), 5.24 (s, 2H), 5.11 (dd, J = 5.14, 13.33 Hz, 1H), 4.38 – 4.46 (m, 1H), 4.22 – 4.30 (m, 1H), 3.54 (s, 2H), 2.85 – 3.01 (m, 5H), 2.59 (br s, 5H), 2.38 – 2.48 (m, 1H), 1.92 – 2.03 (m, 1H). MS (ESI) *m/z* 561.2[M+1]$^+$. Anal. Calcd for C31H30F2N4O4: C, 66.42; H, 5.39; N, 9.99. Found: C, 65.60; H, 5.47; N 9.82; Karl Fischer = 0.25%.

3-(4-((4-((4-(4-Fluorophenyl)piperazin-1-yl)methyl)benzyl)oxy)-1-oxoisoindolin-2-yl)piperidine-2,6-dione (14). To 3-(4-((4-(bromomethyl)benzyl)oxy)-1-oxoisoindolin-2-yl)piperidine-2,6-dione (0.116 g, 0.262 mmol) in ACN (3 mL) was added DIEA (0.091 mL, 0.523 mmol) followed by 1-(4-fluorophenyl)piperazine (0.066 g, 0.366 mmol). The reaction mixture was stirred overnight at RT. The reaction was concentrated under reduced pressure and the residue purified by HPLC and dried to give **14**. (118 mg, 0.217 mmol, 83% yield, HPLC purity >94%). ^{1}H NMR (400 MHz, DMSO-d_6) δ 10.97 (s, 1H), 10.60 (br. s., 1H), 7.54 – 7.64 (m, 4H), 7.47 (t, J = 7.81 Hz, 1H), 7.31 (dd, J = 7.62, 2.54

Hz, 2H), 7.03 – 7.12 (m, 2H), 6.87 – 7.00 (m, 2H), 5.28 (s, 2H), 5.10 (dd, *J* = 13.08, 5.27 Hz, 1H), 4.32 – 4.46 (m, 3H), 4.25 (d, *J* = 17.57 Hz, 1H), 3.69 (d, *J* = 12.89 Hz, 2H), 3.07 – 3.22 (m, 2H), 2.96 – 3.07 (m, 2H), 2.89 (ddd, *J* = 17.67, 13.18, 5.08 Hz, 1H), 2.50 – 2.60 (m, 1H), 2.34 – 2.45 (m, 1H), 1.89 – 2.01 (m, 1H); MS (ESI) *m/z* 543.7 $[M+1]^+$.

3-(4-((4-((4-(3-Fluorophenyl)piperazin-1-yl)methyl)benzyl)oxy)-1-oxoisoindolin-2-yl)piperidine-2,6-dione (15). To 3-(4-((4-(bromomethyl)benzyl)oxy)-1-oxoisoindolin-2-yl)piperidine-2,6-dione (0.130 g, 0.293 mmol) in ACN (3 mL) was added DIEA (0.102 mL, 0.587 mmol) followed by 1-(3-fluorophenyl)piperazine (0.074 g, 0.411 mmol). The reaction mixture was stirred overnight at RT. The reaction was concentrated under reduced pressure and the residue purified by HPLC to give **15** (0.078 g, 0.144 mmol, 49% yield, HPLC purity >96%) ^{1}H NMR (400 MHz, DMSO-d_6) δ 10.97 (s, 1H), 10.39 (br. s., 2H) 7.58 (s, 4H), 7.47 (t, *J* = 7.81 Hz, 1H), 7.31 (dd, *J* = 7.81, 3.91 Hz, 2H), 7.24 (q, *J* = 8.07 Hz, 1H), 6.72 – 6.84 (m, 2 H) 6.61 (t, *J* = 8.40 Hz, 1 H) 5.28 (s, 2 H), 5.10 (dd, *J* = 13.08, 4.88 Hz, 1H), 4.32 – 4.45 (m, 3H), 4.20 – 4.29 (m, 1H), 3.86 (d, *J* = 12.11 Hz, 2H), 3.00 – 3.20 (m, 4H), 2.81 – 2.98 (m, 1H), 2.51 – 2.61 (m, 1H), 2.37 – 2.44 (m, 1H), 1.89 – 2.03 (m, 1H); MS (ESI) *m/z* 543.8 $[M+1]^+$.

3-(4-((4-((4-(2-Fluorophenyl)piperazin-1-yl)methyl)benzyl)oxy)-1-oxoisoindolin-2-yl)piperidine-2,6-dione (16). To 3-(4-((4-(bromomethyl)benzyl)oxy)-1-oxoisoindolin-2-yl)piperidine-2,6-dione (0.119 g, 0.268 mmol) in ACN (3 mL) was added DIEA (0.094 mL, 0.537 mmol) followed by 1-(2-fluorophenyl)piperazine (0.068 g, 0.376 mmol). The reaction mixture was stirred overnight at RT. The reaction was concentrated, and the residue was purified by HPLC to give **16**. (0.026 g, 0.048 mmol, 18% yield, HPLC purity >99%). ^{1}H NMR (400 MHz, DMSO-d_6) δ 10.98 (s, 1H), 7.57 – 7.68 (m, 4H), 7.46 – 7.53 (m, 1H), 7.31 – 7.38 (m, 2H), 7.00 – 7.23 (m, 4H), 5.31 (s, 2H), 5.12 (dd, J = 5.07, 13.27 Hz, 1H), 4.36 – 4.49 (m, 3H), 4.24 – 4.33 (m, 1H), 3.49 (br d, J = 12.47 Hz, 2H), 3.39 (br d, J = 11.74 Hz, 2H), 3.18 – 3.30 (m, 2H), 3.07 – 3.18 (m, 2H), 2.85 – 2.99 (m, 1H), 2.54 – 2.63 (m, 1H), 2.38 – 2.48 (m, 1H), 1.94 – 2.05 (m, 1H); MS (ESI) m/z 543.6 $[M+1]^+$.

3-(4-((4-((4-(2,6-Difluorophenyl)piperazin-1-yl)methyl)benzyl)oxy)-1-oxoisoindolin-2-yl)piperidine-2,6-dione (17). To 3-(4-((4-(bromomethyl)benzyl)oxy)-1-oxoisoindolin-2-yl)piperidine-2,6-dione (0.131 g, 0.296 mmol) in ACN (3 mL) was added DIEA (0.103 mL, 0.591 mmol) followed by 1-(2,6-difluorophenyl)piperazine (0.082 g, 0.414 mmol). The reaction mixture was stirred overnight at RT. The reaction was concentrated under

reduced pressure and the residue was purified by HPLC to give **17**.(0.080 g, 0.143 mmol, 48.3% yield, HPLC purity >97%). ^{1}H NMR (400 MHz, DMSO-d_6) δ ppm 10.97 (s, 1H), 7.54 – 7.66 (m, 4H), 7.47 (t, *J* = 7.81 Hz, 1H), 7.28 - 7.35 (m, 2 H), 6.99 - 7.18 (m, 3H), 5.27 (s, 2H), 5.09 (dd, *J* = 13.28, 5.08 Hz, 1H), 4.32 – 4.48 (m, 3H), 4.15 – 4.32 (m, 1H), 3.39 – 3.53 (m, 2H), 3.22 – 3.31 (m, 3H) 3.06 – 3.21 (m, 2H), 2.81 – 2.95 (m, 1H), 2.55 (d, *J* = 16.79 Hz, 1H), 2.41 (dd, *J* = 13.28, 4.69 Hz, 1H), 1.90 – 2.01 (m, 1H); MS (ESI) *m/z* 561.2 $[M+1]^+$.

3-(4-((4-((4-(2,4-Dichlorophenyl)piperazin-1-yl)methyl)benzyl)oxy)-1-oxoisoindolin-2-yl)piperidine-2,6-dione (18). To 3-(4-((4-(bromomethyl)benzyl)oxy)-1-oxoisoindolin-2-yl)piperidine-2,6-dione (0.100 g, 0.226 mmol) in ACN (3 mL) was added DIEA (0.079 mL, 0.451 mmol) followed by 1-(2,4-dichlorophenyl)piperazine (0.073 g, 0.316 mmol). The reaction mixture was stirred overnight at RT. The reaction was concentrated under reduced pressure and the residue was purified by HPLC to give **18**. (0.110 g, 0.185 mmol, 82% yield, HPLC purity >96%). ^{1}H NMR (400 MHz, DMSO-d_6) δ 10.93 (s, 1H), 7.52 – 7.59 (m, 4 H), 7.40 – 7.47 (m, 1H), 7.35 (dd, *J* = 8.79, 2.54 Hz, 1H), 7.27 (dd, *J* = 7.81, 3.91 Hz, 2H), 7.16 (d, *J* = 8.59 Hz, 1 H), 5.25 (s, 2H), 5.06 (dd, *J* = 13.28, 5.08 Hz, 1H),

4.38 (dd, *J* = 11.33, 5.86 Hz, 3H), 4.16 – 4.26 (m, 1H), 3.34 (s, 2H), 3.37 (s, 2H), 3.17 (d, *J* = 10.55 Hz, 1H), 2.91 – 3.04 (m, 1H), 2.47 – 2.56 (m, 2H) 1.80 – 2.00 (m, 1H); MS (ESI) *m/z* 595.1 $[M+1]^+$.

3-(4-((4-((4-(4-Chlorophenyl)piperazin-1-yl)methyl)benzyl)oxy)-1-oxoisoindolin-2-yl)piperidine-2,6-dione, HCl (19). 3-(4-((4-(Bromomethyl)benzyl)oxy)-1-oxoisoindolin-2-yl)piperidine-2,6-dione (0.282 g, 0.636 mmol) was placed in a flask with 1-(4-chlorophenyl)piperazine (0.125 g, 0.636 mmol), DIEA (0.222 mL, 1.271 mmol), and ACN (6.0 mL). The reaction mixture was heated to 40 °C for 18 h. The reaction mixture was filtered and the residue was purified by HPLC to give a white solid. The solid was taken up in methanol and 6N HCl was added (~3 drops) until the solid fully went into solution. Volatile organics were removed under reduced pressure to give **19** (0.240 g, 0.403 mmol, 63.4% yield, HPLC purity >99%) as a white solid. ^{1}H NMR (400 MHz, DMSO-d_6) δ 10.98 (s, 1H), 7.64 – 7.70 (m, 2H), 7.56 – 7.62 (m, 2H), 7.46 – 7.53 (m, 1H), 7.32 – 7.36 (m, 2H), 7.26 – 7.31 (m, 2H), 6.93 – 7.02 (m, 2H), 5.30 (s, 2H), 5.12 (dd, *J* = 5.14, 13.33 Hz, 1H), 4.41 – 4.49 (m, 1H), 4.38 (br d, *J* = 5.01 Hz, 2H), 4.23 – 4.33 (m, 1H), 3.80 (br d, *J* = 10.27

Hz, 2H), 3.35 (br d, *J* = 8.80 Hz, 2H), 3.05 – 3.22 (m, 4H), 2.84 – 2.98 (m, 1H), 2.58 (br d, *J* = 17.48 Hz, 1H), 2.38 – 2.48 (m, 1H), 1.94 – 2.05 (m, 1H); MS (ESI) *m/z* 559.2 $[M+1]^+$.

3-(4-((4-((4-(4-Methoxyphenyl)piperazin-1-yl)methyl)benzyl)oxy)-1-oxoisoindolin-2-yl)piperidine-2,6-dione (20). To 3-(4-((4-(bromomethyl)benzyl)oxy)-1-oxoisoindolin-2-yl)piperidine-2,6-dione (0.119 g, 0.268 mmol) in ACN (3 mL) was added DIEA (0.094 mL, 0.537 mmol) followed by 1-(4-methoxyphenyl)piperazine (0.072 g, 0.376 mmol). The reaction mixture was stirred overnight at RT. The reaction was concentrated under reduced pressure and the residue was purified by HPLC to give **20**. (0.125 g, 0.225 mmol, 84% yield, HPLC purity >96%). ^{1}H NMR (400 MHz, DMSO-d_6) δ 10.97 (s, 1H), 7.63 – 7.68 (m, 2H), 7.57 – 7.62 (m, 2H), 7.46 – 7.53 (m, 1H), 7.31 – 7.37 (m, 2H), 6.90 – 6.96 (m, 2H), 6.82 – 6.88 (m, 2H), 5.31 (s, 2H), 5.12 (dd, *J* = 5.14, 13.20 Hz, 1H), 4.42 – 4.50 (m, 1H), 4.39 (br d, *J* = 4.40 Hz, 2H), 4.28 (d, *J* = 17.36 Hz, 1H), 3.69 (s, 3H), 3.62 (br d, *J* = 12.96 Hz, 2H), 3.36 (br d, *J* = 11.49 Hz, 2H), 3.10 – 3.23 (m, 2H), 2.98 – 3.07 (m, 2H), 2.85 – 2.97 (m, 1H), 2.58 (br d, *J* = 16.99 Hz, 1H), 2.38 – 2.48 (m, 1H), 1.94 - 2.05 (m, 1H); MS (ESI) *m/z* 555.2 $[M+1]^+$.

3-(1-Oxo-4-((4-((4-phenylpiperazin-1-yl)methyl)benzyl)oxy)isoindolin-2-yl)piperidine-2,6-dione (21). To a solution of 3-(4-(4-(bromomethyl)benzyloxy)-1-oxoisoindolin-2-yl)piperidine-2,6-dione (0.50 g, 1.13 mmol) in ACN (15 mL) was added DIEA (0.373 mL, 2.256 mmol) followed by 1-phenylpiperazine (0.257 mL, 1.692 mmol) at RT. The mixture was stirred at RT overnight. The solvent was evaporated and the resulting white solid was stirred in water (50 mL) and extracted with DCM (2 x 80 mL). The combined organic phases were back-washed with water (50 mL), brine (30 mL), and evaporated to a white solid. The solid was stirred in ACN (8 mL) at 50 °C for 1 h then collected by filtration and dried under vacuum oven to give **21** as a white solid (0.316 g, 53% yield, HPLC purity >95%). ^{1}H NMR (DMSO-d_6) δ 10.98 (s, 1H), 7.42 – 7.55 (m, 3H), 7.28 – 7.41 (m, 4H), 7.15 – 7.25 (m, 2H), 6.91 (d, J = 7.9 Hz, 2H), 6.76 (t, J = 7.3 Hz, 1H), 5.20 – 5.30 (m, 2H), 5.11 (dd, J = 5.1, 13.2 Hz, 1H), 4.20 – 4.48 (m, 2H), 3.50 – 3.62 (m, 2H), 3.12 (t, J = 5.1 Hz, 4H), 2.83 – 2.99 (m, 1H), 2.53 – 2.65 (m, 2H), 2.36 – 2.47 (m, 1H), 1.92-2.06 (m, 1H); ^{13}C NMR (DMSO-d_6) δ 22.36, 31.21, 45.09, 48.18, 51.58, 52.52, 61.71, 69.41, 114.97,

115.24, 115.35, 118.76, 127.68, 128.86, 129.01, 129.82, 129.95, 133.32, 135.30, 137.93, 150.98, 153.50, 168.01, 170.98, 172.83; MS (ESI) *m/z* 525 $[M+1]^+$; Anal Calcd for $C_{31}H_{32}N_4O_4$: C, 70.97; H, 6.15; N, 10.68. Found: C, 70.69; H, 6.01; N, 10.49; mp 195 – 197°C.

3-(4-((4-((4-Isopropylpiperazin-1-yl)methyl)benzyl)oxy)-1-oxoisoindolin-2-yl)piperidine-2,6-dione (22). To a solution of the mixture (~1:1) of 3-(4-(4-(bromomethyl)benzyloxy)-1-oxoisoindolin-2-yl)piperidine-2,6-dione (0.25 g, 0.564 mmol) and 3-(4-(4-(chloromethyl)benzyloxy)-1-oxoisoindolin-2-yl)piperidine-2,6-dione (0.225 g, 0.564 mmol) in ACN was added DIEA (0.292 g, 2.256 mmol) followed by 1-isopropylpiperazine (0.174 g, 1.354 mmol) at RT. The mixture was stirred at RT overnight. The solvent was removed under reduced pressure. The resulting white solid was stirred in water (40 mL) and extracted with DCM (2 x 40 mL). The combined organic phases were washed with water (50 mL) and then evaporated under reduced pressure to give a white oily solid. The solid was stirred in diethyl ether (25 mL) overnight. The suspension was collected by filtration to give an off-white solid, which was suspended in ACN (4 mL) and stirred in a

50 °C oil bath for 30 min. The suspension was collected by filtration to give **22** as a white solid (0.187 g, 34% yield, HPLC purity >95%). ^{1}H NMR (DMSO-d_6) δ 10.97 (s, 1H), 7.38 – 7.54 (m, 3H), 7.26 – 7.36 (m, 4H), 5.22 (s, 2H), 5.11 (dd, J = 5.2, 13.1 Hz, 1H), 4.20 – 4.47 (m, 2H), 3.44 (s, 2H), 3.44 (s, 2H), 2.82 – 2.99 (m, 1H), 2.53 – 2.67 (m, 2H), 2.21 – 2.48 (m, 9H), 1.91 – 2.04 (m, 1H), 0.94 (d, J = 6.4 Hz, 6H); ^{13}C NMR (DMSO-d_6) δ 18.22, 22.36, 31.21, 45.09, 47.95, 51.58, 53.04, 53.55, 61.81, 69.44, 114.97, 115.23, 127.62, 128.86, 129.81, 129.95, 133.31, 135.13, 138.24, 153.51, 168.01, 170.98, 172.83; Anal Calcd for $C_{28}H_{34}N_4O_4$+0.1H_2O: C, 68.30; H, 7.00; N, 11.38. Found: C, 68.21; H, 6.61; N, 11.19; mp 193 – 195°C.

3-(4-((4-((4-Isopropylpiperidin-1-yl)methyl)benzyl)oxy)-1-oxoisoindolin-2-yl)piperidine-2,6-dione (23). *Step A.* To a solution of **12a** (0.5 g, 1.052 mmol) in ACN, was added 4-isopropylpiperidine (0.294 g, 2.314 mmol). The mixture was stirred at RT overnight. The reaction mixture was concentrated under reduced pressure. The resulting oil was taken up in EtOAc (15 mL) and extracted with water (20 mL). The organic layer was washed with brine (10 mL), dried over Na_2SO_4 and concentrated to give methyl 5-amino-4-(4-(4-

((4-isopropylpiperidin-1-yl)methyl)benzyloxy)-1-oxoisoindolin-2-yl)-5-oxopentanoate as an oil.

Step B. To a solution of methyl 5-amino-4-(4-(4-((4-isopropylpiperidin-1-yl)methyl)benzyloxy)-1-oxoisoindolin-2-yl)-5-oxopentanoate (0.548 g, 1.05 mmol) in THF, was added *t*-BuOK (0.12 g, 1.069 mmol) at 0 °C. The mixture was stirred at 0 °C for 30 min. The reaction was quenched by adding 2 mL of HCl (1N) and 5 mL of $NaHCO_3$ (saturated) followed by EtOAc (20 mL) and water (10 mL). The mixture was extracted in EtOAc and the organic layer was washed with water (10 mL), brine (10 mL), and concentrated. The resulting solid was purified by HPLC to give **23** as a white solid (65 mg, 13% yield, HPLC purity >96%). ^{1}H NMR (DMSO-d_6) δ 10.97 (s, 1H), 7.38 – 7.54 (m, 3H), 7.25 – 7.37 (m, 4H), 5.22 (s, 2H), 5.11 (dd, J = 5.1,13.2 Hz, 1H), 4.19 – 4.47 (m, 2H), 3.40 – 3.46 (br. s , 2H), 2.88 – 3.00 (m, 1H), 2.74 – 2.88 (m, 2H), 2.53 – 2.63 (m, 1H), 2.36 – 2.47 (m, 1H), 1.93 – 2.04 (m, 1H), 1.76 – 1.92 (m, 2H), 1.51 – 1.63 (m, 2H), 1.31 – 1.47 (m, 1H), 1.07 – 1.25 (m, 2H), 0.90 – 1.06 (m, 1H), 0.83 (d, J = 6.8 Hz, 6H); ^{13}C NMR (DMSO-d_6) 19.66, 22.36, 28.88, 31.21, 31.94, 41.84, 45.09, 51.58, 53.63, 62.13, 69.45,

114.97, 115. 21, 127.61, 128.80, 129.81, 129.95, 133.31, 135.04, 153.51, 168.01, 170.96, 172.82; MS (ESI) *m/z* 490.3 $[M+1]^+$; Anal Calcd for $C_{29}H_{35}N_3O_4$+0.4 H_2O: C, 70.11; H, 7.26; N, 8.46; Found: C, 70.10; H, 7.37; N, 8.36. mp: 124-126°C.

3-(1-Oxo-4-((4-((4-(trifluoromethyl)piperidin-1-yl)methyl)benzyl)oxy)isoindolin-2-yl)piperidine-2,6-dione (24). *Step A*. In a flask, tert-butyl 5-amino-2-(4-hydroxy-1-oxoisoindolin-2-yl)-5-oxopentanoate (3 g, 8.79 mmol) and triphenyl phosphine on polystyrene (1.6 mmol/g resin, 10.99 g, 17.59 mmol) were slurried in THF (100 mL, 1220 mmol) at RT. The resin was allowed to swell with gentle stirring for 5 min then the mixture was cooled in an ice bath at 0°C. To the mixture, DIAD (3.42 mL, 17.59 mmol) was added using a syringe in a rapid dropwise fashion. After 10 min, (4-(chloromethyl) phenyl)methanol (2.066 g, 13.19 mmol) was added as a solid in one portion. The ice bath was removed and the mixture was stirred at RT for 6 h. The resin was removed by suction filtration and rinsed with successive washes of DCM and MeOH (2 x 50 mL). The combined filtrates and washes were concentrated under reduced pressure. The resulting oil was partitioned between EtOAc (300 mL) and water (100 mL). The organic layer was

washed with brine, dried with Na_2SO_4, and concentrated under reduced pressure to give the crude product as a tan oil. The oil was purified by silica gel column chromatography to give tert-butyl 5-amino-2-(4-(4-(chloromethyl)benzyloxy)-1-oxoisoindolin-2-yl)-5-oxopentanoate as a white foam. (3.6 g, 87% yield). ^{1}H NMR (DMSO-d_6) δ 7.40 – 7.58 (m, 5H), 7.32 (d, J = 2.6 Hz, 1H), 7.29 (d, J = 2.3 Hz, 1H), 7.18 – 7.28 (m, 1H), 6.66 – 6.83 (m, 1H), 5.27 (s, 2H), 4.78 (s, 2H), 4.70 (dd, J = 4.7,10.4 Hz, 1H), 4.43 (s, 2H), 2.14 – 2.35 (m, 1H), 2.00 – 2.14 (m, 3H), 1.39 (s, 9H); ^{13}C NMR (DMSO-d_6) δ 24.69, 27.56, 31.50, 44.78, 45.83, 54.08, 69.13, 81.41, 114.91, 115.26, 127.92, 129.00, 129.73, 130.03, 133.31, 136.78, 137.38, 153.35, 168.09, 169.85, 172.93.

Step B. To a solution of tert-butyl 5-amino-2-(4-(4-(chloromethyl) benzyloxy)-1-oxoisoindolin-2-yl)-5-oxopentanoate (450 mg, 0.95 mmol) and DIEA (0.42 mL, 2.38 mmol) in ACN (9 mL), was added 4-(trifluoromethyl) piperidine hydrochloride (271 mg, 1.43 mmol). The mixture was stirred for 5 h at 60 °C. The crude mixture was partitioned between EtOAc (150 mL) and 1N $NaHCO_3$ (30 mL). The basic aqueous layer was washed with additional EtOAc (100 mL). The organic layers were combined, washed with brine,

dried with Na_2SO_4, and concentrated under reduced pressure to give tert-butyl 5-amino-5-oxo-2-(1-oxo-4-(4-((4-(trifluoromethyl)piperidin-1-yl)methyl)benzyloxy)isoindolin-2-yl)pentanoate as an oil (570 mg). MS (ESI) *m/z* 590 $[M+1]^+$

Step C. To a cooled solution of tert-butyl 5-amino-5-oxo-2-(1-oxo-4-(4-((4-(trifluoromethyl)piperidin-1-yl)methyl)benzyloxy)isoindolin-2-yl)pentanoate (561 mg, 0.95 mmol) in THF (10 mL) in an ice bath, was added t-BuOK (128 mg, 1.14 mmol) as a solid in one portion. The ice bath was removed and the reaction mixture was stirred for 2 h at RT. More t-BuOK (28 mg) was added and the reaction mixture was stirred for 2 h. The reaction mixture was cooled in an ice bath and the reaction quenched with acetic acid (0.163 mL, 2.85 mmol). The mixture was concentrated under reduced pressure and the resulting solid was partitioned between EtOAc (100 mL) and 1N $NaHCO_3$ (30 mL). The aqueous layer was extracted with EtOAc (50 mL), and the combined organic layer was washed with brine, dried with Na_2SO_4, and concentrated under reduced pressure to give a white solid. The solid was triturated with diethyl ether (40 mL), collected by filtration, and washed with additional diethyl ether. The solid was dried and a second trituration was

carried out using water (120 mL). The remaining solid was collected and dried to give **24** as a white solid (328 mg, 67% yield, HPLC >96%). ^{1}H NMR (DMSO-d_6) δ 10.97 (s, 1H), 7.39 – 7.55 (m, 3H), 7.21 – 7.39 (m, 4H), 5.17 – 5.28 (m, 2H), 5.11 (dd, J = 5.0, 13.3 Hz, 1H), 4.42 (d, J = 17.4 Hz, 1H), 4.25 (d, J = 17.6 Hz, 1H), 3.48 (s, 2H), 2.78 – 3.00 (m, 3H), 2.52 – 2.65 (m, 1H), 2.35 – 2.48 (m, 1H), 2.14 – 2.35 (m, 1H), 1.87 – 2.05 (m, 3H), 1.66 – 1.82 (m, 2H), 1.34 – 1.55 (m, 2H); ^{13}C NMR (DMSO-d_6) δ 22.33, 24.19, 31.18, 38.35, 39.07, 45.06, 51.39, 51.55, 61.59, 69.39, 114.96, 115.20, 127.64, 127.82 (q, J = 278 Hz), 128.79, 129.80, 129.93, 133.30, 135.22, 138.11, 153.49, 167.99, 170.96, 172.81; MS (ESI) m/z 516 $[M+1]^+$; Anal Calcd for $C_{27}H_{28}F_3N_3O_4$+0. 35 H_2O: C, 62.15; H, 5.54;N, 8.05; F, 10.92. Found: C, 62.13; H, 5.48; N, 8.06; F, 9.84; mp: 178-180°C.

3-(4-((4-((4,4-Dimethylpiperidin-1-yl)methyl)benzyl)oxy)-1-oxoisoindolin-2-yl)piperidine-2,6-dione (25). *Step A.* To a stirred solution of **12b** (0.55 g, 1.28 mmol) in ACN (15 mL) at RT, were added 4,4-dimethylpiperidine hydrochloride (0.23 g, 1.53 mmol) and DIEA (0.46 mL, 2.81 mmol). The mixture was stirred overnight and then concentrated to give an oil, which was purified by silica gel column chromatography to give methyl 5-amino-4-

(4-(4-((4,4-dimethylpiperidin-1-yl)methyl)benzyloxy)-1-oxoisoindolin-2-yl)-5-oxopentanoate as a light yellow solid (0.60 g, 92% yield).

Step B. To a stirred solution of methyl 5-amino-4-(4-(4-((4,4-dimethylpiperidin-1-yl)methyl)benzyloxy)-1-oxoisoindolin-2-yl)-5-oxopentanoate (0.59 g, 1.16 mmol) in THF (15 mL) in an ice bath, was added t-BuOK (0.33 g, 2.94 mmol). The mixture was stirred for 10 min and the reaction was quenched by 1N HCl (4 mL) and neutralized by saturated sodium bicarbonate (5.5 mL to pH=7). The mixture was then stirred with EtOAc (25 mL). The organic phase was separated, washed with brine (15 mL), and concentrated to an off-white solid, which was purified by silica gel column chromatography to give **25** as a white solid (150 mg, 27% yield, HPLC purity >96%). ^{1}H NMR (DMSO-d_6) δ 10.97 (s, 1H), 7.31 – 7.51 (m, 7H), 5.25 (s, 2H), 5.11 (dd, J = 5.1, 13.2 Hz, 1H), 4.23 – 4.45 (m, 2H), 3.50 (br. s, 2H), 2.86 – 2.98 (m, 3H), 2.51 – 2.60 (m, 1H), 2.37 – 2.43 (m, 1H), 1.96-2.00 (m, 1H), 1.49 (br. s, 4H), 0.95 (s, 6H); ^{13}C NMR (DMSO-d_6) δ 22.35, 27.94, 31.18, 37.16, 45.06, 48.91, 51.56, 69.28, 114.97, 115.26, 127.69, 129.80, 129.94, 133.31, 153.44,

167.98, 170.97, 172.82; MS (ESI) *m/z* 476 $[M+1]^+$; Anal. Calcd for $C_{28}H_{33}N_3O_4$: C, 70.71; H, 6.99; N, 8.84. Found: C, 66.15; H, 6.50; N, 8.02; mp: 168-170°C.

3-(4-((4-((4,4-Difluoropiperidin-1-yl)methyl)benzyl)oxy)-1-oxoisoindolin-2-yl)piperidine-2,6-dione (26). *Step A.* To a stirred solution of **12b** (500 mg, 1.160 mmol) and 4,4-difluoropiperidine hydrochloride (274 mg, 1.741 mmol) in ACN (10 mL) under a nitrogen atmosphere, were added Na_2CO_3 (160 mg, 1.160 mmol) and DIEA (0.507 mL, 2.90 mmol). The resulting solution was stirred at 50 °C for 8 h. The reaction mixture was diluted by DCM (50 mL) and extracted with brine (20 mL). The organic layer was dried with $MgSO_4$ and concentrated under vacuum to give methyl 5-amino-4-(4-((4-((4,4-difluoropiperidin-1-yl)methyl)benzyl)oxy)-1-oxoisoindolin-2-yl)-5-oxopentanoate as an off white solid (630 mg, 105% crude yield). MS (ESI) *m/z* 516 $[M+1]^+$.

Step B. To a stirred solution of methyl 5-amino-4-(4-((4-((4,4-difluoropiperidin-1-yl)methyl)benzyl)oxy)-1-oxoisoindolin-2-yl)-5-oxopentanoate (630 mg, 1.222 mmol) in THF (10 mL) at 0 °C was added t-BuOK (151 mg, 1.344 mmol). The mixture was stirred at 0 °C for 5 min. The reaction mixture was diluted with DCM (50 mL) and acidified by

HCl (1N, aq. 3 mL) to pH=2. The mixture was extracted with a mixture of $NaHCO_3$ (aq. sat., 5 mL) and brine (10 mL). The organic layer was dried over $MgSO_4$ and concentrated. The residue was stirred in ether (50 mL) and the product was collected by vacuum filtration to give a white solid. The solid was triturated in EtOAc (5 mL) and collected by filtration to give **26** as a white solid (215 mg, 36% yield, HPLC purity >99%). ^{1}H NMR (DMSO-d_6) δ 10.97 (s, 1H), 7.40 – 7.54 (m, 3H), 7.33 (d, 4H), 5.23 (s, 2H,), 5.11 (dd, J = 5.1, 13.2 Hz, 1H), 4.42 (d, J = I7.6 Hz, 1H), 4.25 (d, J = 17.6 Hz, 1H), 3.55 (s, 2H), 2.81 – 3.02 (m, 1H), 2.54 – 2.64 (m, 1H), 2.34 – 2.49 (m, 5H), 1.84 – 2.09 (m, 5H); ^{13}C NMR (DMSO-d_6) δ 22.29, 31.12, 33.25 (t, $J_{C\text{-}F}$ = 20.9 Hz), 45.00, 49.12, 51.51, 60.40, 69.29, 114.89, 115.16, 122.68 (t, $J_{C\text{-}F}$ = 239.9 Hz), 127.60, 128.84, 129.73, 129.88, 133.24, 135.32, 137.72, 153.42, 167.93, 170.91, 172.76; Anal. Calcd for $C_{26}H_{27}F_2N_3O_5$+1 H_2O: C, 62.27; H, 5.83; N, 8.39, Found: C, 62.09; H, 5.73; N, 8.17; MS (ESI) *m/z* 484 $[M+1]^+$; mp 193 – 195°C.

3-(4-((4-((4-Methylpiperidin-1-yl)methyl)benzyl)oxy)-1-oxoisoindolin-2-yl)piperidine-2,6-dione (27). 4-Methylpiperidine (0.49 g, 4.94 mmol) was added to a stirred solution of **12b**

(0.71 g, 1.65 mmol) in DMF (15 mL) at 50°C overnight. To the mixture was added K_2CO_3 (0.23 g, 1.65 mmol), and the mixture was heated to 90 °C overnight. The mixture was concentrated to give an oil, which was stirred in EtOAc (10 mL) overnight. The suspension was filtered to give a brown filtrate, which was concentrated under reduced pressure. The residue was purified by silica gel column chromatography to give **27** as a white solid (0.22 g, 29% yield, HPLC purity >98%).^{1}H NMR (400 MHz, DMSO-d_6) δ 10.98 (s, 1H), 10.69 (br. s., 1H), 7.70 – 7.62 (m, 2H), 7.59 – 7.54 (m, 2H), 7.52 – 7.46 (m, 1H), 7.36 – 7.31 (m, 2H), 5.28 (s, 2H), 5.12 (dd, J = 5.0, 13.3 Hz, 1H), 4.44 (d, J = 17.6 Hz, 1H), 4.30 (s, 1H), 4.27 – 4.20 (m, 2H), 3.27 – 3.23 (m, 2H), 2.97 – 2.78 (m, 3H), 2.60 – 2.56 (m, 1H), 2.48 – 2.42 (m, 1H), 2.03 – 1.92 (m, 1H), 1.75 – 1.72 (m, 2H), 1.62 – 1.40 (m, 3H), 0.89 (d, J = 5.8 Hz, 3H); ^{13}C NMR (DMSO-d_6) δ 21.79, 22.36, 30.23, 31.21, 33.89, 45.10, 51.58, 53.22, 62.10, 69.44, 114.97, 115.23, 127.61, 128.86, 129.81, 129.94, 133.31, 135.12, 153.51, 168.01, 170.96, 172.83; MS (ESI) *m/z* 462 $[M+1]^+$; Anal. Calcd for $C_{27}H_{31}N_3O_4$+0.1 H_2O: C, 69.99; H, 6.79; N, 9.07. Found: C, 69.84; H, 6.81; N, 9.12; mp: 189-191°C.

3-(4-((4-((4-(2,4-Dichlorophenyl)-2-oxopiperazin-1-yl)methyl)benzyl)oxy)-1-oxoisoindolin-2-yl)piperidine-2,6-dione (28). 4-(2,4-Dichlorophenyl)piperazin-2-one (124 mg, 0.506 mmol) was dissolved into dry DMF (1.5 mL) and cooled to 0 °C. Sodium hydride (60% dispersion in mineral oil, 25 mg, 0.625 mmol) was added in one portion, and the solution was stirred for 5 min. 3-(4-((4-(Bromomethyl)benzyl)oxy)-1-oxoisoindolin-2-yl)piperidine-2,6-dione (112 mg, 0.253 mmol) was then added as a solid in one portion. After 20 min, another portion of sodium hydride (60% dispersion in mineral oil, 34 mg, 0.850 mmol) was added. After 20 min, another portion of 3-(4-((4-(bromomethyl)benzyl)oxy)-1-oxoisoindolin-2-yl)piperidine-2,6-dione (86.8 mg, 0.196 mmol) was added, with the reaction now at RT. After 5 h, the reaction was added to 1N HCl and poured in a separatory funnel, then diluted with DCM and THF. The organic layer was removed, and the aqueous layer extracted with a mixture of DCM anf THF to solubilize some of the solid. The combined organic solution was dried over $MgSO_4$, filtered, and concentrated. The crude product was purified by HPLC to give **28**. (15.5 mg, 0.026 mmol, 5.0% yield, HPLC purity >98%).^{1}H NMR (500 MHz, DMSO-d_6) δ 10.96 (s, 1H), 7.59 (d, J = 2.52 Hz, 1H), 7.46 – 7.53 (m, 3H), 7.37 – 7.42 (m, 1H), 7.33 (s, 5H), 7.15

– 7.22 (m, 1H), 5.25 (s, 2H), 5.11 (dd, *J* = 13.24, 5.36 Hz, 1H), 4.60 (s, 2H), 4.43 (d, *J* = 17.34 Hz, 1H), 4.27 (d, *J* = 17.65 Hz, 1H), 3.74 (s, 2H), 2.82 – 3.01 (m, 1H), 2.54 – 2.67 (m, 2H), 2.34 – 2.45 (m, 2H), 1.90 – 2.03 (m, 1H); MS (ESI): *m/z* 607.2 $[M+1]^+$.

3-(4-((4-((4-(5-Fluoropyridin-2-yl)piperazin-1-yl)methyl)benzyl)oxy)-1-oxoisoindolin-2-yl)piperidine-2,6-dione (29). To 3-(4-((4-(bromomethyl)benzyl)oxy)-1-oxoisoindolin-2-yl)piperidine-2,6-dione (0.119 g, 0.268 mmol) in ACN (3 mL) was added DIEA (0.141 mL, 0.805 mmol) followed by 1-(5-fluoropyridin-2-yl)piperazine (0.058 g, 0.322 mmol).The reaction was stirred at RT overnight. The mixture was concentrated and the residue was purified by HPLC to give **29**. (0.131 mg, 0.241 mmol, 90% yield, HPLC purity >96%). ^{1}H NMR (400 MHz, DMSO-d_6) δ 11.03 (br. s., 1H), 10.97 (s, 1H), 8.12 (d, *J* = 3.12 Hz, 1H), 7.52 – 7.65 (m, 5H), 7.47 (t, *J* = 7.81 Hz, 1H), 7.24 – 7.35 (m, 2H), 6.95 (dd, *J* = 9.37, 3.51 Hz, 1H), 5.27 (s, 2H), 5.10 (dd, *J* = 13.28, 5.08 Hz, 1H), 4.42 (d, *J* = 17.18 Hz, 1H), 4.34 (d, *J* = 5.08 Hz, 2H), 4.19 – 4.30 (m, 3H), 3.74 (quin, *J* = 6.05 Hz, 1H), 3.32 (d, *J* = 11.72 Hz, 2H), 3.15 – 3.28 (m, 2H), 2.97 – 3.10 (m, 2H), 2.81 – 2.95 (m, 1H), 2.50 – 2.60 (m, 1H), 2.42 (dd, *J* = 13.08, 4.49 Hz, 1H), 1.90 – 2.02 (m, 1H); MS (ESI) *m/z* 544.5 $[M+1]^+$.

3-(1-Oxo-4-((4-((4-(pyridin-2-yl)piperazin-1-yl)methyl)benzyl)oxy)isoindolin-2-yl)piperidine-2,6-dione, HCl (30). 3-(4-((4-(Bromomethyl)benzyl)oxy)-1-oxoisoindolin-2-yl)piperidine-2,6-dione (0.050 g, 0.113 mmol) was placed in a vial with 1-(pyridin-2-yl)piperazine.2HCl (0.029 g, 0.124 mmol), DIEA (0.059 mL, 0.338 mmol), and ACN (1.0 mL). The reaction mixture was stirred at 40 °C for 18 h. The reaction mixture was taken up in DMSO (1.0 mL) and purified by HPLC. Fractions containing the desired product were combined and volatile organics were removed under reduced pressure to give a white solid. The solid was taken up in methanol and three drops of 6N HCl solution were added. Volatile organics were removed under reduced pressure to give **30** (0.038 g, 0.068 mmol, 59.9% yield, HPLC purity >97%) as a white solid. ^{1}H NMR (500 MHz, DMSO-d_6) δ 10.96 (s, 1H), 8.12 – 8.15 (m, 1H), 7.81 (t, J = 7.41 Hz, 1H), 7.65 – 7.69 (m, 2H), 7.59 (d, J = 8.20 Hz, 2H), 7.47 – 7.52 (m, 1H), 7.32 – 7.36 (m, 2H), 7.12 (d, J = 6.94 Hz, 1H), 6.87 (t, J = 5.99 Hz, 1H), 5.30 (s, 2H), 5.12 (dd, J = 5.20, 13.40 Hz, 1H), 4.34 – 4.48 (m, 5H), 4.29 (d, J = 17.65 Hz, 1H), 3.43 – 3.53 (m, 2H), 3.38 (d, J = 12.61 Hz, 2H), 3.12 (d, J = 8.51 Hz, 2H), 2.91 (ddd, J = 5.36, 13.71, 17.50 Hz, 1H), 2.55 – 2.62 (m, 1H), 2.40 – 2.48 (m, 1H), 1.99 (dtd, J = 1.58, 5.12, 12.45 Hz, 1H); MS (ESI) m/z 526.2 $[M+1]^+$.

5-(4-(4-(((2-(2,6-Dioxopiperidin-3-yl)-1-oxoisoindolin-4-yl)oxy)methyl)benzyl)piperazin-1-yl)picolinamide (31). 3-(4-((4-(Bromomethyl)benzyl)oxy)-1-oxoisoindolin-2-yl)piperidine-2,6-dione (0.100 g, 0.226 mmol) was placed in a vial with 5-(piperazin-1-yl)picolinamide (0.047 g, 0.226 mmol), DMF (1.0 mL), and DIEA (0.078 mL, 0.445 mmol). The reaction mixture was stirred at 40 °C for 18 h. DMSO (1 mL) was added to the vial and the crude material was purified by HPLC. Fractions containing the desired product were combined and volatile organics were removed under reduced pressure to give **31** (0.058 g, 0.102 mmol, 45.2% yield, HPLC purity >99%) as a white solid. ^{1}H NMR (400 MHz, DMSO-d_6) δ 10.97 (s, 1H), 8.26 (d, J = 2.69 Hz, 1H), 7.84 (d, J = 8.80 Hz, 1H), 7.77 (br d, J = 2.20 Hz, 1H), 7.44 – 7.53 (m, 3H), 7.27 – 7.41 (m, 6H), 5.25 (s, 2H), 5.12 (dd, J = 5.01, 13.33 Hz, 1H), 4.38 – 4.49 (m, 1H), 4.21 – 4.32 (m, 1H), 3.55 (s, 2H), 2.81 – 3.02 (m, 1H), 2.60 (br s, 1H), 2.37 – 2.48 (m, 1H), 1.89 – 2.07 (m, 1H); MS (ESI) m/z 569.2 $[M+1]^+$.

2-(4-(4-(((2-(2,6-Dioxopiperidin-3-yl)-1-oxoisoindolin-4-yl)oxy)methyl)benzyl)piperazin-1-yl)nicotinonitrile, HCl (32). To 3-(4-((4-(bromomethyl)benzyl)oxy)-1-oxoisoindolin-2-yl)piperidine-2,6-dione (0.119 g, 0.268 mmol) in ACN (3 mL) was added DIEA (0.141 mL, 0.805 mmol) followed by 2-(piperazin-1-yl)nicotinonitrile (0.061 g, 0.322 mmol). The

reaction was stirred overnight at RT, then the mixture was concentrated and purified by HPLC. Fractions containing the desired product were combined and 4 drops of 6 M HCl were added. The solution was frozen and lyophilized to give **32**. (0.037 g, 0.067 mmol, 25% yield, HPLC purity >99%). ^{1}H NMR (400MHz, DMSO-d_6) δ 11.01 (s, 1H), 10.78 (br. s., 1H), 8.49 (dd, J = 4.9, 1.8 Hz, 1H), 8.19 (dd, J = 7.6, 1.8 Hz, 1H), 7.58 – 7.66 (m, 4H), 7.50 (t, J = 7.8 Hz, 1H), 7.31 – 7.38 (m, 2H), 7.09 (dd, J = 7.4, 4.7 Hz, 1H), 5.31 (s, 2H), 5.13 (dd, J = 13.3, 5.1 Hz, 1H), 4.38 – 4.48 (m, 3H), 4.21 – 4.33 (m, 3H), 3.40 – 3.50 (m, 4H), 3.20 (d, J = 11.7 Hz, 2H), 2.87 – 2.98 (m, 1H), 2.56 – 2.64 (m, 1H), 2.38 – 2.48 (m, 1H), 1.96 – 2.03 ppm (m, 1H); MS (ESI) m/z 551.5 $[M+1]^+$.

4-(4-(4-(((2-(2,6-Dioxopiperidin-3-yl)-1-oxoisoindolin-4-yl)oxy)methyl)benzyl)piperazin-1-yl)-3-fluorobenzonitrile (33). 3-(4-((4-(Bromomethyl)benzyl)oxy)-1-oxoisoindolin-2-yl)piperidine-2,6-dione (0.200 g, 0.451 mmol) was placed in a vial with 3-fluoro-4-(piperazin-1-yl)benzonitrile (0.102 g, 0.496 mmol), DIEA (0.236 mL, 1.354 mmol), and ACN (4.0 mL). The reaction mixture was stirred at 40 °C for 18 h. The reaction mixture was taken up in DMSO (4.0 mL) and purified by HPLC to give **33** (0.170 g, 0.300 mmol, 66.4% yield, HPLC purity >99%) as a white solid. ^{1}H NMR (400 MHz, DMSO-d_6) δ 10.97

(s, 1H), 7.69 (dd, *J* = 1.96, 13.45 Hz, 1H), 7.57 (dd, *J* = 1.71, 8.56 Hz, 1H), 7.44 – 7.52 (m, 3H), 7.30 – 7.40 (m, 4H), 7.12 (t, *J* = 8.68 Hz, 1H), 5.24 (s, 2H), 5.12 (dd, *J* = 5.14, 13.20 Hz, 1H), 4.38 – 4.48 (m, 1H), 4.22 – 4.31 (m, 1H), 3.55 (s, 2H), 3.14 – 3.23 (m, 4H), 2.85 – 2.98 (m, 1H), 2.53 (br d, *J* = 4.65 Hz, 5H), 2.39 – 2.48 (m, 1H), 1.93 – 2.05 (m, 1H); MS (ESI) *m/z* 568.2 $[M+1]^+$.

3-(4-((4-((4-Methylpiperazin-1-yl)methyl)benzyl)oxy)-1-oxoisoindolin-2-yl)piperidine-2,6-dione (34). *Step A.* Polymer-supported triphenylphosphine (1.6 mmol/g, 1.36 g, 1.85 mmol) was added to a stirred solution of **11** (0.45 g, 1.54 mmol) in THF (20 mL) at 0 °C followed by addition of DIAD (0.37 mL, 1.88 mmol). After stirring for 30 min, [4-(4-methyl-piperazin-1-ylmethyl)-phenyl]methanol (0.41 g, 1.85 mmol) was added. The mixture was stirred for 3 h then filtered, washed with methanol (3 x 10 mL) and DCM (3 x 10 mL). The combined filtrate was evaporated in vacuo to give an oil, which was purified by silica gel column chromatography to give methyl 5-amino-4-(4-((4-((4-methylpiperazin-1-yl)methyl)benzyl)oxy)-1-oxoisoindolin-2-yl)-5-oxopentanoate as a clear oil (0.50 g, 66% yield).

Step B. Potassium tert-butoxide (0.11 g, 1.01 mmol) was added to a stirred solution of methyl 5-amino-4-(4-((4-((4-methylpiperazin-1-yl)methyl)benzyl)oxy)-1-oxoisoindolin-2-yl)-5-oxopentanoate (0.50 g, 1.01 mmol) in THF (15 mL) at 0 °C. The mixture was stirred for 10 min and the reaction was quenched with 1N HCl (3 mL), the pH was neutralized by saturated sodium bicarbonate (4 mL to pH=7), and the crude product quickly extracted with EtOAc (2 x 30 mL). The combined organic phases were evaporated to give an off-white solid, which was stirred in EtOAc (10 mL) for 1 h. The suspension was filtered and dried to give **34** as an off-white solid (0.12 g, 26% yield, HPLC purity >99%). ^{1}H NMR (DMSO-d_6) δ 10.97 (s, 1H), 7.23 – 7.56 (m, 7H), 5.22 (s, 2H), 5.11 (dd, J = 5.2,13.1 Hz, 1H), 4.17 – 4.50 (m, 2H), 3.45 (s, 2H), 2.80 – 3.05 (m, 1H), 2.55 – 2.66 (m, 1H), 2.20 – 2.46 (m, 9H), 2.14 (s, 3H), 1.90 – 2.04 (m, 1H); ^{13}C NMR (DMSO-d_6) δ 22.36, 31.21, 45.09, 45.72, 51.58, 52.52, 54.71, 61.74, 69.44, 114.98, 115.23, 127.62, 128.88, 129.81, 129.95, 133.31, 135.17, 138.18, 153.51, 168.01,170.96, 172.82; MS (ESI) *m/z* 463 $[M+1]^+$; Anal. Calcd for $C_{26}H_{30}N_4O_4$: C, 67.51; H, 6.54; N, 12.11; Found: C, 67.23; H, 6.67; N, 11.78; mp 188-190 °C.

[4-(Bromomethyl)phenyl]methoxy-tert-butyl-dimethyl-silane (36). *Step A.* To a solution of methyl 4-(hydroxymethyl)benzoate (**35**) (20.0 g, 120.36 mmol) and imidazole (12.29 g, 180.54 mmol) in DMF (250.00 mL) was added TBSCl (27.21 g, 180.54 mmol, 22.12 mL) at 0 °C. The mixture was stirred at 25°C for 16 h. The reaction was quenched with water (300 mL) and extracted with EtOAc (3 x 200 mL). The combined organic phase was washed with brine (3 x 300 mL), dried over anhydrous Na_2SO_4, filtered, and concentrated under reduced pressure. The residue was purified by column chromatography to give crude methyl 4-[[tert-butyl(dimethyl)silyl]oxymethyl]benzoate (36.00 g) as a white solid.^{1}H NMR ($CDCl_3$, 400 MHz) δ 8.01 (d, *J* = 8.0 Hz, 2H), 7.40 (d, *J* = 8.0 Hz, 2H), 4.80 (s, 2H), 3.92 (s, 3H), 0.96 (s, 9H), 0.11 (s, 6H).

Step B. To a mixture of $LiAlH_4$ (7.31 g, 192.56 mmol) in THF (800.0 mL) was added methyl 4-[[tert-butyl(dimethyl)silyl]oxymethyl]benzoate (36.0 g, 128.37 mmol) in THF (800 mL) in one portion at 0 °C under nitrogen. The mixture was stirred at 0 °C for 1 h, then was quenched with water followed by aqueous 20% NaOH. The mixture was filtered and the filtrate was concentrated under reduced pressure. The residue was purified by silica gel

column chromatography to give [4-[[tert-butyl(dimethyl)silyl]oxymethyl]phenyl]methanol (26.00 g, 103.00 mmol, 80.2% yield) as a white solid. ^{1}H NMR ($CDCl_3$, 400 MHz) δ 7.37 – 7.32 (m, 4H), 4.76 (s, 2H), 4.70 (s, 2H), 0.97 (s, 9H), 0.12 (s, 6H).

Step C. To a solution of NBS (8.46 g, 47.54 mmol) in DCM (75.0 mL) at 0 °C was added Me_2S (3.94 g, 63.39 mmol, 4.63 mL). The bright yellow mixture was stirred at 0 °C for 15 min then cooled to -20°C. At this temperature, a pre-cooled solution of [4-[[tert-butyl(dimethyl)silyl]oxymethyl]phenyl]methanol (8.00 g, 31.69 mmol) in DCM (25 mL) was added via syringe. The resulting mixture was warmed to 0 °C and stirred for 15 min, then warmed at 25 °C for 2 h. The mixture was poured into ice-water (50 mL) and stirred for 10 min. The aqueous phase was extracted with DCM (3 x 30 mL). The combined organic phase was washed with brine (2 x 15 mL), dried with anhydrous Na_2SO_4, filtered, and concentrated under reduced pressure. The residue was added to water (30 mL) and extracted with n-hexane (2 x 30 mL). The organic layer was dried with anhydrous Na_2SO_4, filtered, and concentrated under reduced pressure to give crude **36** (8.00 g). The crude material was used in the next step without further purification.

Methyl 5-amino-4-[4-[[4-[[tert-butyl(dimethyl)silyl]oxymethyl]phenyl]methoxy]-1-oxo-isoindolin-2-yl]-5-oxo-pentanoate (37). To a mixture of [4-(bromomethyl)phenyl]methoxy-tert-butyl-dimethyl-silane (10.0 g, 31.71 mmol) and methyl 5-amino-4-(4-hydroxy-1-oxo-isoindolin-2-yl)-5-oxo-pentanoate (11.12 g, 38.05 mmol) in DMF (100 mL) was added K_2CO_3 (26.30 g, 190.26 mmol) in one portion at 25 °C under nitrogen. The mixture was stirred at 25 °C for 16 h. The reaction mixture was poured into ice-water (100 mL) and extracted with EtOAc (3 x 50 mL). The combined organic phase was washed with brine (5 x 50 mL), dried with anhydrous Na_2SO_4, filtered, and concentrated under reduced pressure. The residue was washed with petroleum ether and EtOAc (1:1, 50 mL) to give **37** (7.50 g, 14.24 mmol, 44.9% yield) as a white solid. MS (ESI) *m/z* 549.2 $[M+23]^+$.

3-[4-[[4-(Hydroxymethyl)phenyl]methoxy]-1-oxo-isoindolin-2-yl]-1-methyl-piperidine-2,6-dione (38). *Step A.* To a mixture of potassium *tert*-butoxide (2.40 g, 21.36 mmol) in THF (50 mL) was added **37** (7.50 g, 14.24 mmol) in THF (50 mL) in one portion at 0 °C under nitrogen. The mixture was stirred at 0 °C for 2 h. The reaction mixture was poured into aqueous HCl (1 mol/L) (200 mL). The aqueous phase was extracted with EtOAc (3 x 50

mL). The combined organic phase was washed with brine (2 x 50 mL) and concentrated under reduced pressure to give 3-[4-[[4-[[tert-butyl(dimethyl)silyl]oxymethyl]phenyl]methoxy]-1-oxo-isoindolin-2-yl]piperidine-2,6-dione (6.50 g, crude) as white solid. MS (ESI) *m/z* 495.2 $[M+1]^+$.

Step B. To a mixture of 3-[4-[[4-[[tert-butyl(dimethyl)silyl]oxymethyl]phenyl]methoxy]-1-oxo-isoindolin-2-yl]piperidine-2,6-dione (6.50 g, 13.14 mmol) in THF (100 mL) was added H_2SO_4 (3 M, 30.0 mL) in one portion at 20 °C under nitrogen. The mixture was stirred at 20 °C for 2 h. The pH of the reaction mixture was adjusted with saturated aqueous sodium bicarbonate to pH = 6, then the product was extracted with EtOAc (2 x 50 mL). The combined organic phase was washed with brine (2 x 100 mL), dried over Na_2SO_4, and concentrated. The residue was triturated with petroleum ether:EtOAc (10:1, 50 mL) to give 3-[4-[[4-(hydroxymethyl)phenyl]methoxy]-1-oxo-isoindolin-2-yl]piperidine-2,6-dione (4.20 g, 11.04 mmol, 84.0% yield) as a white solid. ^{1}H NMR (400 MHz, DMSO-d_6) δ 10.90 (s, 1H), 7.45 – 7.33 (m, 3H), 7.25 – 7.22 (m, 4H), 5.15 (s, 2H), 5.03 (dd, *J* = 5.0, 13.2 Hz,

1H), 4.42 (s, 2H), 4.33 (d, *J* = 17.6 Hz, 1H), 4.18 (d, *J* = 17.6 Hz, 1H), 2.93 – 2.75 (m, 1H), 2.53 – 2.51 (m, 1H), 2.39 – 2.30 (m, 1H), 1.95 – 1.85 (m, 1H); MS (ESI) *m/z* 381.2 $[M+1]^+$.

Step C. To a mixture of 3-[4-[[4-(hydroxymethyl)phenyl]methoxy]-1-oxo-isoindolin-2-yl]piperidine-2,6-dione (400 mg, 1.05 mmol) and K_2CO_3 (436 mg, 3.15 mmol) in DMF (5.00 mL) was added methyl iodide (447 mg, 3.15 mmol) in one portion at 0 °C under nitrogen, then heated to 15 °C and stirred for 5 h. The mixture was poured into HCl (1N, 10 mL). The aqueous phase was extracted with EtOAc (3 x 30 mL). The combined organic phase was washed with brine (3 x 30 mL), dried with anhydrous Na_2SO_4, filtered and concentrated under vacuum. The residue was purified by silica gel column chromatography to give **38** (300 mg, 0.761 mmol, 72.4% yield) as a white solid. ^{1}H NMR (400 MHz, DMSO-d_6) δ 7.53 – 7.41 (m, 3H), 7.37 – 7.28 (m, 4H), 5.23 (s, 2H), 5.20 – 5.15 (m, 1H), 4.50 (d, *J* = 5.8 Hz, 2H), 4.40 (d, *J* = 17.6 Hz, 1H), 4.25 (d, *J* = 17.6 Hz, 1H), 3.00 (s, 3H), 2.79 – 2.69 (m, 1H), 2.56 – 2.52 (m, 1H), 2.46 – 2.42 (m, 1H), 2.03 – 1.97 (m, 1H); MS (ESI) *m/z* 395.2 $[M+1]^+$.

3-[4-[[4-[[4-(2,4-Difluorophenyl)piperazin-1-yl]methyl]phenyl]methoxy]-1-oxo-isoindolin-2-yl]-1-methyl-piperidine-2,6-dione (39). *Step A.* To a mixture of **38** (300 mg, 0.761 mmol) and DIEA (245 mg, 1.90 mmol) in DMF (10.0 mL) was added methanesulfonyl chloride (104 mg, 0.913 mmol) in one portion at -5 °C under nitrogen. The mixture was stirred at -5 °C for 1 h. The aqueous phase was extracted with EtOAc (3 x 20 mL). The combined organic phase was washed with brine (2 x 20 mL), dried with anhydrous Na_2SO_4, filtered, and concentrated under vacuum to give crude [4-[[2-(1-methyl-2,6-dioxo-3-piperidyl)-1-oxo-isoindolin-4-yl]oxymethyl]phenyl]methylmethanesulfonate (360 mg) as a colorless oil. The residue was used in the next step without further purification. MS (ESI) *m/z* 473.2 $[M+1]^+$.

Step B. To a mixture of [4-[[2-(1-methyl-2,6-dioxo-3-piperidyl)-1-oxo-isoindolin-4-yl]oxymethyl]phenyl]methyl methanesulfonate (360 mg, 0.762 mmol) and 1-(2,4-difluorophenyl)piperazine (226 mg, 1.14 mmol) in DMF (5.0 mL) was added DIEA (385 mg, 3.81 mmol) in one portion at 25 °C under nitrogen. The mixture was stirred at 25 °C for 16 h. The aqueous phase was extracted with EtOAc (3 x 20 mL). The combined

organic phase was washed with brine (2 x 30 mL), dried with anhydrous Na_2SO_4, filtered, and concentrated in vacuum. The residue was purified by HPLC to give **39** (110 mg, 0.191 mmol, 25.1% yield, HPLC purity >99%) as white solid. ^{1}H NMR (400 MHz, DMSO-d_6) δ 11.89 (br. s., 1H), 7.75 (d, J = 8.0 Hz, 2H), 7.59 (d, J = 8.0 Hz, 2H), 7.54 – 7.47 (m, 1H), 7.41 – 7.32 (m, 2H), 7.26 – 7.21 (m, 1H), 7.15 – 7.10 (m, 1H), 7.05 – 7.00 (m, 1H), 5.29 (s, 1H), 5.20 (dd, J = 5.2, 13.2 Hz, 1H), 4.44 (d, J = 17.6 Hz, 1H), 4.39 (d, J = 4.8 Hz, 2H), 4.38 (d, J = 17.6 Hz, 1H), 3.47 – 3.13 (m, 8H), 3.07 – 2.90 (m, 4H), 2.79 – 2.70 (m, 1H), 2.49 – 2.37 (m, 1H), 2.07 – 1.93 (m, 1H); MS (ESI) m/z 575.3 $[M+1]^+$.

3-(4-(Benzyloxy)-1-oxoisoindolin-2-yl)piperidine-2,6-dione (40). 3-(4-Hydroxy-1-oxoisoindolin-2-yl)piperidine-2,6-dione (0.150 g, 0.576 mmol) was placed in a vial with acetone (2.5 mL), (bromomethyl)benzene (0.099 g, 0.576 mmol), and potassium carbonate (0.199 g, 1.441 mmol). The reaction mixture was heated to 45 °C for 18 h. The reaction mixture was diluted with DMSO (2 mL) and filtered. Acetone was removed under reduced pressure. The remaining mixture was purified by HPLC to give **40** (0.017 g, 0.049 mmol, 8.4% yield, HPLC purity >99%) as a white solid. ^{1}H NMR (500 MHz, DMSO-d_6) δ

10.96 (s, 1H), 7.46 – 7.53 (m, 3H), 7.41 (t, *J* = 7.25 Hz, 2H), 7.31 – 7.38 (m, 3H), 5.27 (s, 2H), 5.12 (dd, *J* = 5.04, 13.24 Hz, 1H), 4.43 (d, *J* = 17.34 Hz, 1H), 4.28 (d, *J* = 17.65 Hz, 1H), 2.92 (ddd, *J* = 5.36, 13.79, 17.42 Hz, 1H), 2.59 (td, *J* = 1.97, 15.29 Hz, 1H), 2.41 – 2.49 (m, 1H), 1.94 – 2.04 (m, 1H); MS (ESI) *m/z* 351.2 $[M+1]^+$.

2-(2,6-Dioxo-3-piperidyl)-4-hydroxy-isoindoline-1,3-dione (42). To a solution of 4-hydroxyisobenzofuran-1,3-dione (**41**) (5.0 g, 30.47 mmol) in acetic acid (60.0 mL) was added sodium acetate (5.0 g, 60.94 mmol) and 3-aminopiperidine-2,6-dione HCl (5.02 g, 30.47 mmol). The mixture was stirred at 100 °C for 2 h. The reaction mixture was concentrated to 20 mL, then poured into ice-water (300 mL). The precipitate was collected by filtration, and the filter cake was washed with ice-water (50 mL). The cake was poured into stirring EtOAc (50 mL) and petroleum ether (50 mL). After 30 min, the precipitate was removed by filtration and the filtrate was concentrated to give **42** (6.00 g, 21.88 mmol, 71.81% yield) as a purple solid. ^{1}H NMR (DMSO-d_6, 400MHz) δ 11.20 (s, 1H), 11.10 (s, 1H), 7.65 (dd, *J* = 8.4, 7.2 Hz, 1 H), 7.32 (d, *J* = 7.2 Hz, 1H), 7.25 (d, *J* =

8.4 Hz, 1H), 5.07 (dd, *J* = 12.8, 5.4 Hz, 1H), 2.93 – 2.84 (m, 1H), 2.61 – 2.53 (m, 2H), 2.04 – 2.00 (m, 1H); MS (ESI) *m/z* 275.1 $[M+1]^+$.

4-[[4-[[tert-Butyl(dimethyl)silyl]oxymethyl]phenyl]methoxy]-2-(2,6-dioxo-3-piperidyl)isoindoline-1,3-dione (43). To a solution of **42** (2.50 g, 9.12 mmol) in DMF (30.0 mL) was added K_2CO_3 (2.52 g, 18.24 mmol) and **36** (3.59 g, 9.12 mmol). The mixture was stirred at 20 °C for 3 h. The mixture was diluted with water (50 mL) and extracted with EtOAc (2 x 30 mL). The combined organic phase was washed with saturated brine (2 x 35 mL), dried with anhydrous Na_2SO_4, filtered, and concentrated under reduced pressure. The residue was purified by silica gel column chromatography to give **43** (1.80 g, 3.54 mmol, 38.8% yield) as a white solid. ^{1}H NMR ($CDCl_3$, 400 MHz) δ 11.12 (s, 1H), 7.82 (dd, *J* = 8.4, 7.2 Hz, 1H), 7.59 (d, *J* = 8.4 Hz, 1H), 7.49 – 7.45 (m, 3H), 7.34 (d, *J* = 8.0 Hz, 2H), 5.36 (s, 2H), 5.09 (dd, *J* = 12.8, 5.4 Hz, 1H), 4.72 (s, 2H), 2.93 – 2.84 (m, 1H), 2.56 – 2.53 (m, 1H), 2.45 – 2.49 (m, 1H), 2.07 – 2.01 (m, 1H), 0.90 (s, 9H), 0.08 (s, 6H); MS (ESI) *m/z* 377.1 $[M\text{-OTBS}]^+$.

[4-[[2-(2,6-Dioxo-3-piperidyl)-1,3-dioxo-isoindolin-4-yl]oxymethyl]phenyl]methylmethanesulfonate (44). *Step A.* To a solution of **43** (1.80 g, 3.54 mmol) in THF (30.00 mL) was added H_2SO_4 (0.5 M, 14.16 mL). The mixture was stirred at 20 °C for 30 min. The mixture was diluted with water (40 mL) and extracted with EtOAc (3 x 20 mL). The combined organic phase was washed with brine (2 x 25 mL), dried with anhydrous Na_2SO_4, filtered, and concentrated under reduced pressure. The crude product was triturated with petroleum ether (2 x 20 mL) to give 2-(2,6-dioxo-3-piperidyl)-4-[[4- (hydroxymethyl)phenyl]methoxy]isoindoline-1,3-dione (1.20 g, 3.04 mmol, 85.9% yield) as a white solid. ^{1}H NMR (DMSO-d_6, 400MHz) δ 11.13 (s, 1H), 7.82 (dd, J = 8.4, 7.2 Hz, 1H), 7.60 (d, J = 8.4 Hz, 1H), 7.4 – 7.45 (m, 3H), 7.36 (d, J = 8.0 Hz, 2H), 5.36 (s, 2H), 5.22 (t, J = 6.0 Hz, 1H), 5.10 (dd, J = 12.8, 5.4 Hz, 1H), 4.51 (d, J = 5.6 Hz, 2H), 2.94 – 2.85 (m, 1H), 2.62 – 2.53 (m, 2H), 2.07 – 2.01 (m, 1H).

Step B. To a solution of 2-(2,6-dioxo-3-piperidyl)-4-[[4-(hydroxymethyl)phenyl]methoxy]isoindoline -1,3-dione (600 mg, 1.52 mmol) in DMF (10.00 mL) was added methanesulfonyl chloride (970 mg, 8.47 mmol, 655.41 µL) and

DIEA (983.11 mg, 7.60 mmol, 1.33 mL) at 0 °C. The mixture was stirred at 20 °C for 2 h. The reaction was quenched by addition of aqueous saturated ammonium chloride (8 mL) at 0 °C. The mixture was diluted with water (30 mL) and extracted EtOAc (3 x 15 mL). The combined organic phase was washed with brine (2 x 5 mL), dried with anhydrous Na_2SO_4, filtered, and concentrated under reduced pressure to give crude **44** (800 mg) as a yellow solid.

4-((4-((4-(2,4-Difluorophenyl)piperazin-1-yl)methyl)benzyl)oxy)-2-(2,6-dioxopiperidin-3-yl)isoindoline-1,3-dione, HCl (45). To a solution of **44** (180 mg, 0.381 mmol) in DMF (5.00 mL) was added DIEA (0.246 g, 1.90 mmol) and 1-(2,4-difluorophenyl)piperazine (113 mg, 0.571 mmol). The mixture was stirred at RT for 16 h. The reaction mixture was diluted with water (10 mL) and extracted with EtOAc (3 x 5 mL). The combined organic phase was washed with brine (2 x 5 mL), dried with anhydrous Na_2SO_4, filtered and concentrated under vacuum. The residue was purified by HPLC and HCl (0.5 M, 3 mL) was added to the collected fractions. Fractions containing desired product were combined and dried under reduced pressure to give **45** (80 mg, 0.127 mmol, 33.5% yield, HPLC purity >97%)

as a white solid. ^{1}H NMR (400 MHz, DMSO-d_6) □ 11.37 (s, 1H), 11.12 (s, 1H), 7.84 (dd, *J* = 8.4, 7.6 Hz, 1H), 7.72 (d, *J* = 8.4 Hz, 2H), 7.63 – 7.59 (m, 3H), 7.49 (d, *J*=7.6 Hz, 1H), 7.25 (ddd, *J* = 12.4, 9.2, 2.8 Hz, 1H), 7.12 (td, *J* = 9.2, 6.0 Hz, 1H), 7.05 – 7.00 (m, 1H), 5.42 (s, 2H), 5.10 (dd, *J* = 12.8, 5.6 Hz, 1H), 4.39 (d, *J* = 4.8 Hz, 2H), 3.42 – 3.32 (m, 4H), 3.24 – 3.16 (m, 4 H), 2.93 – 2.84 (m, 1H), 2.61 – 2.52 (m, 2H), 2.07 – 2.01 (m, 1H); MS (ESI) *m/z* 575.3 $[M+1]^+$.

2-(2,6-Dioxopiperidin-3-yl)-4-((4-((4-(4-fluorophenyl)piperazin-1-yl)methyl)benzyl)oxy)isoindoline-1,3-dione (46). *Step A.* A suspension of 2-(2,6-dioxopiperidin-3-yl)-4-(4-(hydroxymethyl)benzyloxy)isoindoline-1,3-dione (1.05 g, 2.66 mmol) in a mixture of DCM and ACN (25 mL, 10 mL) was stirred in an ice bath. To the mixture was added PBr_3 (0.502 mL, 5.32 mmol) in one portion. After 5 min, the ice bath was removed and the reaction mixture was stirred at room temperature for 20 h. To the reaction mixture was added NaBr (0.822 g, 7.99 mmol) and tetrabutylammonium bromide (0.077 g, 0.240 mmol) and stirring was continued for an additional 14 h at RT. The reaction was concentrated under reduced pressure to an off-white solid. The solid was

slurried in water and filtered. The cake was washed with water and dried to give 4-((4-(bromomethyl) benzyl)-oxy)-2-(2,6-dioxopiperidin-3-yl)isoindoline-1,3-dione as a white solid (1.21 g, 99% yield). ^{1}H NMR (DMSO-d_6) δ 11.11 (s, 1H), 7.83 (dd, J = 7.3, 8.4 Hz, 1H), 7.59 (d, J = 8.5 Hz, 1H), 7.38 – 7.54 (m, 5H), 5.38 (s, 2H), 5.10 (dd, J = 5.4,12.9 Hz, 1H), 5.10 (dd, J = 5.4,12.9 Hz, 1H), 4.72 (s, 2H), 2.79 – 2.99 (m, 1H), 2.42 – 2.70 (m, 2H), 1.94 – 2.15 (m, 1H); MS (ESI) *m/z* 479 $[M+Na]^+$.

Step B. To a suspension of 4-(4-(bromomethyl)benzyloxy)-2-(2,6-dioxopiperidin-3-yl)isoindoline-1,3-dione (0.25 g, 0.547 mmol) in DCM was added 1-(4-fluorophenyl)piperazine (0.108 g, 0.601 mmol) and DIEA (0.212 g, 1.640 mmol). The mixture was stirred at RT overnight. To the reaction mixture was added water (10 mL) and DCM (15 mL) and extracted. The organic layer was concentrated then purified by silica gel column chromatography to give **46** as a yellow solid (0.24 g, 79% yield, HPLC purity >99%). ^{1}H NMR (DMSO-d_6) δ 11.11 (s, 1H), 7.83 (dd, J = 7.4, 8.5 Hz, 1H), 7.61 (d, J = 8.5 Hz, 1H), 7.42 – 7.55 (m, 3H), 7.29 – 7.41 (m, 2H), 6.97 – 7.15 (m, 2H), 6.80 – 6.97 (m, 2H), 5.36 (s, 2H), 5.09 (dd, J = 5.4, 12.7 Hz, 1H), 3.53 (s, 2H), 2.98 – 3.19 (m, 4H),

2.79 – 2.97 (m, 1H), 2.54 – 2.67 (m, 5H), 2.41 – 2.47 (m, 1H), 1.92 – 2.13 (m, 1H); ^{13}C NMR (DMSO-d_6) δ 21.95, 30.90, 48.75, 48.97, 52.51, 61.65, 69.96, 115.03, 115.31, 115.50, 116.98, 117.09, 120.21, 127.28, 129.00, 133.26, 134.79, 136.97, 137.94, 147.92, 154.35, 155.53, 157.47, 165.29, 166.75, 169.87, 172.71; Anal Calcd for $C_{31}H_{29}H_{29}FN_4O_5$+0.2 H_2O: C, 66.47; H, 5.29; N, 10.00; Found: C, 66.16; H, 5.17; N, 9.93; mp: 135 – 137 °C.

4-((4-((4-(2,4-Dichlorophenyl)piperazin-1-yl)methyl)benzyl)oxy)-2-(2,6-dioxopiperidin-3-yl)isoindoline-1,3-dione, HCl (47). To a solution of **44** (180 mg, 0.380 mmol) in DMF (5.00 mL) was added DIEA (0.246 g, 1.90 mmol) and 1-(2,4-dichlorophenyl)piperazine (132 mg, 0.571 mmol). The mixture was stirred at RT for 16 h. The reaction mixture was diluted with water (10 mL) and extracted with EtOAc (3 x 5 mL). The combined organic phase was washed with brine (2 x 5 mL), dried with anhydrous Na_2SO_4 filtered and concentrated under vacuum. The residue was purified by HPLC and HCl (0.5 M, 3 mL) was added to the collected fractions. Fractions containing desired product were combined and dried under reduced pressure to give **47** (0.089 g, 0.138 mmol, 36.1% yield, HPLC purity >99%)

as a white solid. ^{1}H NMR (400 MHz, DMSO-d_6) δ 11.26 (s, 1H), 11.12 (s, 1H), 7.85 (dd, J = 8.4, 7.6 Hz, 1H), 7.72 (d, J = 6.4 Hz, 2H), 7.63 – 7.59 (m, 4H), 7.49 (d, J = 7.2 Hz, 1H), 7.40 (dd, J = 8.4, 2.4 Hz, 1H), 7.20 (d, J = 8.8 Hz, 1H), 5.42 (s, 2H), 5.10 (dd, J = 12.8, 5.6 Hz, 1H), 4.42 (d, J = 4.8 Hz, 2H), 3.43 – 3.35 (m, 4H), 3.23 – 3.15 (m, 4H), 2.93 – 2.84 (m, 1H), 2.61 – 2.52 (m, 2H), 2.07 – 2.01 (m, 1H); MS (ESI) *m/z* 607.2 $[M+1]^+$.

4-((4-(2,4-Difluorophenyl)piperazin-1-yl)methyl)benzaldehyde (49). To a mixture of 1-(2,4-difluorophenyl)piperazine (179 mg, 0.904 mmol) and 4-(bromomethyl)benzaldehyde (**48**) (150 mg, 0.754 mmol) in ACN (5.0 mL) was added TEA (0.153 g, 1.51 mmol) in one portion at 25 °C under nitrogen. The mixture was stirred at 25 °C for 16 h. The mixture was poured into ice-water (20 mL) and stirred for 5 min. The aqueous phase was extracted with EtOAc (3 x 15 mL). The combined organic phase was washed with brine (2 x 15 mL), dried with anhydrous Na_2SO_4, filtered and concentrated under vacuum. The resulting residue was purified by silica gel column chromatography to give **49** (0.228 g, 0.721 mmol, 95% yield) as a yellow oil. MS (ESI) *m/z* 317.1 $[M+1]^+$.

3-(4-((4-((4-(2,4-Difluorophenyl)piperazin-1-yl)methyl)benzyl)amino)-1-oxoisoindolin-2-yl)piperidine-2,6-dione HCl (50). A mixture of **1** (224 mg, 0.865 mmol) and **49** (228 mg, 0.721 mmol) in acetic acid (10.00 mL) was stirred at 100 °C for 3 h under nitrogen. The reaction mixture was cooled to 25 °C and sodium borohydride (0.054 g, 1.44 mmol) was added. The reaction mixture was stirred at 25 °C for 30 min under nitrogen. The mixture was concentrated under reduced pressure and the resulting residue was purified by HPLC to give **50** (215 mg, 0.351 mmol, 48.6% yield, HPLC purity >97%) as yellow solid. ^{1}H NMR (400 MHz, DMSO-d_6) δ 11.66 (s, 1H), 11.04 (s, 1H), 7.64 (d, J = 8.2 Hz, 2H), 7.48 (d, J = 8.2 Hz, 2H), 7.29 – 7.20 (m, 2H), 7.16 – 7.08 (m, 2H), 7.01 – 6.98 (m, 1H), 6.69 (d, J = 8.0 Hz, 1H), 5.13 (dd, J = 5.2, 13.2 Hz, 1H), 4.44 (s, 2H), 4.40 – 4.30 (m, 3H), 4.26 – 4.18 (m, 1H), 3.43 – 3.28 (m, 4H), 3.28 – 3.09 (m, 4H), 3.01 – 2.87 (m, 1H), 2.63 (d, J = 16.8 Hz, 1H), 2.36 – 2.26 (m, 1H), 2.10 – 2.01 (m, 1H); MS (ESI) m/z 560.3 $[M+1]^+$.

Methyl (2*S*)-2-[(*E*)-benzylideneamino]propanoate (52). To a mixture of methyl (2*S*)-2-aminopropanoate HCl (**51**) (20.0 g, 143.3 mmol), $MgSO_4$ (12.07 g, 100.3 mmol) and TEA

(17.40 g, 171.9 mmol, 23.84 mL) in DCM (200 mL) was added benzaldehyde (15.21 g, 143.29 mmol). The reaction was stirred at 15 °C for 16 h. The mixture was filtered and the filtrate washed with brine (3 x 200 mL). The organic layer was dried over anhydrous Na_2SO_4, filtered, and the solvent was evaporated under vacuum to give crude **52** (22.00 g),obtained as a yellow oil. The residue was used in the next step without further purification.

3-Amino-3-methyl-piperidine-2,6-dione HCl (53). *Step A.* To a mixture of **52** (22.00 g, 115.04 mmol) and prop-2-enamide (12.27 g, 172.56 mmol, 11.91 mL) in THF (400 mL) was added t-BuOK (14.20 g, 126.54 mmol) in portions over 20 min at 5 °C. The reaction was stirred at 0 °C for 15 min. Solid ammonium chloride (6.77 g, 126.54 mmol) was added in portions and the mixture was stirred at 0 °C for another 15 min. The mixture was poured into ice water (400 mL) and evaporated under vacuum to ~400 mL. The resulting solid was collected by vacuum filtration and dried under vacuum to give 3-[(*E*)-benzylideneamino]-3-methyl-piperidine-2,6-dione (20.00 g, 86.86 mmol, 75.5% yield) as a white solid. The residue was used in the next step without further purification.

Step B. To a mixture of 3-[(*E*)-benzylideneamino]-3-methyl-piperidine-2,6-dione (20.00 g, 86.86 mmol) in THF (200 mL) was added aqueous HCl (4 M, 26 mL) at 0 °C. The mixture was stirred at 10 °C for 3 h. The mixture was filtered. The solvent was removed under reduced pressure. The resulting residue was washed with EtOAc (20 mL) and dried to give **53** (15.0 g, 83.98 mmol, 96% yield) as a white solid.

[(1*S*,2*R*,5*S*)-2-Isopropyl-5-methyl-cyclohexyl] N-[(3S)-3-methyl-2,6-dioxo-3-piperidyl]carbamate (55). To a mixture of **53** (15.0 g, 83.98 mmol) in THF (250 mL) and water (250 mL) was added [(1*S*,2*R*,5*S*)-2-isopropyl-5-methyl-cyclohexyl] carbonochloridate (**54**) (19.29 g, 88.18 mmol) at 0 °C. $NaHCO_3$ (28.22 g, 335.92 mmol) was added and the mixture was stirred at 0 °C for 2 h. The reaction mixture was extracted with EtOAc (3 x 500 mL). Organic layers were combined and volatile organics were removed under reduced pressure. The resulting residue was purified by silica gel column chromatography. The isolated solid was dissolved in EtOAc (30 mL) and heated to 80 °C for 30 min. The mixture was cooled to 0 °C and filtered. The solid was dissolved in EtOAc (20 mL) and heated to 80 °C for 30 min once more. The solvent was cooled to 0 °C. The

mixture became a white suspension. The mixture was filtered, and the resulting white solid was dried to give **55** (2.50 g, 7.71 mmol, 9.2% yield). MS (ESI) *m/z* 347.1 $[M+Na]^+$; SFC 1.68 min(>99.8% ee).

(3*S*)-3-Amino-3-methyl-piperidine-2,6-dione HBr (56). To a mixture of **55** (2.50 g, 7.71 mmol) in AcOH (25 mL) was added HBr (25 mL) under nitrogen. The mixture was stirred at 90 °C for 6 h. The mixture was cooled to 15 °C and stirred for 30 min. The mixture was filtered and the collected solids were washed with AcOH (3 x 10 mL) and EtOAc (3 x 15 mL). The remaining solid was dried to give **56** (1.50 g, 6.72 mmol, 87.2% yield). VCD analysis confirms absolute configuration of S with 99% confidence. ^{1}H NMR (400 MHz, DMSO-d_6) δ 11.31 (s, 1H), 8.61 (br s, 3H), 2.85 – 2.76 (m, 1H), 2.69 – 2.57 (m, 1H), 2.22 (dt, J = 5.4, 13.2 Hz, 1H), 2.11 – 2.01 (m, 1H), 1.53 (s, 3H).

(3*S*)-3-[4-[*tert*-Butyl(dimethyl)silyl]oxy-1-oxo-isoindolin-2-yl]-3-methyl-piperidine-2,6-dione (57). *Step A.* A mixture of **10** (1.610 g, 4.48 mmol), **56** (1.500 g, 6.72 mmol) and DIEA (1.740 g, 13.44 mmol) in ACN (30 mL) was stirred at 15 °C for 16 h. The mixture was extracted with EtOAc (3 x 50 mL). The organic layer was dried over anhydrous

Na_2SO_4 and solvent was evaporated under vacuum. The residue was purified by silica gel column chromatography to give crude methyl 3-[*tert*-butyl(dimethyl)silyl]oxy-2-[[[(3S)-3-methyl-2,6-dioxo-3-piperidyl]amino]methyl]benzoate (1.20 g) as a yellow oil. MS (ESI) *m/z* 421.2 $[M+1]^+$.

Step B. To a mixture of methyl 3-[*tert*-butyl(dimethyl)silyl]oxy-2-[[[(3*S*)-3-methyl-2,6-dioxo-3-piperidyl]amino]methyl]benzoate (1.200 g, 2.85 mmol) in toluene (15 mL) was added trimethylaluminum (2 M, 0.14 mL) at 15 °C. The mixture was stirred at 110 °C for 2 h. The solvent was evaporated under vacuum and the residue was purified by silica gel column chromatography to give **57** (0.600 g, 1.54 mmol, 54.2% yield) as a yellow solid. MS (ESI) *m/z* 389.0 $[M+1]^+$.

(*S*)-3-(4-((4-((4-(2,4-Difluorophenyl)piperazin-1-yl)methyl)benzyl)oxy)-1-oxoisoindolin-2-yl)-3-methylpiperidine-2,6-dione (58). To a mixture of 1-[[4-(bromomethyl)phenyl]methyl]-4-(2,4-difluorophenyl)piperazine HBr (**63**) (0.711 g, 1.54 mmol) and **57** (0.600 g, 1.54 mmol) in DMF (5 mL) was added K_2CO_3 (0.641 g, 4.63 mmol) at 15 °C. The mixture was stirred at 15 °C for 16 h. The mixture was filtered and the solvent was evaporated under

vacuum. The residue was purified by HPLC to give a white solid. The solid was further purified by preparative chiral HPLC to give **58** (0.221 g, 0.38 mmol, 73.7% yield, HPLC purity >98%) as a white solid. ^{1}H NMR (400MHz, DMSO-d_6) δ 10.85 (br s, 1H), 7.56 – 7.43 (m, 3H), 7.42 – 7.29 (m, 3H), 7.27 – 7.13 (m, 2H), 7.11 – 6.92 (m, 2H), 5.26 (br s, 2H), 4.75 – 4.52 (m, 2H), 3.55 (br s, 2H), 2.97 (br s, 4H), 2.82 – 2.55 (m, 7H), 1.89 (br d, J = 11.9 Hz, 1H), 1.69 (s, 3H); MS (ESI) *m/z* 575.3 $[M+1]^+$; SFC 3.41 min(>99.8% ee).

(*R*)-3-(4-((4-((4-(2,4-Difluorophenyl)piperazin-1-yl)methyl)benzyl)oxy)-1-oxoisoindolin-2-yl)-3-methylpiperidine-2,6-dione (59). The title compound (0.109 g, 0.19 mmol, 21.4% yield, HPLC purity >98%) was obtained as a white solid which originated from the same synthetic route used to make **58**, the only difference being that intermediate **55** was only crystallized once instead of twice. Preparative chiral HPLC after the final step provided **59**. ^{1}H NMR (400 MHz, DMSO-d_6) δ 11.54 (br. s., 1H), 10.87 (s, 1H), 7.72 (d, J = 8.2 Hz, 2H), 7.61 (d, J = 8.0 Hz, 2H), 7.50 – 7.43 (m, 1H), 7.35 – 7.21 (m, 3H), 7.13 (dt, J = 5.8, 9.4 Hz, 1H), 7.07 – 6.99 (m, 1H), 5.38 – 5.27 (m, 2H), 4.77 – 4.56 (m, 2H), 4.44 – 4.35

(m, 2H), 3.48 – 3.30 (m, 5H), 3.22 (d, J = 8.3 Hz, 4H), 2.81 – 2.58 (m, 2H), 1.96 – 1.85 (m, 1H), 1.70 (s, 3H); MS (ESI) *m/z* 575.3 $[M+1]^+$; SFC 4.05 min(>99.8% ee).

(S/R)-3-(4-((4-((4-(2,4-Difluorophenyl)piperazin-1-yl)methyl)benzyl)oxy)-1-oxoisoindolin-2-yl)piperidine-2,6-dione (60, 61). Compounds **60** and **61** resulted from the chiral separation of racemic compound **13** (0.300 g, 0.535 mmol) using preparative chiral HPLC. The conditions used are as follows:

Isocratic Method: 15% B in 40 min. Column: Astec_Chirobiotik_V2, 21.2 x 250mm, 5u. A: 0.1% formic acid in water, B: 0.1% formic acid in ACN.

Fractions containing the desired product were combined and volatile organics were removed under reduced pressure to give (S)-3-(4-((4-((4-(2,4-difluorophenyl)piperazin-1-yl)methyl)benzyl)oxy)-1-oxoisoindolin-2-yl)piperidine-2,6-dione (**60**) (0.135 g, 0.234 mmol, 45.0% yield, HPLC purity >99%, ee > 99%) and (R)-3-(4-((4-((4-(2,4-difluorophenyl)piperazin-1-yl)methyl)benzyl)oxy)-1-oxoisoindolin-2-yl)piperidine-2,6-dione (**61**) (0.131 g, 0.241 mmol, 43.7% yield, HPLC purity > 99%, ee > 99%) as white

solids. Absolute stereochemistry of **60** was later confirmed by resynthesis using the chiral synthetic route described in scheme 8.

60: ^{1}H NMR (400 MHz, DMSO-d_6) δ 10.97 (br s, 1H), 7.41– 7.54 (m, 3H), 7.30 – 7.39 (m, 4H), 7.17 (ddd, J = 2.81, 9.17, 12.35 Hz, 1H), 7.01 – 7.10 (m, 1H), 6.93 – 7.01 (m, 1H), 5.24 (s, 2H), 5.11 (dd, J = 5.01, 13.33 Hz, 1H), 4.37 – 4.48 (m, 1H), 4.21 – 4.31 (m, 1H), 3.54 (s, 2H), 2.84 – 3.00 (m, 5H), 2.54 – 2.61 (m, 5H), 2.37 – 2.47 (m, 1H), 1.92 – 2.04 (m, 1H); MS (ESI) m/z 561.2[M+1]$^+$.

61:^{1}H NMR (400 MHz, DMSO-d_6) δ 10.97 (s, 1H), 7.42 – 7.53 (m, 3H), 7.29 – 7.39 (m, 4H), 7.17 (ddd, J = 2.87, 9.17, 12.41 Hz, 1H), 7.01 – 7.10 (m, 1H), 6.94 – 7.01 (m, 1H), 5.24 (s, 2H), 5.11 (dd, J = 5.01, 13.20 Hz, 1H), 4.36 – 4.47 (m, 1H), 4.20 – 4.31 (m, 1H), 3.54 (s, 2H), 2.84 – 3.01 (m, 5H), 2.59 (br s, 5H), 2.35 – 2.47 (m, 1H), 1.92 – 2.04 (m, 1H); MS (ESI) m/z 561.2[M+1]$^+$.

(4-((4-(2,4-Difluorophenyl)piperazin-1-yl)methyl)phenyl)methanol (62). To a mixture of **49** (1.70 g, 5.37 mmol) in MeOH (20 mL) was added sodium borohydride (0.30 g, 8.06 mmol)

at 0 °C. The mixture was stirred at 0 °C for 2 h. The solvent was evaporated under vacuum and the remaining residue was washed with water (3 x 10 mL) to give **62** (1.500 g, 4.71 mmol, 87.7%yield) as a yellow oil. MS (ESI) *m/z* 319.1 $[M+1]^+$.

1-[[4-(Bromomethyl)phenyl]methyl]-4-(2,4-difluorophenyl)piperazine HBr (63). To a mixture of **62** (1.500 g, 4.71 mmol) in DCM (20 mL) was added thionyl bromide (1.960 g, 9.42 mmol, 0.73 mL) at 15 °C. The mixture was stirred at 15 °C for 2 h. Petroleum ether (20 mL) was added to the reaction mixture and the mixture was filtered. The collected solid was dried under vacuum to give **63** (2.00 g, 4.33 mmol, 91.9% yield) as a yellow solid. MS (ESI) *m/z* 381.0 $[M+1]^+$.

***tert*-Butyl-4-[[2-(1-carbamoyl-4-methoxy-4-oxo-butyl)-1-oxo-isoindolin-4-yl]oxymethyl]benzoate (65).** To a suspension of **11** (210.0 g, 718.46 mmol) and tert-butyl 4-(bromomethyl)benzoate (**64**) (194.81 g, 718.46 mmol) in NMP (2.10 L) was added K_2CO_3 (297.90 g, 2.16 mol). The reaction mixture was stirred at 25 °C for 4 h, then was poured into water (3 L), extracted with EtOAc (3 x 5 L). The organic phase was washed with brine (5 L), dried with Na_2SO_4, and concentrated under reduced pressure.

During the process of concentration, a white solid was formed. Collected by filtration, the filter cake was washed with a 1:1 mixture of petroleum ether;EtOAc (350 mL), to give after drying **65** (200.0 g, 414.9 mmol, 57.7% yield) as white solid. ^{1}H NMR (400 MHz, DMSO-d_6) □ 7.93 (d, J = 8.38 Hz, 2H), 7.61 (d, J = 7.94 Hz, 3H), 7.41 – 7.48 (m, 1H), 7.28 (dd, J = 7.94, 18.52 Hz, 2H), 7.21 (s., 1H), 5.34 (s, 2H), 4.74 (dd, J=4.85, 10.14 Hz, 1H), 4.54 – 4.61 (m, 1H), 4.41 – 4.48 (m, 1H), 3.50 (s, 3H), 3.29 (t, J = 6.84 Hz, 1H), 2.69 (s, 1H), 2.23 – 2.30 (m, 2H), 2.14 – 2.23 (m, 1H), 2.02 – 2.12 (m, 1H), 1.89 (m, 1H), 1.54 (s, 9H). MS (ESI) *m/z* 483 $[M+1]^+$.

***tert*-Butyl 4-[[2-(2,6-dioxo-3-piperidyl)-1-oxo-isoindolin-4-yl]- oxymethyl]benzoate (66).** A solution of **65** (99.60 g, 206.42 mmol) in THF (3.00 L) was cooled in a dry ice/acetone bath to -70 °C. While stirring, t-BuOK (25.48 g, 227.06 mmol) was added in one portion to the clear solution. The reaction mixture turned pale yellow and was stirred for 1.5 h at -70 °C. A cooled 1N aqueous solution of HCl (900 mL) was rapidly added to the reaction mixture while maintaining the temperature at -70 °C. The mixture immediately turned milky white and the dry ice-acetone bath was removed. The mixture was concentrated to

remove most of the THF. Upon concentration, a white solid precipitated out. The solid was collected by vacuum filtration and the filter cake was washed with water (200 mL). The material was dried to give **66** (68.34 g, 151.7 mmol, 73.5% yield) as a white solid. ^{1}H NMR (400 MHz, DMSO-d_6) ☐ 10.99 (s, 1H), 7.92 (d, J = 8.22 Hz, 2H), 7.60 (d, J = 8.22 Hz, 2H), 7.44 – 7.51 (m, 1H), 7.31 (dd, J = 7.83, 19.56 Hz, 2H), 5.35 (s, 2H), 5.12 (dd, J = 5.09, 13.30 Hz, 1H), 4.41 – 4.49 (m, 1H), 4.26 – 4.34 (m, 1H), 2.85 – 2.98 (m, 1H), 2.59 (d, J = 17.61 Hz, 1H), 2.38 – 2.48 (m, 1H), 2.01 (s, 1H), 1.54 (s, 9H).

Perfluorophenyl 4-(((2-(2,6-dioxopiperidin-3-yl)-1-oxoisoindolin-4-yl)oxy)methyl)benzoate (67). *Step A.* To a mixture of **66** (350.0 g, 776.95 mmol) in DCM (1.22 L) was added TFA (1.88 kg, 16.51 mol, 1.22 L). The mixture was stirred at 25 °C for 12 h. The reaction mixture was filtered and the filter cake was washed with DCM (3 x 500 mL). The filtrate was concentrated and filtered. The resulting filter cake was washed with DCM (3 x 200 mL). The two solids were combined and dried to give 4-(((2-(2,6-dioxopiperidin-3-yl)-1-oxoisoindolin-4-yl)oxy)methyl)benzoic acid (325.0 g, 824 mmol, 100% yield) as white solid. ^{1}H NMR (400 MHz, DMSO-d_6) ☐ 10.98 (s, 1H), 7.97 (d, J =

7.94 Hz, 2H), 7.61 (d, *J* = 7.94 Hz, 2H), 7.45 – 7.52 (m, 1H), 7.32 (dd, *J* = 7.72, 13.45 Hz, 2H), 5.35 (s, 2H), 5.12 (dd, *J* = 4.85, 13.23 Hz, 1H), 4.41 – 4.50 (m, 1H), 4.26 – 4.35 (m, 1H), 2.84 – 2.98 (m, 1H), 2.58 (d, *J* = 18.08 Hz, 1H), 2.39 – 2.46 (m, 1H), 1.94 – 2.04 (m, 1H). MS (ESI) *m/z* 393 $[M-1]^+$.

Step B. Perfluorophenyl 2,2,2-trifluoroacetate (0.805 mL, 4.68 mmol) was added to a heterogeneous solution of 4-(((2-(2,6-dioxopiperidin-3-yl)-1-oxoisoindolin-4-yl)oxy)methyl)benzoic acid (739 mg, 1.874 mmol) in THF (5 mL), and DIEA (1.3 mL, 7.44 mmol) at RT. DMF (10.0 mL) was added in portions until the solution was pink and homogeneous. The reaction was diluted with water (5 mL) giving a copious white precipitate. The precipitate was collected by filtration, washed with water, and dried to provide **67** (598.1 mg, 1.067 mmol, 57.0% yield) as a light grey solid. MS (ESI) *m/z* 561.2 $[M+1]^+$.

3-(4-((4-(4-(2,4-Difluorophenyl)piperazine-1-carbonyl)benzyl)oxy)-1-oxoisoindolin-2-yl)piperidine-2,6-dione (68). A flask containing **67** (407 mg, 0.726 mmol) and 1-(2,4-difluorophenyl)piperazine (309 mg, 1.559 mmol) was treated with DMF (2.0 mL) and DIEA

(0.254 mL, 1.452 mmol) for 10 min. The reaction mixture was purified directly by semi-preparative HPLC to provide **68** (310.9 mg, 0.541 mmol, 74.5% yield, HPLC purity >99%) as a white powder. ^{1}H NMR (500 MHz, DMSO-d_6) δ 10.97 (s, 1H), 7.59 (d, J = 8.20 Hz, 2H), 7.43 – 7.54 (m, 3H), 7.35 (dd, J = 7.88, 1.89 Hz, 2H), 7.22 (ddd, J = 12.30, 9.14, 2.84 Hz, 1H), 7.11 (td, J = 9.46, 5.99 Hz, 1H), 7.02 (td, J = 8.35, 2.21 Hz, 1H), 5.32 (s, 2H), 5.13 (dd, J = 13.40, 5.20 Hz, 1H), 4.46 (d, J = 17.34 Hz, 1H), 4.30 (d, J = 17.65 Hz, 1H), 3.66 – 3.88 (m, 2H), 3.37 – 3.60 (m, 2H), 2.84 – 3.11 (m, 5H), 2.54 – 2.69 (m, 2H), 2.46 (d, J = 8.83 Hz, 2H), 1.94 – 2.04 (m, 1H); MS (ESI) m/z 575.2 $[M+1]^+$.

3-(4-((4-(4-(4-Fluorophenyl)piperazine-1-carbonyl)benzyl)oxy)-1-oxoisoindolin-2-yl)piperidine-2,6-dione (69). A solution of **67** (100 mg, 0.178 mmol) in DMF (1.0 mL) was added to a vial containing 1-(4-fluorophenyl)piperazine (50.8 mg, 0.282 mmol), DIEA (0.060 mL, 0.344 mmol), and DMF (0.5 mL) for 10 min. The reaction mixture was purified by semi-preprative HPLC to give **69** (73.6 mg, 0.132 mmol, 74.1% yield, HPLC purity >99%) as a white solid. ^{1}H NMR (500 MHz, DMSO-d_6) δ 10.97 (s, 1H), 7.59 (d, J = 8.20 Hz, 2H), 7.49 – 7.54 (m, 1H), 7.48 (d, J = 8.20 Hz, 2H), 7.35 (dd, J = 7.88, 2.84 Hz, 2H), 7.04 – 7.13 (m, 2H), 6.94 – 7.02 (m, 2H), 5.32 (s, 2H), 5.13 (dd, J = 13.40, 5.20 Hz, 1H),

4.46 (d, *J* = 17.34 Hz, 1H), 4.30 (d, *J* = 17.34 Hz, 1H), 3.76 (br. s., 2H), 3.49 (br. s., 2H), 3.11 (br. s., 4H), 2.92 (ddd, *J* = 17.50, 13.56, 5.52 Hz, 1H), 2.54 – 2.68 (m, 1H), 2.35 – 2.48 (m, 1H), 1.94 – 2.05 (m, 1H); MS (ESI) *m/z* 557.2 $[M+1]^+$.

3-(4-((4-(4-(4-Chlorophenyl)piperazine-1-carbonyl)benzyl)oxy)-1-oxoisoindolin-2-yl)piperidine-2,6-dione (70). A portion of **67** (102.1 mg, 0.182 mmol) was added to a vial containing 1-(4-chlorophenyl)piperazine (45.7 mg, 0.232 mmol), DIEA (0.08 mL, 0.458 mmol), and DMF (1.5 mL). The reaction was heated to 60 °C for 10 min. The reaction mixture was purified by semi-preparative HPLC to give **70** (54.1 mg, 0.094 mmol, 51.8% yield, HPLC purity >99%) as a white solid. ^{1}H NMR (500 MHz, DMSO-d_6) δ 10.97 (s, 1H), 7.59 (d, *J* = 8.51 Hz, 2H), 7.43 – 7.55 (m, 3H), 7.35 (dd, *J* = 7.88, 2.52 Hz, 2H), 7.20 – 7.29 (m, 2H), 6.92 – 7.03 (m, 2H), 5.32 (s, 2H), 5.13 (dd, *J* = 13.24, 5.04 Hz, 1H), 4.46 (d, *J* = 17.34 Hz, 1H), 4.30 (d, *J* = 17.34 Hz, 1H), 3.75 (br. s., 2H), 3.39 – 3.57 (m, 2H), 3.19 (br. s., 4H), 2.86 – 2.98 (m, 1H), 2.54 – 2.68 (m, 2H), 2.35 – 2.47 (m, 2H), 1.94 – 2.05 (m, 1H); MS (ESI) *m/z* 573.2 $[M+1]^+$.

3-(4-((4-(4-(2,4-Dichlorophenyl)piperazine-1-carbonyl)benzyl)oxy)-1-oxoisoindolin-2-yl)piperidine-2,6-dione (71). A solution of **67** (103.1 mg, 0.184 mmol) in DMF (1.0 mL) was added to a vial containing 1-(2,4-dichlorophenyl)piperazine (87.1 mg, 0.377 mmol). DIEA (0.10 mL, 0.573 mmol) was added. The reaction was stirred at RT for 10 min. The reaction mixture was purified by semi-preparative HPLC to give **71** (56.1 mg, 0.092 mmol, 50.2% yield, HPLC purity >97%). ^{1}H NMR (500 MHz, DMSO-d_6) δ 10.97 (s, 1H), 7.55 – 7.61 (m, 3H), 7.46 – 7.54 (m, 3H), 7.39 (dd, J = 8.83, 2.52 Hz, 1H), 7.32 – 7.37 (m, 2H), 7.20 (d, J = 8.51 Hz, 1H), 5.32 (s, 2H), 5.13 (dd, J = 13.24, 5.04 Hz, 1H), 4.46 (d, J = 17.34 Hz, 1H), 4.30 (d, J = 17.65 Hz, 1H), 3.79 (br. s., 2H), 3.44 – 3.55 (m, 1H), 2.85 – 3.09 (m, 5H), 2.54 – 2.68 (m, 2H), 2.35 – 2.47 (m, 2H), 1.92 – 2.06 (m, 1H); MS (ESI) *m/z* 607.2 $[M+1]^+$.

4-(4-(4-(Chloromethyl)benzyl)piperazin-1-yl)-3-fluorobenzonitrile (73). 1,4-bis(chloromethyl)benzene (51.2 g, 292 mmol) was placed in a flask with ACN (195 mL) and DMF (195 mL) and allowed to stir at RT until all the solids dissolved. DIEA (51.1 mL, 292 mmol) was then added followed by 3-fluoro-4-(piperazin-1-yl)benzonitrile (**72**) (20 g,

97 mmol) in one portion. The reaction was heated to 60 °C for 1 h. Acetonitrile was removed under reduced pressure and the remaining mixture was partitioned between EtOAc (1.0 L), water (700 mL), and brine (300 mL). The organic layer was separated, and the aqueous layer was extracted with EtOAc twice more. The organic layers were combined and volatile organics were removed under reduced pressure. The resulting solid was purified by silica gel column chromatography to give **73** (22.7 g, 66.0 mmol, 67.7% yield) as an off-white solid. ^{1}H NMR (400 MHz, CHLOROFORM-*d*) δ 7.33 – 7.39 (m, 5H), 7.29 (d, *J* = 1.96 Hz, 1H), 7.25 (d, *J* = 1.96 Hz, 1H), 6.91 (t, *J* = 8.56 Hz, 1H), 4.60 (s, 2H), 3.58 (s, 2H), 3.19 – 3.27 (m, 4H), 2.58 – 2.66 (m, 4H); MS (ESI) *m/z* 344.2 $[M+1]^+$.

***tert*-Butyl (4S)-5-amino-4-(4-hydroxy-1-oxo-isoindolin-2-yl)-5-oxo-pentanoate (74).** *Step A.* To a solution of tert-butyl (4S)-4,5-diamino-5-oxo-pentanoate (130 g, 643 mmol) in ACN (4.0 L) was added **10** (210 g, 584 mmol) and DIEA (113 g, 877 mmol). The reaction mixture was stirred at 50 °C for 16 h, then was concentrated to remove most of the ACN. The residue was dissolved in methyl tert-butyl ether (2.0 L) and water (1.5 L). The organic layer was washed with saturated monopotassium phosphate (1.0 L x 2), brine (1.0 mL),

dried over anhydrous Na_2SO_4, filtered and concentrated to give crude tert-butyl (4S)-5-amino-4-[4-[tert-butyl(dimethyl)silyl]oxy-1-oxo- isoindolin-2-yl]-5-oxo-pentanoate (524 g). The material was used in the next step without further purification.

Step B. To a solution of tert-butyl (4S)-5-amino-4-[4-[tert-butyl(dimethyl)silyl]oxy-1-oxo-isoindolin -2-yl]-5-oxo-pentanoate (275 g, 613 mmol,) in MeOH (2.0 L) was added tetrabutylammonium fluoride trihydrate (38.7 g, 123 mmol). The mixture was stirred at 18 °C for 16 h. The reaction mixture was concentrated to remove most of the MeOH. The residue was partitioned between DCM/water (3L/2L). The organic layer was washed with brine (1.0 L), dried over anhydrous Na_2SO_4, filtered, and concentrated. The crude material was purified by silica gel column chromatography to give the product (260 g). The solid was added into ACN (750 mL), and the mixture was stirred at 60 °C for 2 h, then cooled to 18 °C and stirred for another 2 h. The solid was collected by filtration and the cake was dried to give **74** (248 g, 60.5% yield) as gray solid. (Purity 100%, ee value 100%) ^{1}H NMR (400 MHz, DMSO-d_6) δ 10.00 (s, 1H), 7.54 (s, 1H), 7.29 (t, J = 7.6 Hz, 1H), 7.14 (d, J = 4.8 Hz, 2H), 4.72 – 4.68 (m, 1H), 4.49 – 4.28 (m, 2H), 2.17 – 1.97 (m, 4H), 1.31 (s, 9H).

(S)-*tert*-Butyl 5-amino-4-(4-((4-((4-(4-cyano-2-fluorophenyl)piperazin-1-yl)methyl)benzyl)oxy)-1-oxoisoindolin-2-yl)-5-oxopentanoate (75). A portion of **74** (22.05 g, 65.9 mmol) was placed in a flask with **73** (22.67 g, 65.9 mmol), K_2CO_3 (18.23 g, 132 mmol), and DMF (330 mL). The reaction mixture was heated to 45 °C for 16 h. The reaction was diluted with EtOAc (50 mL) and filtered. The filtrate was partitioned with EtOAc (900 mL), water (600 mL), and brine (200 mL). The organic layer was isolated and washed again with water (600 mL). The organic layer was separated, dried over Na_2SO_4, and volatile organics were removed under reduced pressure. The resulting residue was treated with 20% EtOAc in hexanes and volatiles were removed under reduced pressure to give **75** (44.02 g, 68.6 mmol, 100% yield) as an off-white solid. ^{1}H NMR (400 MHz, CHLOROFORM-*d*) δ 7.43 – 7.49 (m, 2H), 7.40 (s, 4H), 7.36 (dd, *J* = 8.38, 1.28 Hz, 1H), 7.29 (d, *J* = 1.96 Hz, 1H), 7.26 (d, *J* = 1.83 Hz, 1H), 7.11 (dd, *J* = 7.64, 1.16 Hz, 1H), 6.92 (t, *J* = 8.50 Hz, 1H), 6.23 (br s, 1H), 5.24 – 5.32 (m, 1H), 5.15 (s, 2H), 4.86 – 4.94 (m, 1H), 4.38 – 4.55 (m, 2H), 3.61 (s, 2H), 3.18 – 3.32 (m, 4H), 2.58 – 2.70 (m, 4H), 2.09 – 2.47 (m, 4H), 1.43 (s, 8H); MS (ESI) *m/z* 642.4 $[M+1]^+$.

(S)-4-(4-(4-(((2-(2,6-Dioxopiperidin-3-yl)-1-oxoisoindolin-4-yl)oxy)methyl)benzyl)piperazin-1-yl)-3-fluorobenzonitrile (4). A portion of **75** (12.1 g, 18.86 mmol) was placed in a vial with ACN (190 mL) and benzenesulfonic acid (3.96 g, 24.51 mmol). The reaction mixture was placed under vacuum and purged with nitrogen. This was repeated once more and the mixture was then heated to 85 °C overnight under a nitrogen atmosphere. The reaction mixture was poured warm directly into 2 separatory funnels containing DCM (1.0 L) and EtOAc (300 mL). To this mixture, a saturated solution of $NaHCO_3$ (900 mL), water (100 mL), and brine (450 mL) were added. The pH of the aqueous layer was tested to verify it was basic. The organic layer was isolated and the aqueous layer was extracted once more with DCM (800 mL) and EtOAc (200 mL). The organic layer was separated and all organic layers were combined and dried over anhydrous $MgSO_4$, and concentrated to give a solid. To the solid was added EtOAc (400 mL) and hexanes (50 mL). Volatiles were removed under reduced pressure. To the resulting solid was added EtOAc (150 mL) and the mixture was stirred at 40 °C for 30 min until it became an homogeneous slurry. Solids were collected by vacuum filtration, washed with EtOAc (100 mL), and dried to afford **4** as a white solid (7.7 g, 13.5 mmol,

72% yield, HPLC purity >99%, ee value >97%). ^{1}H NMR (400 MHz, DMSO-d_6) δ 10.96 (s, 1H), 7.68 (dd, J = 13.45, 1.83 Hz, 1H), 7.56 (dd, J = 8.44, 1.83 Hz, 1H), 7.43 – 7.52 (m, 3H), 7.29 – 7.39 (m, 4H), 7.11 (t, J = 8.80 Hz, 1H), 5.24 (s, 2H), 5.11 (dd, J = 13.20, 5.14 Hz, 1H), 4.22 – 4.46 (m, 2H), 3.54 (s, 2H), 3.12 – 3.22 (m, 4H), 2.85 – 2.97 (m, 1H), 2.53 – 2.62 (m, 2H), 2.38 – 2.48 (m, 2H), 1.93 – 2.03 (m, 1H); MS (ESI) m/z 568.2 $[M+1]^+$.

Fluorescence Resonance Energy Transfer-based Cereblon Binding Description: This assay monitors time-resolved fluorescence resonance energy transfer (TR-FRET) between a Cy5-conjugated CELMoD bound in the tri-tryptophan pocket of CRBN and a europium-conjugated anti-His antibody bound to a 6×His tag on the N-terminus of CRBN. The FRET efficiency (the ratio of FRET to non-FRET emission = 665 nM/615 nM) is determined by exciting the europium at 340 nM and monitoring emissions at 615 nM (non-FRET emission) and 665 nm (FRET emission). When a competing compound is added to displace the Cy5-conjugated CELMoD from cereblon, the FRET efficiency is

decreased. Consequently, the concentration-dependent loss of FRET signal can be used to determine the IC_{50} of CRBN binding.

Fluorescence Resonance Energy Transfer-based Cereblon Binding Assay: A solution containing 60 nM purified 6×His-CRBN_005-DDB1_026 (CRBN a.a. 1-442, DDB1 a.a. 1-1140, generated in-house) 3 nM Eu-anti-His Tag Antibody (catalog number PV5596, Thermo Fisher), and 30 nM CC0782985 was pre-mixed in FRET-assay buffer (50 mM HEPES pH 7, 150 mM NaCl, 0.005% Tween 20). Thirty microliters of assay mixture were distributed into the wells of white, solid bottom 384-well plates containing compounds previously distributed by acoustic dispensing. The plates were then mixed on a shaker for 5 seconds and spun down, with a total pre-incubation time of approximately 10 minutes, before scanning on a Pherastar plate reader with excitation at 340 nM. Emissions were monitored at 615 nM (non-FRET emission) and 665 nm (FRET emission), using a 700 µs TR-FRET delay. The FRET/non-FRET emission ratio (ratio of signal from 665/615) was used to determine FRET efficiency, and the loss of FRET

efficiency was plotted against compound concentration to determine the relative binding affinity (IC_{50}).

ePL Degradation Description: To monitor protein degradation, we used the DiscoverX Enzyme Fragment Complementation Assay (EFC) technology. This system relies on having two different components of the β-galactosidase enzyme expressed for activity. The large protein fragment of β-galactosidase is included in the InCELL Hunter™ detection reagent that is added at the end of the assay. The small peptide fragment (the enhanced ProLabel (ePL)) that is required for β-galactosidase activity is expressed on the protein of interest (example: Aiolos and GSPT1). When the ePL tagged protein has been degraded through the E3-ligase mechanism, there is a loss in the β-galactosidase activity. The active β-galactosidase hydrolyzes a substrate that is turned over by luciferase to give a chemiluminescent signal.

ePL Degradation Assay: DF15 multiple myeloma cells stably expressing ePL-tagged Aiolos and GSPT1 were generated via lentiviral infection with pLOC-ePL-Aiolos and pLOC-ePL-GSPT1. Cells were dispensed into 384-well plates (Corning #3712) that were pre-spotted with compounds. Compounds were dispensed by an acoustic dispenser

(ATS acoustic transfer system from EDC Biosystems) into a 384-well in a 10-point dose−response curve using a 3-fold dilution. A DMSO control is added to the assay. Twenty-five microliters of media (RPMI-1640 + 10% Heat Inactivated FBS +25mM Hepes+1mM Na Pyruvate+1X NEAA + 0.1% Pluronic F-68 + 1x Pen Strep Glutamine) containing 5000 cells was dispensed per well. Assay plates were incubated at 37°C with 5% CO_2 for four hours. After incubation, 25 µL of the InCELL Hunter™ Detection Reagent Working Solution (DiscoverX, cat #96-0002, Fremont, CA) was added to each well and incubated at room temperature for 30 min protected from light. After 30 min, luminescence was read on a PHERAstar luminometer (Cary, NC).

To determine the half-maximal effective concentration (EC_{50}) values for Aiolos or GSPT1 degradation, a four parameter logistic model was used: (Sigmoidal Dose-Response Model) (FIT= (A+((B-A)/1+((C/x)^D)))) where C is the inflection point (EC_{50}), D is the correlation coefficient, and A and B are the low and high limits of the fit respectively). The lower limit of the fit (value A) is referred to as Y_{min}. A luciferase inhibitor at a concentration of 20 µM was used as the control with a Ymin value = 0. The maximum limit is the Y_{max}

for the DMSO control. The curves were processed and evaluated using Activity Base (IDBS).

Immunoblot Analysis. H929 R10-1 cells were treated with DMSO and test compounds for 4h and 72h as indicated in Figure 11a. Cells were then washed with 1 X PBS and lysed in Chris Buffer [0.5% NP-40 (Igepal CA-630), 50mM Tris pH 8, 10% Glycerol, 1mM EDTA 200mM NaCl, complete ULTRA protease inhibitor tablet (Roche), PhosSTOP phosphatase inhibitor tablet (Roche) and 0.2mM p-APMSF (Calbiochem)]. Clarified cell lysates were subjected to immunoblot analysis with the following antibodies: rabbit anti-Ikaros monoclonal antibody (#9034, Cell Signaling), rabbit anti-Aiolos polyclonal antibody (#12720, Cell Signaling), mouse anti-β-Tubulin monoclonal antibody (#T5201, Sigma), rabbit anti-IRF4 monoclonal antibody (#4299, Cell Signaling), rabbit anti-c-Myc monoclonal antibody (#ab32072, Abcam), mouse anti-p27 monoclonal antibody (#610241, BD Transduction Laboratories), rabbit anti-Phospho-Rb S807/811 polyclonal antibody (#9308, Cell Signaling), rabbit anti-Survivin monoclonal antibody (#2808, Cell Signaling), rabbit anti-BIM monoclonal antibody (#2933, Cell Signaling), rabbit anti-

Cleaved-Caspase-1 monoclonal antibody (#4199, Cell Signaling), rabbit anti-Cleaved-Caspase-7 polyclonal antibody (#9491, Cell Signaling), rabbit anti-Cleaved-Caspase-3 polyclonal antibody (#9661, Cell Signaling), rabbit anti-Cleaved-PARP monoclonal antibody (#5625, Cell Signaling), goat anti-rabbit IgG (H+L) Alexa Fluor 700 (#A21038, Invitrogen) and goat anti-mouse IgG (H+L) IRDye 800 (#610-132-121, Rockland).

Growth Inhibition Assay. H929 R10-1 cells were maintained in log-phase at 37ºC with 5% CO_2 using the indicated media. Cell density and viability were monitored by trypan blue exclusion using the Vi-Cell XR cell viability analyzer. Seeding densities were established after a 5-day growth CellTiter-Glo® (CTG) assay. Compounds were dispensed as 10-point duplicate DRCs starting at 10μM with (1:3) dilutions using the EDC ATS-100 acoustic dispenser into black clear-bottom 384-well plates in 0.1% DMSO with a final volume of 40μl. Cells were plated using the Integra VIAFLO384 pipette at 5000 cells/well followed by centrifugation at 600rpm for 1min. Any remaining bubbles were removed from culture wells using ethanol vapor and plates incubated for 5 days with 2 dummy plates on top and bottom of plate stacks. Compound effect on proliferation was

measured using the standard CTG assay which quantifies ATP production through luminescence. Relative luminescence units (RLUs) were generated by dispensing 20µl per well of CTG using a Multidrop™ Combi Reagent Dispenser, plates shaken for 15 seconds, incubated in the dark at room temperature for 1 hour and read on an Envision luminescence detector.

IN VIVO STUDIES

In Vivo Studies. All animal studies were performed under protocols approved by the Celgene Institutional Animal Care and Use Committee (IACUC). Animals were acclimatized to the animal housing facility for a period of 7 days prior to the beginning of the experiment. Female 6-8 weeks old CB17 SCID (severe combined immunodeficiency) (Charles River Laboratories) mice were housed in a barrier facility in micro-isolator cages at 10 animals per cage. Mice were fed with Harlan-Teklad LM- 485 Mouse/Rat Sterilizable Diet and autoclaved water ad libitum and maintained on a 12 h light/dark cycle.

NCI-H929-1051, a lenalidomide-resistant version of NCI-H929 plasmacytoma cells were generated in vitro. Parental NCI-H929 cells lines were obtained from the American

Tissue Culture Collection (Gaithersburg, MD). The cells were grown in growth medium containing RPMI 1640 with 2 mM L-glutamine adjusted to contain 90% medium and 10% FBS. The lenalidomide-resistant H929-1051 cell line was generated by growth in the continual presence of 10 μM lenalidomide. Cells that were expanded for implantation in vivo were grown in the continuous presence of 10 μM lenalidomide.

SCID mice were inoculated subcutaneously with 10×10^6 NCI-H929-1051 cells. Tumor volumes were determined prior to the initiation of treatment and considered as the starting volumes. Mice with tumors of approximately 150 mm^3 were randomized and treated orally at various doses of compound 4 (n =8−10/group). Tumors were measured twice a week for the duration of the study. The long and short axes of each tumor were measured using a digital caliper in millimeters and the tumor volumes were calculated using the formula: $width^2 \times length/2$. The tumor volumes were expressed in cubic millimeters (mm^3).

Xenograft data are expressed as mean ± standard error of the mean (SEM). Statistical analyses were performed using GraphPad Prism. A one-way analysis of variance (ANOVA) was performed for tumor volume measurements. Post-hoc analysis

was performed using Dunnett's test where all treatment groups are compared with the vehicle control.

AUTHOR INFORMATION

Corresponding Author

Joshua Hansen, Tel: 858-795-4910, jhansen@celgene.com

Notes

The authors declare no competing financial interest. All authors are currently employees of Celgene, except Courtney G. Havens, Veronique Plantevin, Timothy Kercher, Brian Cathers, Thomas Daniel, Katerina Leftheris, and Mehran Moghaddam who were employees of Celgene at the time of their contribution to this work.

ACKNOWLEDGMENT

Thanks to George Muller and his chemistry team for their efforts leading to the development of lenalidomide and pomalidomide which served to enable starting points and comparators for this work.

ABBREVIATIONS

CRBN, Cereblon; CUL4, cullin protein; DDB1, damaged DNA-binding protein 1; RBX1, RING box-domain protein; GSPT1, G1 to S phase transition 1; DUB, deubiquitinating enzyme; eRF1, eukaryotic translation termination factor 1; NBS, N-bromosuccinimide, ACN, acetonitrile; EtOAc, ethyl acetate; HCl, hydrochloric acid; DMA, dimethylacetamide; DMF, diemthylformamide; TLC, thin layer chromatography; HPLC, high performance liquid chromatography.

ASSOCIATED CONTENT

Supporting Information.

Standard error of measurement for all biological data present and

Molecular Formula Strings, Excel document

TABLE OF CONTENTS GRAPHIC

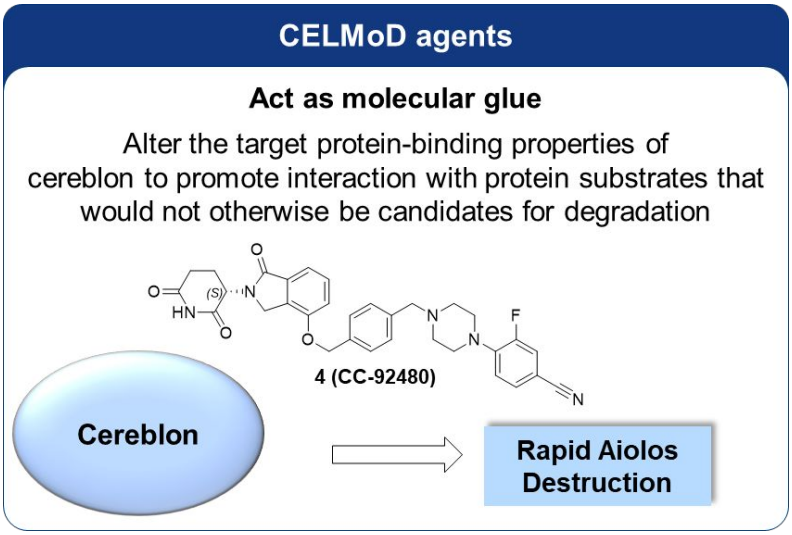

REFERENCES

1. American Cancer Society, Cancer Statistic Center Page. https://cancerstatisticscenter.cancer.org/?_ga=2.200904942.1379280727.1580495928-1064148705.1580495928#!/cancer-site/Myeloma (accessed Jan 2020).

2. Nijhof, I. S.; van de Donk, N.W. C. J.; Zweegman, S.; Lokhorst, H. M. Current and New Therapeutic Strategies for Relapsed and Refractory Multiple Myeloma: An Update. *Drugs* **2018**, *78*, 19–37.

3. Ito, T.; Ando, H.; Suzuki, T.; Ogura, T.; Hotta, K.; Imamura, Y.; Yamaguchi, Y.; Handa, H. Identification of a Primary Target of Thalidomide Teratogenicity. *Science* **2010**, *327*, 1345-1350.

4. Kronke, J.; Udeshi, N. D.; Narla, A.; Grauman, P.; Hurst, S. N.; McConkey, M.; Svinkina, T.; Heckl, D.; Comer, C.; Li, X.; Hartman, E.; Munshi, N.; Schenone, M.; Schreiber, S. L.; Carr, S. A.; Ebert, B. L. Lenalidomide Causes Selective Degradation of IKZF1 and IKZF3 in Multiple Myeloma Cells. *Science* **2014**, *343*, 301-305.

5. Lu. G.; Middleton, R. E.; Sun, H.; Naniong, M.; Ott, C. J.; Mitsiades C. S.; Wong, K. K.; Bradner, J. E.; Kaelin, W. G. Jr. The Myeloma Drug Lenalidomide Promotes the Cereblon-Dependent Destruction of Ikaros Proteins. *Science* **2014**, *343*, 305-309.

6. Zhu, Y. X.; Braggio, E.; Shi, C. X.; Bruins, L. A.; Schmidt, J. E.; Van Wier, S.; Chang, X-B.; Bjorklund, C.; Fonseca, R.; Bergsagel, L.; Orlowski, R.; Cereblon Expression is Required for the Antimyeloma Activity of Lenalidomide and Pomalidomide. *Blood* **2011**, *118*, 4771–4779.

7. Lopez-Girona, A.; Mendy, D.; Ito, T.; Miller, K.; Gandhi, A.K.; Kang, J.; Karasawa, S.; Carmel, G.; Jackson, P.; Abbasian, M.; Mahmoudi, A.; Cathers, B.; Rychak, E.; Gaidarova, S.; Chen, R.; Schafer, P.; Handa, H.; Daniel, T. Cereblon is a Direct Protein Target for Immunomodulatory and Antiproliferative Activities of Lenalidomide and Pomalidomide. *Leukemia* **2012**, *26*, 2326–2335.

8. Gandhi, A. K.; Kang, J.; Havens, C. G.; Conklin, T.; Ning, Y.; Wu, L.; Ito, T.; Ando, H.; Waldman, M.; Thakurta, A; Klippel, A; Handa, H.; Daniel, T.; Schafer, P.; Chopra, R. Immunomodulatory Agents Lenalidomide and Pomalidomide Co-stimulate T Cells by Inducing Degradation of T Cell Repressors Ikaros and Aiolos via Modulation of the E3 Ubiquitin Ligase Complex CRL4(CRBN). *Br. J. Haematol*. **2014**, *164*, 811–821.

9. Zhu, Y. X.; Kortuem, K. M.; Stewart, A. K. Molecular Mechanism of Action of Immune-modulatory Drugs Thalidomide, Lenalidomide and Pomalidomide in Multiple Myeloma. *Leuk. Lymphoma*. **2013**, *54*, 683–687.

10. Guirguis, A. A.; Ebert, B. L. Lenalidomide: Deciphering Mechanisms of Action in Myeloma, Myelodysplastic Syndrome and Beyond. *Curr Opin Cell Biol.* **2015**, *37*, 61–67.

11. Hansen, J.D.; Condroski, K.; Correa, M.; Muller, G.; Man, H.W.; Ruchelman, A.; Zhang, W.; Vocanson, F.; Crea, T.; Liu, W.; Lu, G.; Baculi, F.; LeBrun, L.; Mahmoudi, A.; Carmel, G.; Hickman, M.; Lu, C.C. Protein Degradation via CRL4CRBN Ubiquitin Ligase: Discovery and Structure-Activity Relationships of Novel Glutarimide Analogs That Promote Degradation of Aiolos and/or GSPT1. *J. Med. Chem.* **2018**, *61*, 492-503.

12. Muller, G. W.; Ruchelman, A. L. 5-substituted Isoindoline Compounds for the use in Cancer. WO 2010053732, **2010**.

13. Siegel, D.; Schiller, G. J.; Song, K. W.; Agajanian, R.; Stockerl-Goldstein, K.; Kaya, H.; Sebag, M.; Samaras, C.; Malek, E.; Talamo, G.; Seet, C. S.; Mouro, J.; Zafar, F.; Chung, W.; Srinivasan, S.; Qian, M.; Agarwal, A.; Thakurta, A.; Bahlis, N. J. Pomalidomide (POM) + Low-Dose Dexamethasone (LoDEX) Safety and Efficacy in

Patients (pts) with Relapsed and/or Refractory Multiple Myeloma (RRMM) Previously Treated with a Proteasome Inhibitor (PI) and in Whom Last Prior Therapy with Lenalidomide (LEN) Failed. *Blood* **2017,** 130, 1812.

14. Chamberlain, P. P.; Lopez-Girona, A.; Miller, K.; Carmel, G.; Pagarigan, B.; Chie-Leon, B.; Rychak, E.; Corral, L. G.; Ren, Y. J.; Wang, M.; Riley, M.; Delker, S. L.; Ito, T.; Ando, H.; Mori, T.; Hirano, Y.; Handa, H.; Hakoshima, T.; Daniel, T. O.; Cathers, B. E. Structure of the Human Cereblon-DDB1-lenalidomide Complex Reveals Basis for Responsiveness to Thalidomide Analogs. *Nat. Struct. Mol. Biol.* **2014**, *21*, 803-809.

15. Teo, S. K.; Chen, Y.; Muller, G.; Chen, R.; D. Thomas, S.; Stirling, D.; Chandula, R. Chiral Inversion of the Second Generation IMiD CC-4047 (ACTIMID) in Human Plasma and Phosphate-buffered Saline. *Chirality* **2003**, *15*, 348–351.

16. Eriksson, T.; Björkman, S.; Roth, B.; Fyge, A.; Höglund, P. Stereospecific Determination, Chiral Inversion In Vitro and Pharmacokinetics in Humans of the Enantiomers of Thalidomide. *Chirality* **2003**, *7,* 44–52.

17. Mori, T.; Ito, T.; Liu, S.; Ando, H.; Sakamoto, S.; Yamaguchi, Y.; Tokunaga, E.; Shibata, N.; Handa, H.; Hakoshima, T. Structural Basis of Thalidomide Enantiomer Binding to Cereblon. *Sci Rep*. **2018,** *8*, 1294-1308.

18. Li, Z. S.; Schmauss, C.; Cuenca, A.; Ratcliffe, E.; Gershon, M. D. Physiological Modulation of Intestinal Motility by Enteric Dopaminergic Neurons and the D2 Receptor: Analysis of Dopamine Receptor Expression, Location, Development, and Function in Wild-Type and Knock-Out Mice. *J. Neuroscience* **2006**, 26, 2798–2807.

19. Deshaies, R. J. Protein Degradation: Prime Time for PROTACs. *Nat. Chem. Biol.* **2015**, *11*, 634–635.

20. Winter, G. E.; Buckley, D. L.; Paulk, J.; Roberts, J. M.; Souza, A.; Dhe-Paganon, S.; Bradner, J. E. Drug Development. Phthalimide Conjugation as a Strategy for In Vivo Target Protein Degradation. *Science* **2015**, *348*, 1376–1381.

21. Lu, J.; Qian, Y.; Altieri, M.; Dong, H.; Wang, J.; Raina, K.; Hines, J.; Winkler, J. D.; Crew, A. P.; Coleman, K.; Crews, C. M. Hijacking the E3 Ubiquitin Ligase Cereblon to Efficiently Target BRD4. *Chem. Biol*. **2015**, *22*, 755–763.

22. Matyskiela, M.; Lu, G.; Ito, T.; Pagarigan, B.; Lu, C. C.; Miller, K.; Fang, W.; Wang, N. Y.; Nguyen, D.; Houston, J.; Carmel, G.; Tran, T.; Riley, M.; Nosaka, L.; Lander, G. C.; Gaidarova, S.; Xu, S.; Ruchelman, A. L.; Handa, H.; Carmichael, J.; Daniel, T. O.; Cathers, B. E. Lopez-Girona, A.; Chamberlain, P. P. A Novel Cereblon Modulator Recruits GSPT1 to the CRL4CRBN Ubiquitin Ligase. *Nature* **2016**, *535*, 252-257.